Reconstructing visual speed: behavior, perception, models, and the neural basis of an illusion of increased speed

by

Mark M. Churchland

DISSERTATION

Submitted in partial satisfaction of the requirements for the degree of

DOCTOR OF PHILOSOPHY

in

Neuroscience

in the

GRADUATE DIVISION

of the

UNIVERSITY OF CALIFORNIA SAN FRANCISCO

Date University Librarian

Degree Conferred: .....

To my father,

who made science aesthetic, and the world with it

(or perhaps it was the other way around)

Many thanks to the colleagues who made this work possible, foremost among them Nicholas Priebe, Anne Churchland and Justin Gardner. Equal thanks to those who have kept me happy throughout: my wife Clarissa, my sister Anne, my parents Paul and Pat, and my other parents Penny and Bob. And of course many thanks to Steve, for firm but gentle guidance and considerable faith.

Reconstructing visual speed: behavior, perception, models, and the neural basis of an illusion of increased speed

Mark M. Churchland

We recorded motor, perceptual and neural responses to visual stimuli designed to reveal how the brain estimates speed. One set of experiments asked if the speed-tuning of area MT neurons subserves the estimate of speed that guides smooth-pursuit eye movements. We measured the pursuit evoked by stimuli containing a local component, designed to excite neurons with a particular speed-tuning, and a displacement component that produced a different net speed. Pursuit eye movements were driven primarily by the local component, and were affected only weakly by the net speed. A model based on the speed-tuning of recorded MT neurons was similarly weakly influenced by the net speed. We conclude that the neural estimate of speed used by pursuit is based on the speed tuning of MT neurons. A second set of experiments documented the pursuit of apparent motion targets. The flash separation of the target was varied while holding speed constant. For small separations, motion appeared smooth and produced normal pursuit. Larger flash separations induced a number of changes in both the magnitude and latency of the initial pursuit response. The perception of speed in humans was similarly influenced by apparent motion. We conclude that apparent motion changes the magnitude and latency of the neural estimate of speed. One such change was unexpected: some flash separations produced an increase in both initial pursuit and the perception of speed. The same flash separations produced diminished neural responses in

MT neurons, relative to
ffected than were fast-p
higher speeds. A simple
averaging, was applied t
relevant flash separation
ursuit latency. We c
agnitude and latency c
ccounted for if the brai
verage.

MT neurons, relative to smooth motion. However, slow-preferring neurons were more affected than were fast-preferring neurons, shifting the population response towards higher speeds. A simple decoding model, based on opponent motion and vector averaging, was applied to the neural responses. The model successfully predicts, for the relevant flash separations, the increases and decreases in initial pursuit, and the changes in pursuit latency. We conclude that apparent motion induces a number of changes in the magnitude and latency of the neural estimate of speed, and that these changes can be accounted for if the brain estimates speed from MT via a particular kind of vector average.

Table of contents

List of tables and figures

Chapter 1

Chapter 2

Chapter 3

Chapter 3

Figure 16.....

General Introduction

For many neurons in the brain, the firing of action potentials is influenced by sensory stimuli. Such neurons are termed sensory, and their firing is said to convey information about sensory stimuli. Two questions we might ask about such neurons are 1) how, exactly, is their firing related to the sensory input, and 2) how is their firing interpreted by the brain to create estimates of the external world? This thesis is concerned primarily with this second question, as it applies to the estimation of visual motion. In particular, we sought to understand how the brain estimates the speed of moving objects from the firing of neurons responsive to visual motion.

Using awake monkeys, we recorded the responses of motion sensitive neurons to a moving stimulus. Monkeys were trained to perform a task in response to the stimulus. The task, ocular smooth pursuit, is known to depend upon the neurons from which we recorded, and allowed us to infer how fast the stimulus appeared to the monkeys' visual system. We were thus able to simultaneously observe the response of a population of motion sensitive cells and the estimate of speed extracted from this population. Our goal was to deduce how the responses of neurons within the population are combined to yield the estimate of speed used by the monkey. This goal was aided by the use of a number of specialized stimuli, in particular apparent motion. Apparent motion produces changes in the both the response of motion sensitive neurons and in the visual system's estimate of speed. By observing the covariance of the neural population response and the estimate of speed, we are able to draw conclusions about how the estimate of speed is extracted from the population response. Apparent motion thus functions as a tool. Its utility lies in its ability to create changes in the estimate of speed used by the visual system. Some of

these changes appear p

methods by which spee

The first chapter

system makes its estima

cortical area MT. This

second chapter describe

movements of monkeys

apparent motion and tha

motion on pursuit are l

experiments lay the fou

third chapter describes

also the results of exper

responses, perception a

speed.

these changes appear paradoxical, and are particularly useful to us as they constrain the methods by which speed could be estimated.

The first chapter describes a series of experiments demonstrating that the pursuit system makes its estimate of speed based on the speed tuning of motion sensitive cells in cortical area MT. This chapter lays the foundation for the models we later explore. The second chapter describes in detail the effect of apparent motion on the smooth pursuit eye movements of monkeys. We describe in detail the relationship between the parameters of apparent motion and the evoked smooth pursuit. We discuss which effects of apparent motion on pursuit are likely due to changes in the neural estimate of speed. These experiments lay the foundation for the strategy described in the paragraphs above. The third chapter describes recordings from motion sensitive neurons in cortical area MT, and also the results of experiments on human perception. This last section links neural responses, perception and pursuit via models of how the brain extracts its estimate of speed.

Reconstruction of

Nicholas J. P.

Chapter 1

Reconstruction of target speed for the guidance of pursuit eye movements

Nicholas J. Priebe*, Mark M. Churchland*, and Stephen G. Lisberger

(* contributing equally. *J Neurosci,* in press)

Abstract

We studied how
selective cells for the g
mation. In theory, the
of the active populatior
activation across the co
movements evoked by
component designed to
displacement compone
fields. Pursuit eye mov
were affected to only a
space. Extracellular re
sponses of cells in vis
but were influenced by
eye movements. We co
reconstruction of target
cells.

Abstract

We studied how object speed is reconstructed from the responses of motion selective cells for the generation of a behavior that is tightly linked to the speed of visual motion. In theory, the speed of an object could be estimated either from the speed tuning of the active population of motion selective cells, or from the rate of displacement of activation across the cortical map of visual space. We measured the pursuit eye movements evoked by stimuli containing two conflicting motion components: a local component designed to excite motion selective cells with a particular speed tuning, and a displacement component designed to excite cells with a sequence of spatial receptive fields. Pursuit eye movements were driven primarily by the local motion component, and were affected to only a small degree by the rate of target displacement across visual space. Extracellular single unit recordings using the same stimuli revealed that the responses of cells in visual area MT depended primarily on the local motion component, but were influenced by the displacement component to the same degree as were pursuit eye movements. We conclude that the initiation of pursuit is consistent with a reconstruction of target speed based on the speed tuning of the active population of MT cells.

Note added for thesis

The work in Chapter 1 demonstrates that the estimate of speed that guides pursuit is based on the speed tuning of MT neurons. The explanations and models presented in Chapter 3 assume this conclusion. Their success provides a confirmation of the conclusions of Chapter 1.

Introduction

Visual motion is critical for the guidance of movement. For example, smooth pursuit eye movements respond to the motion of visual targets (Rashbass 1961). Pursuit is guided by estimates of both the direction and speed of the object to be tracked. In monkeys, the middle temporal visual area (MT) is necessary for the normal initiation of smooth pursuit eye movements, and micro-stimulation of MT drives pursuit (Newsome et al 1985, Komatsu and Wurtz 1989). Neurons in MT are excited by moving targets (Dubner and Zeki 1971) and are tuned for both target direction and target speed (Maunsell and Van Essen 1983). Thus, the question of how the nervous system estimates or "reconstructs" target motion from the responses of neurons in MT may be addressed by measuring the smooth eye movements guided by that reconstruction.

In principle, there are two different approaches that might be used by the nervous system to reconstruct target speed. The first approach would rely on the speed-tuning of MT neurons. When a target moves at a constant speed, MT neurons with preferred speeds near the target speed will be the most active. Any of a variety of neural computations could be used to reconstruct target speed by estimating the preferred speed of the most active neurons. The second approach would measure the rate of displacement of a target across adjacent receptive fields of a sequence of MT neurons. This approach would not be sensitive to the speed tuning of the active neurons, but only to their receptive field locations. There is a precedent for displacement computations, as they must be used at some level of the nervous system to create direction-selective neurons. In primates displacement computations create direction-selective neurons in the primary visual cortex (V1) from the non-direction selective neurons in the lateral geniculate nucleus (LGN)

(Saul and Humphrey 1992). A displacement computation could solve the problem that the speed-tuning of MT neurons is not constant, but varies as a function of target features such as contrast and spatial frequency (Movshon et al 1986, Cassanello et al 2000). The variance of speed-tuning would adversely impact the accuracy of a reconstruction of target speed based on the speed-tuning of MT cells, but would not affect a reconstruction based on a displacement computation.

The goal of the present paper was to test whether target speed is reconstructed from the firing of MT neurons by a displacement computation or a speed-tuning computation. We contrived stimuli that would cause different estimates of target speed, depending on which computation is actually used. Stimuli provided two components of motion. The first component was local, and was intended to excite MT neurons with preferred speeds near the speed of the local motion. The second component consisted of a displacement of the local motion across the visual field, at a different speed. We evaluated the neural estimate of target speed by measuring the initiation of smooth pursuit. Eye acceleration during pursuit initiation is closely related to target speed (Lisberger and Westbrook 1985). By measuring eye acceleration, we were therefore able to assess the estimate of speed used by pursuit. Our data indicate that pursuit is driven by a reconstruction of target speed based on the speed-tuning of the active neurons in area MT, and not by a displacement computation based on the spatial location of the activity.

Methods

Pursuit experiments

Pursuit experiments were run on three male rhesus monkeys (*Macaca mulatta*) that had been trained to pursue spot targets. The experimental and training protocol has been described before (e.g. Lisberger and Westbrook 1985). Eye movements were measured with the scleral search coil method (Judge et al. 1980), using eye coils that had been implanted with sterile procedure while the animal was anesthetized with isofluorane. In a separate surgery, stainless steel plates were secured to the skull and attached with dental acrylic to a cylindrical receptacle that could be used for head restraint. During experiments, the head was immobilized by attaching a post to both the receptacle and the ceiling of a specially-designed primate chair. Eye velocity was obtained by analog differentiation of the eye position outputs from the search coil electronics (DC-25 Hz, -20 dB/decade). During experiments, animals were rewarded with juice or water for accurate tracking. Experiments were run daily, typically lasting two hours.

Single unit recording experiments

Single unit recordings were made in two anesthetized, paralyzed macaque monkeys (*Macaca fascicularis*). After the induction of anesthesia with ketamine (5-15 mg/kg) and midazolam (0.7 mg/kg), cannulae were inserted into the saphenous vein and the trachea. The animal's head was then fixed in a stereotaxic frame and the surgery was continued under an anesthetic combination of isoflurane (2%) and oxygen. A small craniotomy was performed directly above the superior temporal sulcus (STS) and the underlying dura was reflected. The animal was maintained under anesthesia using an

intravenous opiate, sufentanil citrate (8-16 micrograms/kg/hr) for the duration of the experiment. To minimize drift in eye position, paralysis was maintained with an infusion of vecuronium bromide (Norcuron, 0.1 mg/kg/hr) for the duration of the experiment and the animals were artificially ventilated with medical grade air. Body temperature was kept at 37°C with a thermostatically controlled heating pad. The electrocardiogram, electroencephalogram, autonomic signs, and rectal temperature were continuously monitored to ensure the anesthetic and physiological state of the animal. The pupils were dilated using topical atropine and the corneas were protected with +2D gas-permeable hard contact lenses. Supplementary lenses were selected by direct ophthalmoscopy to make the lens conjugate with the display. The locations of the foveae were recorded using a reversible ophthalmoscope.

Tungsten-in-glass electrodes were introduced by a hydraulic microdrive into the anterior bank of the superior temporal sulcus (STS) and were driven down through the cortex and across the lumen of the STS into area MT. Location of unit recordings in MT was confirmed by histological examination of the brain after the experiment, using methods described in Lisberger and Movshon (1999). After the electrode was in place, agarose was placed over the craniotomy to protect the surface of the cortex and reduce pulsations. Single units were isolated and recorded for subsequent analysis. The responses included here are from five electrode penetrations at different sites in 2 monkeys.

All methods for both awake and anesthetized monkeys had received prior approval by, and were in compliance with the regulations of the *Institutional Animal Care and Use Committee* at UCSF.

Stimulus Presentation

Visual stimuli were presented on an analog oscilloscope (Hewlett-Packard models 1304A and 1321B, P4 phosphor), using signals provided by digital-to-analog converter outputs from a PC-based digital signal processing board (Spectrum Signal Processing, "Detroit" system). This method affords extremely high spatial and temporal resolution, with a frame refresh rate of 500 or 250 Hz and a spatial resolution of 64K by 64K pixels. The apparent motion created by our display is effectively smooth at these sampling rates (Mikami et al. 1986, Churchland and Lisberger, 2000). The display was positioned 30 cm from the animal and subtended 48.4° horizontally by 38.6° vertically. Experiments were performed in a dimly lit room. Due to the dark screen of the display, background luminance was beneath the threshold of the photometer, less than one mcd/m^2. The same display technology was used for the pursuit and unit recording experiments.

Spot targets were round and smaller than 0.25°. The spot targets were used both as fixation points and tracking targets and had net luminances of 1.6 and 25 cd/m^2, respectively. Because spot targets were small, these luminances were bright but not dazzling. Motion of the target was achieved by flashing the spot in a new location every 2 or 4 ms. Each flash lasted approximately 160 μs.

Patch targets consisted of six dots randomly placed within a 3° x 3° virtual window that the monkey was required to follow. Each dot had a luminance of 1.6 cd/m^2. Patch targets were surrounded by a field of stationary random dots of the same density (1 dot per 1.5 deg^2) and luminance as the patch target. The dots in the patch target and the borders of the virtual window always moved in the same direction, though sometimes at different speeds. As the patch target moved across the display, the dots in the background

texture remained static

defined by the patch ta

patch target. Boundary

limits of the window o

occurred, a new dot w

to the constraint provi

move a maximum of 1

placed randomly in the

assigned an initial spat

asynchronously. Becau

single dot was reposit

within a patch was cyc

For the pursuit

with the appearance o

within 600 ms after its

200 to 800 ms. The fi

target that was either a

appeared eccentric and

Rashbass 1961). The

or the speed of the tar

extinguished earlier. I

experiments, the target

the monkey was requi

texture remained stationary, but were displayed only when outside of the virtual window defined by the patch target. Thus, there was no luminance boundary to demarcate the patch target. Boundary conditions arose when a dot inside the patch moved beyond the limits of the window or when the limits of the window moved past a dot. When this occurred, a new dot was randomly placed within the bounds of the window. In addition to the constraint provided by the edges of the window, each single dot was allowed to move a maximum of 1° before it was extinguished and replaced with a new dot that was placed randomly in the patch window. At the beginning of a trial, each dot was randomly assigned an initial spatial lifetime between 0 and 1°, so that dots were replaced asynchronously. Because of boundary constraints and limits on the distance moved, a single dot was repositioned on average every 4 ms during these trials and the set of dots within a patch was cycled completely at least every 40 ms.

For the pursuit experiments, targets were presented in individual trials that began with the appearance of a fixation point. The monkey was required to fixate the point within 600 ms after its appearance and to maintain fixation within 2° for an additional 200 to 800 ms. The fixation spot was then extinguished and replaced with a tracking target that was either a spot or a patch, depending on the experiment. The tracking target appeared eccentric and immediately began to move toward the point of fixation (Rashbass 1961). The duration of target motion varied from 270 to 1200 ms, depending on the speed of the target. Faster targets neared the edge of the monitor sooner and were extinguished earlier. For the very fast targets and short durations of motion used in some experiments, the target stopped and remained visible near the edge of the monitor, and the monkey was required to fixate the stationary target for 600 ms. This approach was

designed to motivate the monkeys to track to the best of their abilities even for very brief target motions. If fixation requirements were met for the duration of the trial, then a juice reward was delivered. Each pursuit experiment consisted of multiple repeats of a list of up to 50 types of trials, where each trial type presented a different stimulus. The trials were sequenced by shuffling the list and requiring the monkey to complete each trial successfully once. Failed trials were placed at the end of the list and presented again after all the other trials had been completed. After all trials had been completed once, the list was shuffled and presented again.

For single unit recording experiments, we initially mapped the receptive fields of the individual MT neurons by hand using bars on a tangent screen. The receptive fields of the cells included in this study were all within 10° of the fovea and were 4 to 10 degrees of visual arc in diameter (mean: 6.1°, SD: 1.7°). After the receptive field location was determined, a mirror was positioned such that a random dot texture on the display oscilloscope fell within the receptive field of the cell. Textures were used to characterize the preferred direction and speed of the cell (Lisberger and Movshon 1999). We then studied each cell with a sequence of trials that provided motion of the same spot and patch targets that had been used to analyze pursuit. To render the stimuli identical with those used in the pursuit experiments, the spot trials began with the appearance and immediate motion of the target from its initial position. The patch trials began with the appearance of a stationary, uniform random dot texture that was visible for 256 ms before a patch target like those described above provided motion in either the preferred or null direction of the cell being recorded. Target movement continued for 256 ms or until the target reached the end of the display.

Data Acquisition and Analysis

Experiments were controlled by a computer program running on a UNIX workstation. The workstation sent commands to a Pentium PC that both controlled the stimuli and acquired data. For the pursuit experiments, signals proportional to horizontal and vertical eye position and eye velocity were sampled at 1 kHz on each channel. For the unit recording experiments, a hardware discriminator was used to convert the extracellular action potentials to TTL pulses and the time of each pulse was recorded by the computer to the nearest 10 μs. After each trial, data were sent via the local area network to the UNIX workstation and saved for later analysis, along with a record of the commands given to generate the stimulus.

For pursuit, we aligned the responses to multiple repetitions of the same stimulus on the onset of target motion and computed the average eye velocity as a function of time, in 1 ms bins. We then estimated the time of the initiation of pursuit from the averages and defined our analysis interval to start at the initiation of pursuit and have a duration equal to one open-loop interval. The duration of the open-loop interval was estimated as the latency of the eye velocity response to a change in target velocity during sustained pursuit. Both the latency of pursuit and the open loop interval varied slightly between monkeys and as a function of the form of the target, and the latency of pursuit also varied as a function of target direction. The latency of pursuit initiation was typically slightly longer (75-110 ms) than the duration of the open-loop interval (60-85 ms). For each trial type, we measured the change in average eye velocity during the analysis interval, and computed average eye acceleration as the change in eye velocity divided by the duration of the open-loop interval. Standard errors were computed by

measuring the eye acceleration on a trial-by-trial basis. We did not analyze the later, closed-loop and maintenance periods of pursuit, as the retinal stimulus driving pursuit differs from the presented target motion, making interpretation difficult. Trials with saccades during the open-loop interval following pursuit initiation were excluded from all analyses.

For the single unit data, we aligned the responses to multiple repetitions of the same stimulus on the onset of target motion and computed the average firing rate as a function of time, in 16 ms bins. The number of repetitions of each trial ranged from 12 to 56 and averaged 18.8. We then measured firing rate in the interval from 80 to 176 ms after the onset of stimulus motion, an interval chosen because it approximates the period during which MT responses drive eye acceleration at the initiation of pursuit. To quantify the speed tuning of each MT neuron, we presented textures that were stationary for 256 ms before starting to move at constant speeds of 0.125, 0.25, 0.5, 1, 2, 4, 8, 16, 32, 64, and 128°/s. We computed the average firing rate in the analysis interval for each speed, plotted average firing rate as a function of speed, and fit the data with the function:

$$G(s) = R_{max}\left(e^{-\left[\frac{\log\left(\frac{s}{\mu_s}\right)}{\sigma_s+\zeta\log\left(\frac{s}{\mu_s}\right)}\right]} - e^{-\left(\frac{1}{\zeta^2}\right)}\right) \qquad (1)$$

where R_{max} is the maximal firing rate, μ_s is the optimal speed, s is the speed of the stimulus, σ_s is the tuning width and ζ is the skew of the cell, after the background firing rate has been subtracted. The quality of the fits was excellent. For the 20 MT neurons in our sample, the fitted parameters yielded a mean chi square of 4.98±4.06, where there were 6 degrees of freedom. To allow comparison across neurons, each neuron's response to each stimulus was normalized by the value of R_{max} from Equation 1.

Results

The basis for our experimental design is illustrated in Figure 1, where each graph places a population of MT neurons on two axes: the horizontal axis corresponds to the spatial locations of the neurons' receptive fields and the vertical axis corresponds to their preferred speeds. Stimulus motion excites cells with appropriate preferred speeds, and with receptive fields at the location of the target. In principle, displacement computations could estimate target speed according to how quickly the activity peak is displaced along the horizontal axis, represented by the filled arrows along the top of each graph. Speed-tuning computations based on the preferred speeds of the active population of neurons could estimate target speed by measuring the location of the peak of the activity along the vertical axis, represented by the open arrows along the right of each graph. If the stimulus is conceptualized in this way, then each target motion has two components: one related to local motion and one related to the rate of displacement of the motion. We will refer to the two stimulus components as "local motion" and "displacement" components.

Figure 1A presents the usual situation, where computations based on either the local motion or the rate of displacement would yield the same estimate of target speed. In Figure 1B, the stimulus contains fast local motion but is displaced slowly across visual space. In Figure 1C, the stimulus contains slow local motion but is displaced quickly across visual space. We created the latter two situations in the first three experiments, by contriving stimuli that contained conflicting displacement and local-motion components. As we will show below, the result of each experiment is consistent with the idea that pursuit is driven by the local-motion component of the

stimuli. In the fourth experiment, we used the same target motions as visual stimuli while recording from cells in area MT. This allowed us to be sure that the speed tuning of the active population of MT neurons was determined primarily by the local motion component of our stimuli.

Experiment 1: The Gaps Experiment

Gap targets achieved the dissociation between the speed of local motion and the rate of displacement by using alternate periods in which the target was visible and invisible. For example, the top trace in Figure 2A shows the velocity profile of a spot target that started with a visible period (solid trace) in which it moved at 10°/s for 16 ms. Target motion was sampled at 4 ms intervals, so that each visible period delivered 5 flashes of the target. During the subsequent gap period (dashed part of the trace), the target was invisible for 16 ms. At the end of the gap period, the target reappeared at a new position as if it had moved at 20°/s during the gap, a displacement of 0.32 degrees. After 3 cycles of visible and gap periods, the target reappeared and moved uninterrupted at 15°/s so that the monkey could establish accurate tracking of an unambiguous target motion. We refer to the target motion in Figure 2A as the "10-visible condition". Its companion, in which the first, visible motion was at 20°/s and gap motion was at 10°/s, is termed the "20-visible" condition (not illustrated). Both targets were displaced at a rate of 15°/s, but during their visible periods should have excited populations of cells tuned for different speeds. The 10-visible condition is expected to preferentially excite cells with preferred speeds near 10°/s, while the 20-visible condition is expected to excite cells with preferred speeds near 20°/s. The bottom traces in Figure 2A show averages of eye velocity from one experiment to illustrate the general finding that the 10-visible and 20-

visible conditions evoked different initial pursuit responses, even though the target was displaced at the same average rate in both conditions.

Figure 2B shows that the mean eye acceleration during the open-loop interval was lower in the 10-visible condition than in the 20-visible condition for both monkeys we tested. Each group of 4 bars shows the average results for a single experiment. These results are the first piece of evidence we present to suggest that eye acceleration at the initiation of pursuit is sensitive to the speed tuning of the population of active MT cells. Note, however, that the rate of displacement of the target was held constant in this experiment, so it is not possible to know if a displacement computation also contributes to pursuit initiation.

We performed two control experiments to ensure that our results were not related to other features of the stimulus that differed between the 10-visible and 20-visible conditions. First, to control for any effects of the order of the speeds within the first versus second interval, we used a "20-reversed" stimulus in which visible motion was at 20°/s but the gap-interval was first and the visible-interval was second. Second, to control for the fact that the two stimuli provided targets that moved different distances during the visible period we employed a "20-short" stimulus in which visible motion was at 20°/s but the visible periods were only 8 ms in duration: gap period duration was 16 ms and velocity was 10°/s, as before. Figure 2B shows that both of these stimuli elicited eye accelerations that were consistent with the visible component of the stimulus, which provided target motion at 20°/s. Note that the rate of stimulus displacement across the visual field was reduced to 13.3°/s for the 20-short stimulus. If a pure displacement computation were employed to extract speed information, then the 20-short stimulus

ought to yield lower eye accelerations than any of the other stimulus conditions. However, the data show that initial eye acceleration was similar to that evoked by the 20-visible condition, and higher than that evoked by the 10-visible condition.

Experiment 2: The Jumps Experiment

Jumps targets dissociated the speed of local motion from the rate of displacement by interrupting motion at one speed with sudden steps of target displacement. The test target (illustrated by the dashed target trace in Fig. 3A) moved at 8°/s for successive 16-ms intervals, but underwent 2° jumps in the direction of target motion between intervals, producing a net displacement rate of 133°/s. After five or six intervals separated by jumps, the target ceased jumping and moved at a constant speed of either 8°/s (illustrated) or 133°/s with equal probability. This "2-deg-jumps" target was designed to excite MT cells with speed tunings near 8°/s, but to traverse visual space at a much faster rate. A jump size of 2° was selected to exceed the maximum spatial integration distance of MT neurons (Mikami et al. 1986), and therefore not to excite cells with fast preferred speeds, despite the rapid displacement of the stimulus. We confirm in a later section that the stimulus design was successful in creating this effect. Two control targets moved at either 8°/s or 133°/s (illustrated, respectively, by the thin and thick target traces in Fig. 3A). All target motion was sampled at 2 ms intervals, so that the 2-deg-jumps target was flashed 9 times during each 16-ms interval of smooth motion.

The average eye velocity traces in Figure 3A show that the initial pursuit response to the 2-deg-jumps target (dashed trace) is similar to that evoked by the 8°/s target (fine, solid trace), and much smaller than that evoked by the 133°/s target (bold, solid trace). The bar graphs in Figure 3B show that mean eye acceleration in the open-loop interval

for the 2-deg-jumps target was slightly larger than that for the 8°/s target but much smaller than that for the 133°/s target. The 2-deg-jumps target was designed to contain two components: local motion at 8°/s and a net rate of displacement of 133°/s. The response to the 2-deg-jumps target was close to that for the control 8°/s target and therefore was dominated by the speed of the local motion. However, the faster displacement component did have an impact. The response to the 2-deg-jumps target was larger than that for the 8°/s target, and the difference was statistically significant for both monkeys shown in Figure 3 ($p<0.05$).

We quantified the relative contributions of the local motion and displacement components of the 2-deg-jumps stimulus using the equation:

$$R_{local\,/\,displacement} = l*(R_{local}) + (1-l)*(R_{displacement}) \qquad (2)$$

where l is the proportion of the response governed by local motion. $R_{local/displacement}$ is the measured smooth eye acceleration for the target with conflicting local and displacement speeds (the 2-deg-jumps target for these experiments). R_{local} is the measured smooth eye acceleration to the control target whose speed was the same as the local-motion component of the conflicting stimulus (the 8°/s target). $R_{displacement}$ is the measured smooth eye acceleration to a control target whose speed was the same as the rate of displacement of the conflicting stimulus (the 133°/s target). If the response to the 2-deg-jumps target were the same as the response to the 8°/s or 133°/s targets, then l would be equal to one or zero, respectively. Smooth eye acceleration was measured as the average acceleration during the open loop interval, as described in methods. For rightward pursuit in monkeys Ka and Mo, l was 0.83 and 0.81, indicating that the majority of the response to the 2-deg-jumps stimulus can be accounted for as a response to the local

motion component of target motion. To insure these results generalized, we ran 8 additional jumps experiments, for a total of 10 experiments on 3 monkeys, including tests of both horizontal and vertical pursuit. Although pursuit accelerations differed dramatically among the four directions tested, the *l*-value did not depend on whether pursuit was along the vertical or horizontal axis (Table 1).

We conducted two controls for the 2-deg-jumps experiment. The first control was run for the experiments illustrated in Figure 4, and asked whether the jumps could influence the initiation of pursuit if they were smaller. We measured the response to a "0.2-deg-jumps" target that was identical to the 2-deg-jumps target except that each jump was only 0.2°. Smaller jumps are expected to fall within the spatial integration ability of MT neurons and to excite cells with preferred speeds near the net speed created by the jumps. The bars labeled "0.2-deg-jumps" in Figure 3C indicate that initial pursuit acceleration was consistently larger for the 0.2-deg-jumps target than for the 8°/s target ($p<0.05$ for both monkeys), and larger even than for the 2-deg-jumps target ($p<0.05$ for monkey Mo, not significant for monkey Ka).

For the second control, we asked whether the slightly larger eye acceleration for the 2-deg-jumps target versus the control 8°/s target is due to the fact that the two targets had different average eccentricities (0.74° and 3.74° respectively) during the first 64 ms of target motion (approximately the open loop interval). Less eccentric targets typically evoke larger eye accelerations (Lisberger and Westbrook 1985), potentially accounting for the larger acceleration evoked by the 2-deg-jumps target. To test this hypothesis we recorded pursuit as a function of the initial eccentricity of the pure 8°/s target. Starting eccentricities of 4°, 1.5°, and 1° yielded average eccentricities of 3.74°, 1.24°, and 0.74°

in the first 64 ms of target motion and had small and variable effects on eye acceleration in the open-loop interval. For the rightward pursuit of monkey Mo, average open-loop acceleration was 118 ± 4°/s, 102 ± 3°/s, and 109 ± 3°/s, respectively. For the rightward pursuit monkey Ka, average open-loop acceleration was 105 ± 3°/s, 100 ± 3°/s, and 110 ± 3°/s. By comparison, the 2-deg-jumps target evoked an average eye acceleration of 164 ± 7°/s for monkey Mo, and 123 ± 6°/s for monkey Ka. We conclude that the increase in initial eye acceleration produced by the 2-deg-jumps target is not simply a product of the change in average target eccentricity.

This control was also performed for the subsequent 8 experiments using the jumps stimuli, described in Table 1. For some of these experiments, the change in acceleration as a function of eccentricity was large enough to potentially account for the increase in eye acceleration produced by the 2-deg-jumps target (relative to the pure 8°/s target). For these experiments, we cannot be sure if the displacement component of the 2-deg-jumps target influenced pursuit, or if the changes in eye acceleration were due to the difference in average eccentricity. However, for many of the experiments, the response to the pure 8°/s target was, for both eccentricities, smaller than that to the 2-deg-jumps target. Therefore, it does appear that the displacement component makes a small contribution to the initial pursuit response, even though the values of *l* we report may slightly underestimate the dominance of the local component.

Experiment 3: The Patch Experiment

Patch targets dissociated the speed of local motion from the rate of displacement by painting dots within a 3° x 3° window surrounded by a static random dot field, and contriving to have the dots within the window and the borders of the window move at

different speeds (see Methods for details). Window and dot speed could each be either 10°/s or 30°/s, yielding four combinations, two of which put the window and dot speeds in conflict. Motion was sampled every 2 ms.

Figure 4A and B show typical eye position responses to stimuli in which the dots moved slower or faster than the boundaries of the window. When dot speed was 10°/s and the window was displaced at 30°/s (top traces in Fig. 4A), the smooth component of eye velocity was slower than the window displacement and the monkey made a staircase of rightward saccades to keep eye position (solid trace) close to window position (dashed trace), which was the requirement to receive a reward. When dot speed was 30°/s and the window traversed visual space at 10°/s (bottom traces in Fig. 4A), smooth eye movement started briskly so that eye position led target position and a backwards saccade was required to fulfill the reward requirements.

Averages of eye velocity in the open-loop interval for the four stimulus conditions show that the initiation of pursuit depended primarily on the speed of dot motion and not the rate of window displacement (Fig. 4B). As long as dot motion was at 10°/s, the pursuit response depended little on whether the window was displaced at 10°/s (bold solid trace) or 30°/s (bold dashed trace). Similarly, as long as dot motion was at 30°/s, pursuit depended little on whether the window was displaced at 30°/s (fine solid trace) or 10°/s (fine dashed trace). The bar graphs in Figure 4C show means and standard errors of the initial eye acceleration for all four conditions, revealing a consistent dependence on dot speed but not window movement.

We again used Equation 2 to estimate the contribution of the local-motion signal provided by dot speed to the signals driving pursuit. For monkey Na, the value of l was

0.99 and 0.82 when the dots moved slower or faster than the window. For monkey Mo, the value of *l* was 0.98 and 0.78 when the dots moved slower or faster than the window. Thus, pursuit responses were determined primarily by the local motion of the dots, but were weakly influenced by the rate of window displacement, especially when fast moving dots were paired with slow displacement of the window. As in the jumps experiment, the effect of the displacement component was particularly large near the end of the open-loop interval. A total of 8 patch experiments were run on 3 monkeys, including tests of both horizontal and vertical pursuit. As summarized in Table 2, the results were consistent across experiments and were statistically significant in all animals. Again, the *l*-value did not depend on whether pursuit was along the horizontal axis, or in the upward direction. The value of *l* was lower for fast dots and slow window displacement that for the converse situation in all but one experiment. This unexpected asymmetry may result from a weak disruption of pursuit gain in the unfamiliar situation where the dot and window speeds do not match. For the 3 monkeys tested, the patch targets evoked little downward pursuit, and that it was not possible to conduct the experiment for this direction.

Experiment 4: Single Unit Responses in Area MT

Experiment 4 was designed as to ask whether neurons in area MT responded solely to the local-motion component of our stimuli, as we had assumed when we designed Experiments 1-3, or whether the displacement component of motion influenced their responses. Single MT cells were recorded in anesthetized monkeys. After a neuron's preferred direction and speed were determined using moving random dot textures, we recorded responses to the target motions used in the patch and jumps experiments. For

each cell, the stimulus was shown moving in both the cell's preferred and null direction. The speed of the stimulus was not customized for each cell, as we wished to know how neurons with different preferred speeds responded to the stimuli we had used to measure pursuit.

Figure 5 shows the responses of two neurons when presented with the stimuli used in the patch experiment. For the neuron that responded to fast speeds (preferred speed = 33°/s), a brisk response was elicited when dot speed was 30°/s, whether the speed of window displacement was 10 or 30°/s. For a neuron that responded to slower speeds (preferred speed = 10°/s), a strong response was elicited when dot speed was 10°/s, whether the speed of the window was 10 or 30°/s. For both example neurons, the amplitude of the responses was determined primarily by the speed of dot motion. The time course of the response was shorter when the window moved at 30°/s, presumably because the patch exited the spatial confines of the receptive field more quickly than when the window moved at 10°/s. The variation in time course is expected to have minimal impact on our analysis, which considered the firing rate only in the interval from 80-172 ms after the beginning of stimulus movement, a period analogous to the open-loop interval in the pursuit experiments.

To summarize these data, for each target we first computed the directional component of each neuron's firing rate. The directional component of the firing rate is defined as the response to motion in the preferred direction minus the response to motion in the null direction. We then normalized the firing rate for each target by the maximal response of the same neuron in the speed tuning experiments, grouped the neurons according to their preferred speed into bins that were one octave wide, and computed the

mean and standard deviation of the response, in each bin, for each target. The general trend in Figure 6A shows that neurons with preferred speeds in the 4 and 8°/s bins responded best when the dot speed was 10°/s (yellow and red bars) and neurons with preferred speeds in the 32 and 64°/s bins responded best when the dot speed was 30°/s (green and blue bars). Neurons with preferred speeds of 16°/s gave the same response for all 4 stimuli. In general, neurons responded strongly only when the local motion provided by dot speed was near their preferred speed. In addition, the window speed did have a small effect. For example, for dot motion at 10°/s, neurons with preferred speeds in the 4 and 8°/s bins responded better when the window speed was 10°/s (yellow bars) than when it was 30°/s (red bars). Because responses to motion in the null-direction were almost always small, the same basic trends appeared when the analysis was based solely on the response to the preferred direction (data not shown). These results validate our assumption that the preferred speeds of the active population are determined primarily by the local motion of the dots themselves.

The targets used in the jumps experiment also evoked MT responses that were driven primarily by the local motion component (Fig. 6B). Both the control 8°/s target (yellow bars) and the 2-deg-jumps target (red bars) evoked responses that were larger for neurons with slower preferred speeds. The 133°/s target (blue bars) evoked the largest response in neurons with preferred speeds in the 32 and 64°/s bins. The same basic trends seen in Figure 6B, which plots the difference between responses to the preferred and null directions, are seen in the responses to the preferred direction (data not shown). Thus, MT neurons respond mainly to the 8°/s local motion in the 2-deg-jumps target, as we had assumed in interpreting the jumps experiment.

Quantitative comparison of population responses in MT and pursuit behavior

Although MT neurons responded primarily to the local motion component of our stimuli, the displacement component also had an effect. We quantitatively compared the relative influences of the two components on the MT population response. This was done by reconstructing target speed from the responses of our sample population of neurons for each stimulus condition. We then computed the *l*-value from these reconstructions of target speed to measure the relative effect of the local and displacement components of motion on the reconstruction of target speed.

We normalized the speed tuning curve for each neuron (Equation 1) to have a peak response of 1, weighted each normalized curve by the neuron's response to the stimulus, summed these curves over all MT neurons in our sample, and normalized for the sum of the responses:

$$P(s) = \frac{\sum_i \frac{R_i}{R_{max_i}} * G_i}{\sum_i R_i} \qquad (3)$$

where $P(s)$ is the population response for stimulus speed s, R_i is the normalized directional response of the i^{th} MT neuron to stimulus s, G_i is the speed tuning curve of cell i, and the sum is taken over all 20 MT neurons we recorded. This approach uses each neuron's speed tuning curve as a filter to smooth the population code, compensating for our relatively sparse sampling of the population.

Figure 6C shows the population response obtained for each of the four target motions used in the patch experiment. Each curve plots the normalized activation of the population as a function of the preferred speed of the neurons. The curves form two pairs. The two curves with peaks at lower preferred speeds were obtained from responses

to the 'dots 10/window 10' target (yellow trace) and the 'dots 10/window 30' target (red trace). The two curves with peaks at higher preferred speeds were obtained from responses to the 'dots 30/window 10' target (green trace) and the 'dots 30/window 30' target (blue trace). In addition, there is a small effect of window speed: the curves for a window speed of 30°/s (red, blue) lie slightly to the right of those for a window speed of 10°/s (yellow, green). Like pursuit, the MT population response is dominated by the local component, but is influenced by the displacement component.

For the jumps experiment (Fig. 6D) the population responses for the 8°/s target (yellow) and 2-deg-jumps target (red) are similar. They both peak at lower preferred speeds than the population response for the pure 133°/s target (blue curve) and the curve for the 2-deg-jumps target (red) has a slightly higher peak than that for the 8 deg/s target (yellow curve). Because of our incomplete sampling of MT neurons, including few neurons with preferred speeds above 30°/s, the population response to the 133°/s target peaks at a much lower preferred speed, just under 23°/s. However, it is the relative locations of the peaks that are important. Faster target speeds lead to larger estimates of speed, even if the estimates are not exact. As with the patch targets, the population response to the jumps targets is influence by the local and displacement components of motion in the same way as pursuit.

To reconstruct target speed from the population responses and compare it with the pursuit responses, we measured the preferred speed of the neurons at the peak of the population response. For the patch experiment (leftmost 4 bars in Fig. 7), the primary determinant of the reconstructed target speed was the speed of the local motion provided by the dots, though the reconstruction was biased slightly towards the speed of the

window. The effect of both the dot and window speed was statistically significant based on using a jackknife technique (Sokal and Rohlf 1995) to compute error bars for each stimulus condition and pairwise t-tests to determine significance of the differences between the reconstructions. Application of Equation 1 to the reconstructions from the unit recordings revealed that the *l*-values for the reconstruction of speed from MT neurons were 0.90 and 0.85 for the dots 10/window 30 and dots 30/window 10 target, comparable to those for pursuit (mean values of 0.95 and 0.79, respectively).

For the jumps experiment (rightmost 3 bars in Fig. 7), the reconstructed target speed was slightly higher for the 2-deg-jumps target than for the 8°/s target motion, and was much higher for the 133°/s target motion. All the differences were statistically significant. For the 2-deg-jumps target, the *l*-value for the reconstruction was 0.86, indicating that the reconstruction of speed from MT neurons was determined primarily by the speed of the local motion, but was influenced slightly by the rate of the target displacement. For pursuit, the mean *l*-value was similar: 0.87.

Discussion

The goal of our experiments was to determine how the pursuit system reconstructs an estimate of target speed. We contrived targets that placed into conflict the speed of local motion and the overall rate of displacement of the stimulus. Our behavioral experiments show that initial pursuit eye acceleration is determined primarily by the speed of local motion and argue that the reconstruction of target speed is based primarily on the speed tuning of MT cells. The rate of displacement of the stimulus did have a small effect on the initiation of pursuit, suggesting that a displacement-based computation might also contribute to the reconstruction of target speed. However, the rate of displacement also had a small effect on the responses of MT neurons, so that the speed-tuning reconstruction was sufficient to account for the behavioral data. It is therefore unnecessary to suppose that a displacement-based computation contributes anything to the estimate of target speed used during pursuit initiation. We conclude that the estimate of target speed driving eye acceleration during the initiation of pursuit is derived purely from a speed-tuning based estimate of target speed.

Our experiments raise four technical questions that we will consider now.

1) Why did the displacement component of motion in our stimuli affect the peak of the active population of MT neurons at all? For the jumps experiment, we chose to elevate the rate of target displacement from 8°/s to 133°/s by the addition of 2° jumps because such large jumps should not support direction-selective responses in the majority MT cells (Mikami et al. 1986). Some cells, particularly those with a combination of selectivity for low spatial frequencies and high speeds, may have sufficient spatial integration to

respond directionally to the 2° jumps. Alternately, the response to local motion may facilitate a response to the 2° target displacements. For the patch experiment, the displacement of the window fails to provide any moving luminance borders, and is an example of "second-order motion." As second-order motion evokes a response from some MT neurons (Albright 1992; O'Keefe and Movshon 1998), it is not surprising that window displacement did have a small effect on both the response of MT neurons and the initiation of pursuit

2) Would our results have been different if we had used a different computational approach to reconstruct target speed? For simplicity, we took the speed at the peak of the population curve as our estimate of the target speed. This corresponds to a category of approaches that falls under the rubric of "winner-take-all". An alternative approach involves estimating the center of mass of the population response, commonly termed "vector averaging". Inspection of the population responses in Figures 6C and 6D makes it clear that population responses were unimodal and well-behaved, and that we would have obtained the same results from almost any sensible method. Note that the simpler method of taking the average firing rate over all MT neurons would not have worked. It fails even on control target motions: the output of such a model will actually be lower for a target speed of 133°/s than for 8°/s. Finally, though we based our estimates of target speed on the directional component of MT neuron responses, calculated by taking the difference between firing rate for motion in the preferred and null directions,

we obtained the same general results when we repeated the computations based on responses for motion in the preferred direction only.

3) Were our results altered by smoothing the population responses using the speed tuning curves as filters? In fact, results were very similar when we computed the population response via a vector-average that weighted each neuron's normalized response according to its preferred speed (data not shown). However, this approach would not have allowed the clean graphical presentation in Figures 6C and 6D.

4) Would our estimate of the value of *l*, the relative contribution of local motion signals to the response of MT cells, differ if we had a larger sample of MT neurons? The distribution of preferred speeds we sampled resembles that found by other researchers (Mikami et al 1986). Therefore we do not believe that a skewed sampling of preferred speeds has influenced our estimate of the value of *l*. Although the reconstructions of target speed from this population of MT neurons did not yield quantitatively accurate estimates of actual target speed (Figure 7), the estimates did increase monotonically with the target speed. Because the *l*-value is computed from the relative locations of the peaks, it would be influenced minimally by systematic inaccuracies in the absolute estimate of speed.

Our results provide a major constraint on how the responses of the population of MT neurons are pooled to drive smooth pursuit eye movements: the estimate of speed used by pursuit is extracted by a computation based on the speed-tuning of the active neurons. A number of different neural computations could be used, all of which can be

termed 'labeled-line computations' because they rely on knowing both a neuron's firing rate and its preferred speed or speed tuning. Labeled-line computations provide reliable estimates of stimulus parameters only if the neurons' tunings for that parameter remain fixed independent of other stimulus parameters. Consistent labeled-line estimates could be made for orientation and direction of motion, since tuning may broaden or narrow, strengthen or weaken, but the location of the peak is invariant with stimulus form or contrast (Sclar and Freeman 1982; Jones and Palmer 1987; Albright 1992). However, the preferred speed of most of the neurons in V1, MT, and V2 depends on the spatial frequency content of the stimulus (Movshon et al. 1986; Movshon et al. 1988; Cassanello et al. 2000). If a labeled line computation based on speed-tuning is used, then the estimate of speed may vary as a function of spatial frequency.

It is unknown whether the initiation of pursuit varies as a function of the spatial frequency of the visual stimulus, although ocular following is known to do so (Miles et al. 1986). Psychophysical experiments have demonstrated that changes in both contrast and spatial frequency consistently affect the perception of speed (Diener et al. 1976; Campbell and Maffei 1981; Thompson 1983; McKee et al. 1986; Stone 1992). However, other approaches imply that representations of speed that are invariant with spatial frequency do exist in the brain (Schrater and Simoncelli 1998, Reisbeck and Gegenfurter 1999). It is unclear whether these representations are based upon a subset of MT neurons that have invariant speed tunings, or are based on responses in areas downstream of MT.

We stress that our results do not exclude the use of displacement-based algorithms earlier in the visual motion pathway. In primary visual cortex, a displacement-based algorithm is used to convert the firing of LGN neurons into direction selective responses

(Saul and Humphrey 1990; Saul and Humphrey 1992). Further, cells in area MT may use displacement-based algorithms as part of the mechanism that creates their responses from the activity of cells in V1. A computation that reads the displacement of activation across the cortical map of visual space in V1 would account for the observation that MT neurons retain directional responses even when apparent motion causes the majority of V1 neurons to lose direction selectivity (Mikami et al. 1986). Finally, displacement-based reconstructions of target speed from the firing of MT neurons may be used for some purposes, such as the detection of long-range apparent motion (Braddick 1980), but do not drive eye acceleration at the initiation of smooth pursuit eye movements.

References

Albright TD (1992). Form-cue invariant motion processing in primate visual cortex. Science **255**: 1141-1143.

Braddick O (1980). Low-level and high-level processes in apparent motion. Philos Trans R Soc Lond B Biol Sci **290**: 137-151.

Campbell FW and Maffei L (1981). The influence of spatial frequency and contrast on the perception of moving patterns. Vision Research **21**: 713-721.

Cassanello C, Priebe NJ and Lisberger SG (2000). The speed tuning of single units in macaque visual area MT depends upon spatial form. Soc. Neurosci. Abstr., New Orleans, LA.

Churchland MM and Lisberger SG (2000). Apparent motion produces multiple deficits in visually guided smooth pursuit eye movements of monkeys. Journal of Neurophysiology 84: 216-235.

Diener HC, Wist ER, Dichgans J, Brandt T (1976). The spatial frequency effect on perceived velocity. Vision Research **16**: 169-176.

Jones J and Palmer L (1987). The two-dimensional structure of simple receptive fields in cat striate cortex. Journal of Neurophysiology **58**: 1187-1211.

Judge SJ, Richmond BJ, and Chu FC (1980). Implantation of magnetic search coils for measurement of eye position: an improved method. Vision Research **20**: 535-538.

Lisberger SG and Movshon JA (1999). Visual motion analysis for pursuit eye movements in area MT of macaque monkeys. Journal of Neuroscience **19**: 2224-2246.

Lisberger SG and Westbrook LE (1985). Properties of visual inputs that initiate horizontal smooth pursuit eye movements in monkeys. Journal of Neuroscience **5**: 1662-1673.

Komatsu, H., and Wurtz, R.H. Modulation of Pursuit Eye Movements by Stimulation of Cortical Areas MT and MST. J. Neurophysiol. 62: 31-47, 1989.

McKee SP, Silverman G, Nakayama K (1986). Precise velocity discrimination despite random variations in temporal frequency and contrast. Vision Research **26**: 609-619.

Mikami A, Newsome WT and Wurtz RH (1986). Motion selectivity in macaque visual cortex. II. Spatiotemporal range of directional interactions in MT and V1. Journal of Neurophysiology **55**: 1328-1339.

Miles FA, Kawano K and Optican LM (1986). Short-Latency Ocular Following Responses of Monkey. I. Dependence on Temporospatial Properties of Visual Input. Journal of Neurophysiology **56**: 1321-1354.

Movshon JA, Newsome WT, Gizzi MS and Levitt JB (1988). Spatio-temporal tuning and speed sensitivity in macaque visual cortical neurons. Investigative Opthalmology and Visual Science (Supplement) **24**: 106.

Movshon JA, Adelson EH, Gizzi MS and Newsome WT (1986). The analysis of moving visual patterns. Experimental Brain Research Supplementum II: Pattern Recognition Mechanisms: 117-151.

O'Keefe LP and Movshon JA (1998). Processing of first- and second-order motion signals by neurons in area MT. Visual Neuroscience **15**: 305-317.

Rashbass C (1961). The relationship between saccadic and smooth tracking eye movements. Journal of Physiology London **159**: 326-338.

Reisbeck T and Gegenfurtner K (1999). Velocity tuned mechanisms in human motion processing. Vision Research **39**: 3267-3285.

Salinas E and Abbott LF (1994). Vector reconstruction from firing rates. Journal of Computational Neuroscience **1**: 89-107.

Saul AB and Humphrey AL (1990). Spatial and temporal response properties of lagged and nonlagged cells in cat lateral geniculate nucleus. Journal of Neurophysiology **64**: 206-224.

Saul AB and Humphrey AL (1992). Evidence of input from lagged cells in the lateral geniculate nucleus to simple cells in cortical area 17 of the cat. Journal of Neurophysiology **68**: 1190-1208.

Sclar G and Freeman RF (1982). Orientation selectivity in the cat's striate cortex is invariant with stimulus contrast. Experimental Brain Research **46**: 457-461.

Sokal R. and Rohlf F(1995). Biometry. New York, W. H. Freeman and Company.

Stone LS (1992). Human speed perception is contrast dependent. Vision Research **32**: 1535-1549.

Thompson P (1983). Perceived rate of movement depends on contrast. Vision Research **22**: 337-380.

Acknowledgements

We are grateful to Michael Shadlen for initially advancing the idea of displacement motion computations, Jessica Hanover and Kenneth Britten for helpful comments on earlier versions of the manuscript, Scott Ruffner for creating the target presentation software, and Leslie Osborne and Carlos Cassanello for assisting with the physiology experiments. Research was supported by the Howard Hughes Medical Institute, and by NIH grants R01-EY03878 and T32-EY07120.

	8 °/s (4°)	8 °/s (1°)	2-deg-jumps (4°)	133 °/s (4°)	*L*
Monkey Mo (right, 1st)†	118 °/s^2	109 °/s^2	165 °/s^2	367 °/s^2	0.81
Monkey Ka (right)†	106 °/s^2	110 °/s^2	123 °/s^2	245 °/s^2	0.87
Monkey Qu (right)	69 °/s^2	112 °/s^{2*}	116 °/s^2	392 °/s^2	0.85
Monkey Qu (left)	55 °/s^2	109 °/s^{2*}	97 °/s^2	322 °/s^2	0.84
Monkey Qu (up)	29 °/s^2	46 °/s^2	67 °/s^2	125 °/s^2	0.61
Monkey Qu (down)	43 °/s^2	60 °/s^2	51 °/s^2	184 °/s^2	0.94
Monkey Mo (right, 2nd)	78 °/s^2	98 °/s^2	112 °/s^2	460 °/s^2	0.91
Monkey Mo (left)	78 °/s^2	104 °/s^{2*}	101 °/s^2	490 °/s^2	0.94
Monkey Mo (up)	54 °/s^{2*}	72 °/s^2	59 °/s^2	136 °/s^2	0.94
Monkey Mo (down)	61 °/s^{2*}	87 °/s^2	67 °/s^2	324 °/s^2	0.97
Physiology (peak response)	6.4 °/s		8.7 °/s	22.8 °/s	0.86

Table 1: Summary of the jumps experiments. From left to right, the columns show data for: the control 8°/s target starting at 4° eccentric from fixation, the control 8°/s target starting at 1°, the 2-deg-jumps target starting at 4°, the control 133°/s target starting at 4°, and the value of *l* computed from equation 2. The upper 10 rows report eye acceleration during the initiation of pursuit for target motion in different directions, using different monkeys or recorded on different days. For some experiments using vertical directions, initial pursuit was weak and it was necessary to increase the starting eccentricity of the targets to reduce the prevalence of early saccades. For these experiments the eccentricity of all targets was increased by 1 or 2°. Relative eccentricities remained unchanged. The

bottom row gives the target speed reconstructed for each target type from the population response recorded in area MT. An (*) indicates that there was *not* a significant difference between the responses to the indicated control 8°/s target and the 2-deg-Jumps target (paired t-test). An (†) indicates data shown in Figure 3. All measurements were based on averages of at least 50 trials.

	Dots 10 Window 10	Dots 10 Window 30	Dots 30 Window 10	Dots 30 Window 30	$l_{10/30}$	$l_{30/10}$
Monkey Mo (right, 1st)†	52.1 °/s² *	53.2 °/s² *	125.1 °/s²	146.2 °/s²	0.98	0.78
Monkey Na (right)†	31.8 °/s² *	32.1 °/s² *	55.9 °/s²	61.4 °/s²	0.99	0.82
Monkey Qu (right)	48.8 °/s²	53.1 °/s²	66.5 °/s²	75.3 °/s²	0.84	0.67
Monkey Qu (left)	34.7 °/s² *	34.5 °/s² *	44.5 °/s²	49.8 °/s²	1.01	0.65
Monkey Qu (up)	13.5 °/s² *	13.1 °/s² *	18.5 °/s²	20.2 °/s²	1.06	0.75
Monkey Mo (right, 2nd)	64.9 °/s²	72.3 °/s²	110.0 °/s²	112.9 °/s²	0.85	0.94
Monkey Mo (left)	44.7 °/s² *	44.9 °/s² *	68.8 °/s²	70.7 °/s²	0.99	0.93
Monkey Mo (up)	31.4 °/s² *	33.9 °/s² *	47.6 °/s²	53.4 °/s²	0.89	0.74
Physiology (peak response)	6.4 °/s	7.6 °/s	16.1 °/s	17.8 °/s	0.90	0.85

Table 2: Summary of the patch experiments. The upper 8 rows report eye accelerations during the initiation of pursuit for target motion in different directions, using different monkeys, or on different days. The bottom row gives the target speed reconstructed for each target from the population response recorded in area MT. An (*) indicates that the conditions "Dots10/Window10" and "Dots 10/Window 30" did *not* evoke statistically significant differences in pursuit acceleration. Note that for the two l-values greater than one, there was no significant difference between the "Dots10/Window10" and "Dots 10/Window 30" conditions. An (†) indicates data shown in Figure 4. All measurements were based on at least 28 trials.

Figure 1. A schematic representation of the population of neurons in area MT, showing how speed could be reconstructed either from the speed-tuning of the active neurons or from the rate of displacement of the active site across the map of visual space. In each panel, the activation of MT cells is indicated by the shading, where the darkest cells have the greatest activity. The length of the dark arrow above each graph indicates the reconstruction of speed based upon a displacement computation. The length of the hollow arrow on the right of each graph indicates the reconstruction of speed based upon the speed tuning of the active population of cells. *A*: The local and displacement motion signals are in agreement, yielding equivalent reconstructions from displacement and speed tuning computations. *B*: The local motion signal is fast while the target is displaced slowly across the visual field. *C*: The local motion signal is slow while the target is displaced rapidly across the visual field.

Figure 1

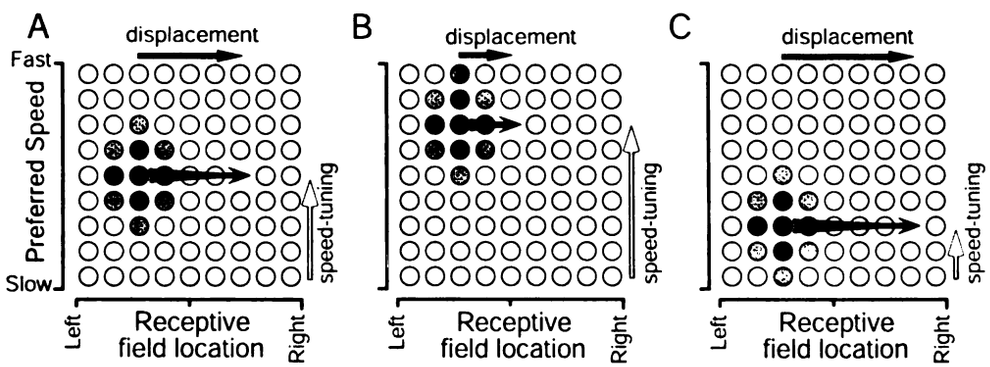
A
displacement
Fast
Preferred Speed
Slow
speed-tuning
Left
Receptive field location
Right
B
displacement
speed-tuning
Left
Receptive field location
Right
C
displacement
speed-tuning
Left
Receptive field location
Right

Figure 2. Pursuit responses in the gaps experiment. *A*: The top trace shows the velocity of the spot target in the "10-visible" condition. Solid lines indicate when the target was visible and moving; dashed lines indicate when the target was not visible but was moving. Average eye velocity is shown in the bottom traces. The thin and thick traces show the pursuit responses to the "10-visible" and the "20-visible" conditions. The upward arrow indicates the end of the open-loop interval. For this and all figures, upward deflections indicate rightward movement. The scale bar on the right refers to both target and eye velocity. *B*: Bar graphs showing the average open-loop eye acceleration measured during the initiation of pursuit for one experiment in each of two monkeys. Error bars give the standard errors of the mean.

Figure 2

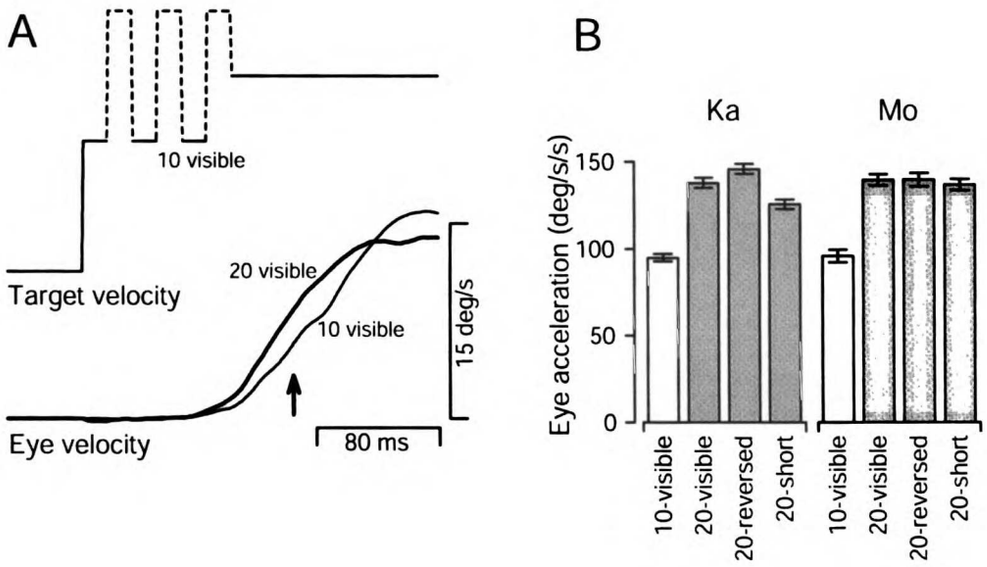
A
10 visible
20 visible
Target velocity
10 visible
15 deg/s
Eye velocity
80 ms
B
Ka
Mo
Eye acceleration (deg/s/s)
150
100
50
0
10-visible
20-visible
20-reversed
20-short
10-visible
20-visible
20-reversed
20-short

Figure 3. Pursuit responses in the jumps experiment. *A*: The top trace shows target position for three conditions. The thin and thick solid traces represent control 8°/s and 133°/s targets. The dashed trace represent the 2-deg-jumps target, which moved at 8°/s, but jumped 2° in the direction of target movement every 16 ms. The bottom traces indicate the average eye velocity for the three different conditions. *B*: Bar graphs showing the average open-loop pursuit acceleration for one experiment in each of two monkeys. Error bars indicate the standard error of the mean.

Figure 3

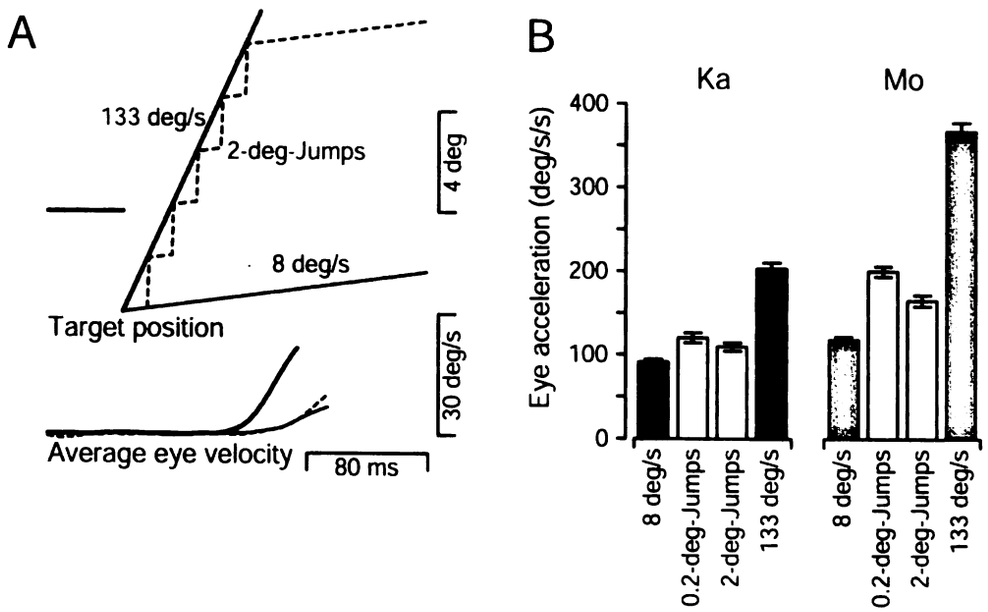
A
133 deg/s
2-deg-Jumps
8 deg/s
4 deg
Target position
30 deg/s
Average eye velocity
80 ms
B
Ka
Mo
Eye acceleration (deg/s/s)
400
300
200
100
0
8 deg/s
0.2-deg-Jumps
2-deg-Jumps
133 deg/s
8 deg/s
0.2-deg-Jumps
2-deg-Jumps
133 deg/s

Figure 4. Pursuit responses in the patch experiment. *A*: Eye and target position are shown for conditions where the displacement and local motion signals are in conflict. The solid traces correspond to eye position and the dashed lines indicate the position of the virtual window defining the patch target. The top traces demonstrate the condition where the dots moved at 10°/s, but the window moved at 30°/s. The bottom traces correspond to the converse condition: dots 30°/s, window 10°/s. *B*: Average eye velocity for the four combinations of dot and window velocity, for the open-loop interval only. The solid and dashed traces plot responses to conditions in which dot and window motion were at the same or different speeds. Thick and thin traces indicate dot motion at 10°/s or 30°/s. The downward arrow indicates the initiation of pursuit. *C*: Bar graphs show the average open-loop pursuit eye acceleration for one experiment on each of two monkeys. Error bars indicate the standard error of the mean.

Figure 4

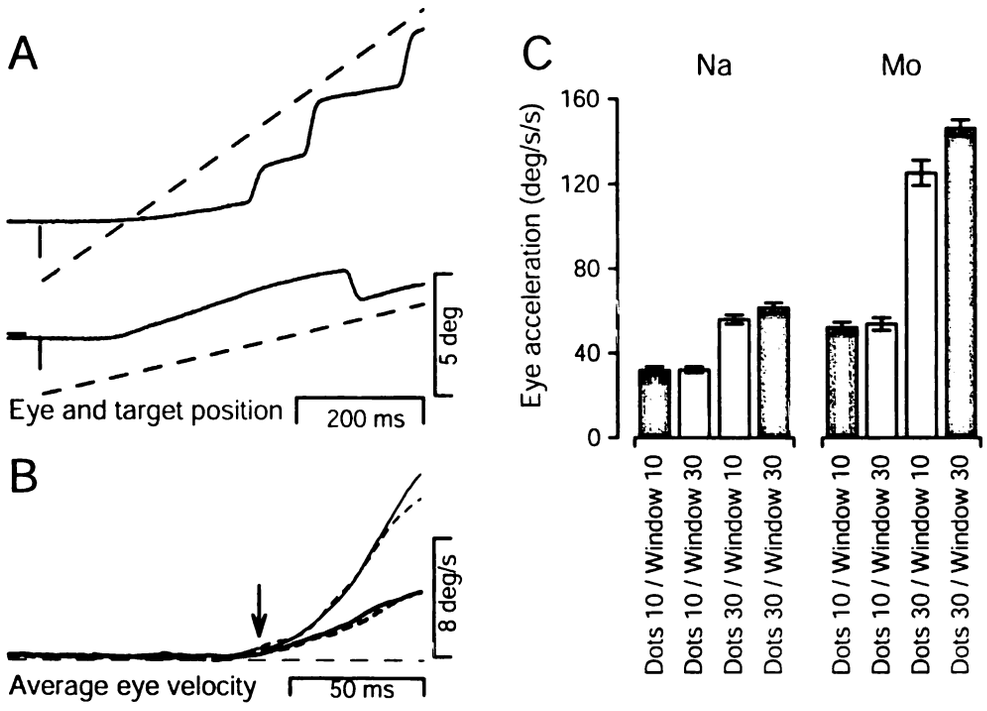
A
5 deg
Eye and target position
200 ms
B
8 deg/s
Average eye velocity
50 ms
C
Na
Mo
Eye acceleration (deg/s/s)
160
120
80
40
0
Dots 10 / Window 10
Dots 10 / Window 30
Dots 30 / Window 10
Dots 30 / Window 30
Dots 10 / Window 10
Dots 10 / Window 30
Dots 30 / Window 10
Dots 30 / Window 30

Figure 5: Representative single unit responses to the four combinations of dot and window velocity in the patch experiment. The top row provides schematic drawings of the stimulus, where the solid dots and arrows indicate the speed of dot motion and the open arrows indicate the speed of window motion. The middle and bottom rows show the responses of two MT neurons to the four stimuli. The neuron in the middle row had a preferred speed of 33°/s. The neuron in the bottom row had a preferred speed of 10°/s. Each histogram shows the firing rate of the neuron in response to the stimulus shown above the histogram. Bin width was 16 ms. The bars underneath each histogram indicate the interval of stimulus motion.

Figure 5

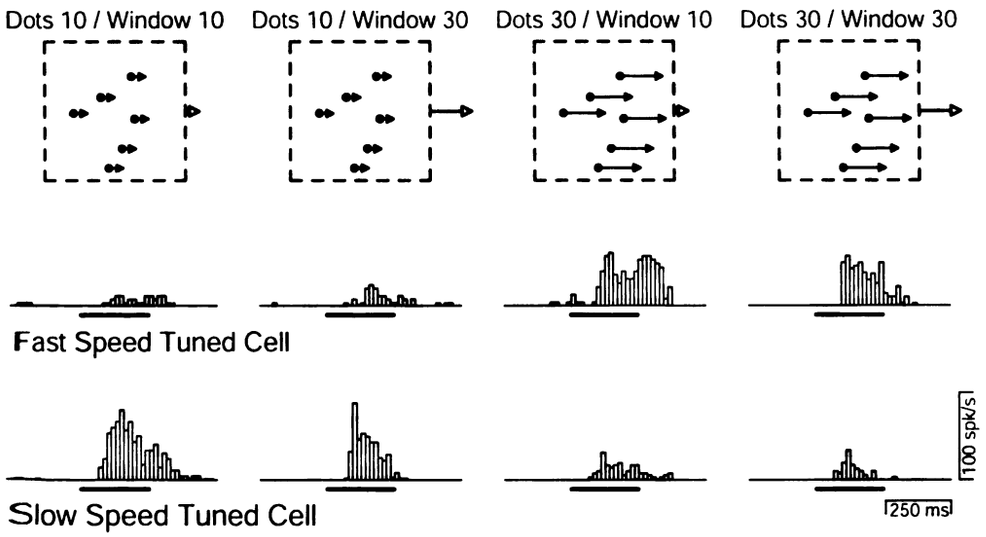
Dots 10 / Window 10
Dots 10 / Window 30
Dots 30 / Window 10
Dots 30 / Window 30
Fast Speed Tuned Cell
Slow Speed Tuned Cell
100 spk/s
250 ms

Figure 6: The response of the population of MT neurons to the stimuli used to record pursuit eye movements. Responses to patch and jumps stimuli are summarized in the left and right columns. In A and B, cells were pooled into five groups based upon their preferred speed. Each bar graph shows the average normalized response of MT neurons to each stimulus minus the response to the null direction, as a function of preferred speed. In C and D, the population response is plotted as a function of preferred speed. *A, C*: Patch targets. The color coding for both bars and curves is: yellow, dots 10/windows 10; red, dots 10/windows 30; green, dots 30/windows 10; blue, dots 30/windows 30. *B, D*: Jumps targets. The color coding for both bars and curves is: yellow, control 8°/s target motion; red 2-deg-jumps; blue bars, control 133°/s target motion.

Figure 6

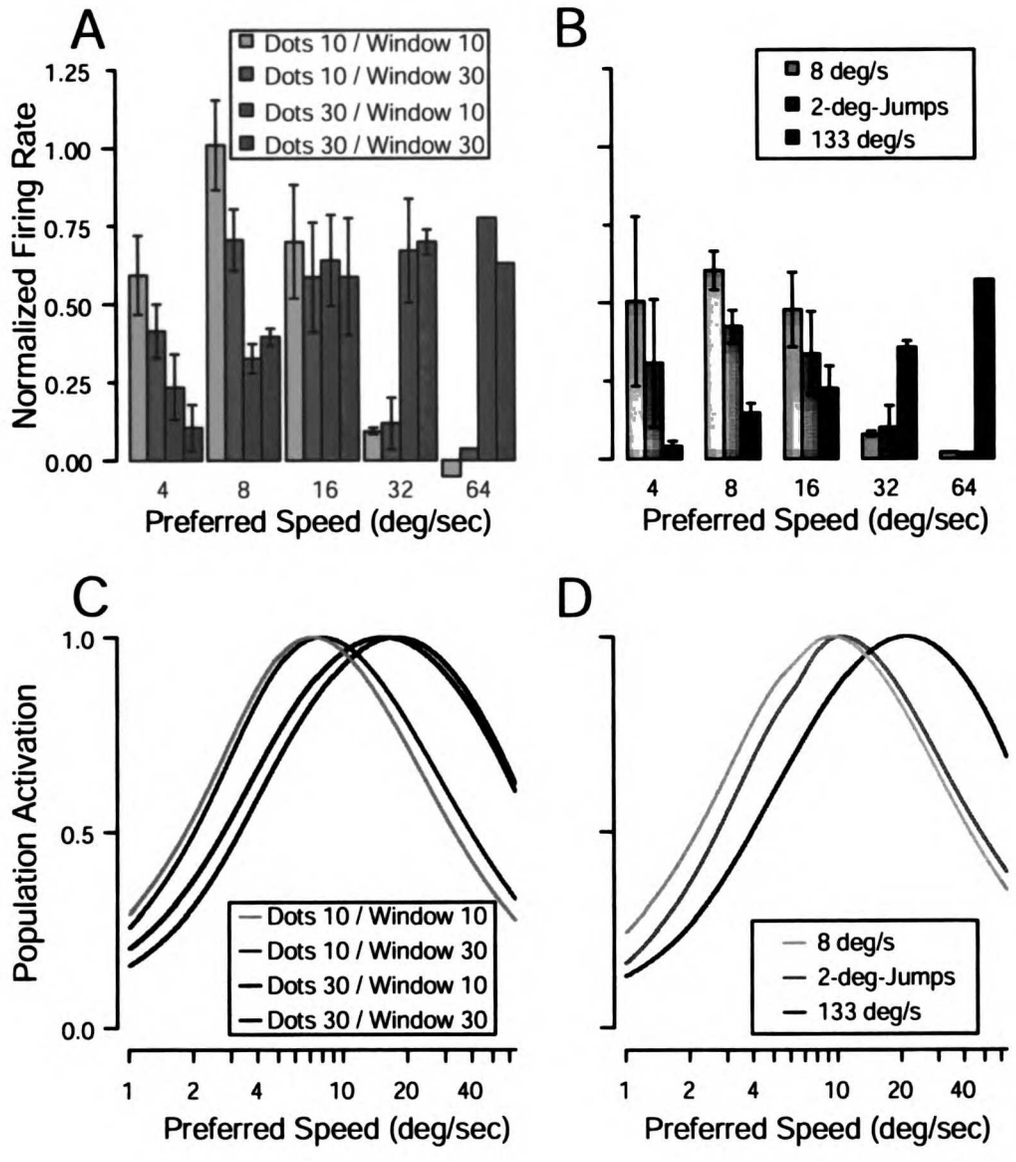
A
Dots 10 / Window 10
Dots 10 / Window 30
Dots 30 / Window 10
Dots 30 / Window 30
Normalized Firing Rate
1.25
1.00
0.75
0.50
0.25
0.00
4
8
16
32
64
Preferred Speed (deg/sec)
B
8 deg/s
2-deg-Jumps
133 deg/s
4
8
16
32
64
Preferred Speed (deg/sec)
C
Population Activation
1.0
0.5
0.0
Dots 10 / Window 10
Dots 10 / Window 30
Dots 30 / Window 10
Dots 30 / Window 30
1
2
4
10
20
40
Preferred Speed (deg/sec)
D
8 deg/s
2-deg-Jumps
133 deg/s
1
2
4
10
20
40
Preferred Speed (deg/sec)

Figure 7: Reconstructions of speed based upon the population of responses from cells in area MT. The left and right panels plot reconstructions for the patch and jumps experiment, respectively. Error bars indicate the standard error of the mean reconstructed speed.

Figure 7

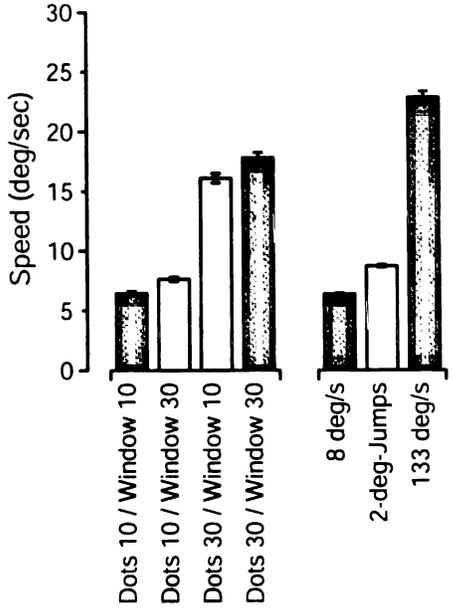
Speed (deg/sec)
30
25
20
15
10
5
0
Dots 10 / Window 10
Dots 10 / Window 30
Dots 30 / Window 10
Dots 30 / Window 30
8 deg/s
2-deg-Jumps
133 deg/s

Chapter 2

Apparent motion produces multiple deficits in visually-guided smooth pursuit eye movements of monkeys

Mark M. Churchland and Stephen G. Lisberger

(originally published in *J Neurophysiol* 85: 216-235, 2000)

Abstract

We used apparent motion targets to explore how degraded visual motion alters smooth pursuit eye movements. Apparent motion targets consisted of brief stationary flashes with a spatial separation (Δx), temporal separation (Δt), and apparent target velocity equal to $\Delta x/\Delta t$. Changes in pursuit initiation were readily observed when holding target velocity constant and increasing the flash separation. As flash separation increased, the first deficit observed was an increase in the latency to peak eye acceleration. Also seen was a paradoxical increase in initial eye acceleration. Further increases in the flash separation produced larger increases in latency, and resulted in decreased eye acceleration. By varying target velocity, we were able to discern that the visual inputs driving pursuit initiation show both temporal and spatial limits. For target velocities above 4-8°/s, deficits in the initiation of pursuit were seen when Δx exceeded 0.2-0.5°, even when Δt was small. For target velocities below 4-8°/s, deficits appeared when Δt exceeded 32-64 ms, even when Δx was small. Further experiments were designed to determine if the spatial limit varied as retinal and extra-retinal factors changed. Varying the initial retinal position of the target for motion at 18°/s revealed that the spatial limit increased as a function of retinal eccentricity. We then employed targets that increased velocity twice, once from fixation and again during pursuit. These experiments revealed that, as expected, the spatial limit is expressed in terms of the flash separation on the retina. The spatial limit is uninfluenced by either eye velocity or the absolute velocity of the target. These experiments also demonstrate that 'initiation' deficits can be observed during ongoing pursuit, and are thus not deficits in initiation *per se*. We conclude that such deficits result from degradation of the retino-centric motion signals that drive

pursuit eye acceleration. For large flash separations, we also observed deficits in the maintenance of pursuit: sustained eye velocity failed to match the constant apparent target velocity. Deficits in the maintenance of pursuit depended on both target velocity and Δt and did not result simply from a failure of degraded image motion signals to drive eye acceleration. We argue that such deficits result from a low gain in the eye velocity memory that normally supports the maintenance of pursuit. This low gain may appear because visual inputs are so degraded that the transition from fixation to tracking is incomplete.

Note added for thesis

The experiments Chapter 2 provide a thorough documentation of the effects of apparent motion on pursuit. Effects are divided into two classes: those attributed to changes in the visuo-motor drive of eye acceleration, and those attributed to changes in pursuit engagement and the resulting recruitment of eye-velocity memory. We propose that the effects attributed to visuo-motor drive are due to changes in the estimate of speed extracted from MT. In Chapter 3, it is these changes that we attempt to account for. The large proportion of Chapter 2 devoted to deficits in the engagement of pursuit is largely peripheral to the rest of this thesis, with the exception that we wish to explicitly exclude these deficits from the explanations of Chapter 3.

Introduction

Smooth pursuit eye movements are used by primates to track small moving targets. Step-ramp target trajectories, consisting of a step in target position concurrent with the onset of target motion, have become a standard approach for analyzing non-predictive features of pursuit (Rashbass 1961; Lisberger and Westbrook 1985). Shortly after the onset of target motion, the eye accelerates rapidly towards target velocity. Following this rapid acceleration, eye velocity settles near target velocity. Pursuit of step-ramp targets is thus often described as having 'initiation' and 'maintenance' phases.

While dividing the response into initiation and maintenance phases is descriptively useful, there is no evidence that the pursuit system makes an active transition from one phase to the other, or that its responsiveness differs between the two states. Instead, analysis of pursuit has revealed two functional mechanisms that do not map directly onto the two phases of pursuit initiation and maintenance. One mechanism, called "visuo-motor drive", relies on visual motion inputs represented in a population code in area MT, and transforms that code into commands for smooth eye acceleration (Newsome et al. 1985; Dursteler et al. 1987, Morris and Lisberger 1987; Groh et al. 1997). The other mechanism, called "eye velocity memory", converts commands for eye acceleration into signals for desired smooth eye velocity and ensures that eye velocity will decay only slowly from its current value in the absence of image motion (Young et al. 1968; Robinson 1971; Robinson 1986; Morris and Lisberger 1987). Acting as an acceleration to velocity integrator, eye velocity memory is conceptually similar to, but functionally distinct from, the well known 'neural integrator' that converts commands for eye velocity into commands for eye position (Robinson, 1989). Visuo-motor drive and

eye velocity memory are both active during both the initiation and maintenance of pursuit. However, for step ramp targets, changes in pursuit initiation can typically be attributed to changes in visuo-motor drive, assuming that the status of eye velocity memory remains constant. Likewise, the analysis of maintenance can be used to evaluate the status of eye velocity memory, assuming that visuo-motor drive is sufficient to drive the eye to the constant target velocity.

Recent reports from our laboratory have emphasized a third mechanism that we have previously called a "pursuit switch" or "on-line gain control" and that we will refer to here as the "engagement" of pursuit. The existence of different levels of engagement of pursuit was previously demonstrated using brief perturbations of target motion to probe the gain of visuo-motor drive (Goldreich et al. 1992; Schwartz and Lisberger 1994). The gain of the evoked pursuit response depended on whether the monkey was fixating or tracking when the probe was presented, and on the ongoing eye/target velocity during pursuit maintenance. These experiments demonstrate that the pursuit system is engaged to differing degrees during fixation and ongoing pursuit. A deficit in engagement of pursuit was also proposed as an explanation for a number of deficits in sustained eye velocity during the maintenance of pursuit (Kiorpes et al. 1996; Grasse and Lisberger 1992). We have thus assumed that both visuo-motor drive and eye-velocity memory are modulated by the state of engagement of the pursuit system. That the engagement of pursuit influences eye velocity memory was first suggested by Robinson (Robinson, 1986; Luebke and Robinson, 1988), and is assumed by the pursuit model of Krauzlis and Lisberger (1994). Visual motion thus serves a dual role in pursuit. It is the

primary input for the visuo-motor drive of eye acceleration during pursuit, but is also necessary to engage pursuit in the first place.

One approach to understanding the perception and neural processing of visual motion has been to degrade the quality of motion using 'apparent motion' stimuli, consisting of flashes of a target at a sequence of positions. Studies of human perception using different types of targets have revealed very different spatial limits for 'short-range' and 'long-range' perception of motion (Tyler 1973; Braddick 1980; Newsome et al. 1986; Barlow and Levick 1965). Parallel analysis of human motion perception and neuronal responses in awake monkeys have revealed a broad similarity in the spatial limit of motion perception and the spatial limit of direction selectivity for MT neurons (Mikami et al. 1986; Newsome et al. 1986). Previous studies of pursuit eye movements using apparent motion along periodic trajectories have revealed tracking deficits when the flash separation was increased past 80-150 ms (Morgan and Turnbull 1978; Van der Steen et al. 1983; Schor et al. 1984; Fetter and Buettner 1990). However, the continuous nature of the target trajectories used in these prior studies makes it difficult to determine if the deficits arose because the degraded motion failed to support normal visuo-motor drive of eye acceleration, or because the degraded motion was insufficiently convincing to fully engage pursuit.

We now report the pursuit evoked by step-ramp target trajectories consisting of apparent motion with a range of spatial and temporal separations of the flashes. Our data reveal separable effects of apparent motion on both visuo-motor drive and eye velocity memory. Effects on visuo-motor drive were manifested as changes in the latency and magnitude of eye acceleration at the initiation of pursuit, including a paradoxical

facilitation of eye acceleration over a narrow range of parameters. Effects on eye-velocity memory were manifested as sustained maintenance phase eye velocities much lower than target velocity. We interpret eye-velocity memory deficits as resulting from a failure of the visual stimulus to provide a sufficiently convincing motion signal to fully engage pursuit. Our data indicate that the engagement and subsequent visuo-motor guidance of pursuit eye movements both depend upon the quality of the visual motion. We suggest that the motion signals governing engagement may not be the same as those driving eye acceleration. While deficits in visuo-motor drive were independent of extra-retinal factors such as eye and target velocity, deficits in eye velocity memory were not.

Materials and Methods

Parameterizing apparent motion stimuli

The solid line in Figure 1A illustrates the spatio-temporal trajectory of a horizontally moving point. As time passes, the point moves rightwards. The filled circles along this line illustrate the trajectory of an apparently moving spot, with spatial and temporal separations Δx and Δt respectively. The apparent velocity is given by $\Delta x/\Delta t$. Smooth and apparent motion may also be represented in the frequency domain. The transform of a single spot contains a broad range of spatial frequencies. For a smoothly moving spot, each spatial frequency is associated with a different temporal frequency, where velocity = temporal frequency /spatial frequency (Watson and Ahumada, 1984; Adelsen and Bergen, 1984). The solid diagonal line in Figure 1B illustrates this relationship. Apparent motion is equivalent to sampling a smoothly moving stimulus, and produces aliasing. In the frequency domain aliasing produces 'replicas' of the original spatio-temporal frequency content, as shown by the dashed lines in figure in Figure 1B.

The range over which apparent motion effectively emulates real motion can be described in the space-time domain in terms of the effective combinations of Δx and Δt. The same range can also be described in the frequency domain by outlining the 'window of visibility': the range of temporal and spatial frequencies to which the system of interest is sensitive. Apparent motion becomes noticeably un-smooth when the replicas produced by aliasing enter this window of visibility. We choose to describe our stimuli and the effective range of apparent motion in the space-time domain for two reasons. First, the spots we used are simply and intuitively described in the space-time domain. Secondly,

because our stimuli were actually spots, not sine wave gratings, linearity becomes an issue when one attempts to describe the response of either pursuit or of neural motion sensors in terms of the responses to individual frequency components. As an example, some of the components of an apparently rightwards moving spot are in fact moving leftwards (those aliasing components in the lower right hand quadrant of Figure 1B). A leftwards tuned motion sensor would, if linear, respond to these components just as surely as if the stimulus had actually been a leftwards moving grating. If non-linear, the sensor might or might not be expected to respond. Unpublished experiments from this laboratory indicate that the responses of many MT cells fail to respond in the way expected given the assumptions of linearity. We therefore choose to describe the limits of apparent motion in terms of maximum Δx and Δt, and not in terms of the border of the window of visibility. This is not to deny that the latter description could be constructed, provided that the relevant non-linearities were understood and accounted for. Such a description is, however, outside the scope of this paper, the goal of which is to parameterize the limits of apparent motion for pursuit in a simple descriptive manner that might then be compared with a similar description of the effects of apparent motion on the response of the population of MT neurons.

Surgical procedures

Experiments were performed on 6 adult male rhesus monkeys that had been trained to pursue single moving targets. Our basic experimental methods have been presented before (e.g. Lisberger and Westbrook 1985). Briefly, monkeys were trained to track visual targets, and were rewarded with drops of water or Tang. Eye movements were monitored using scleral search coils that had been implanted with the technique of

Judge et al. (1980), using sterile procedure while the monkey was anesthetized with Isofluorane. Post-surgical analgesia was provided for a minimum of 2 days with Buprenex (0.01 mg/kg every 12 hours). During experiments, monkeys sat in a primate chair with their heads affixed to the ceiling of the chair using a dental acrylic fixture that had been implanted at the same time as the eye coil. Experiments lasted two to three hours. Methods had been approved in advance by the Institutional Animal Care and Use Committee at UCSF.

Visual stimuli and presentation of targets

Stimuli were presented on a 12-inch diagonal analog oscilloscope (Hewlett Packard model 1304, P4 phosphor) driven by the digital-to-analog converter outputs from a digital-signal-processing board in a pentium PC computer. This system provided us with a spatial resolution of 65,536 by 65,536 pixels and a maximum temporal resolution of 4 ms (2 ms in a few later experiments). We positioned the display 30 cm from the monkey so that it subtended a vertical visual angle of 40° and a horizontal visual angle of 50°.

Stimuli were sequences of flashes with a wide range of temporal flash separations (Δt) and spatial flash separations (Δx), which were systematically varied. When Δt and Δx were small, the series of flashes produced the perception of a smoothly-moving target (Newsome et al. 1986). Thus, we will refer to the series of flashes as a target, with a given Δt, Δx, and apparent velocity. As the apparent velocity of a target is given by $\Delta x/\Delta t$, the stimulus is fully defined by any 2 of these 3 parameters. To maintain a constant mean luminance of the target, the luminance of each flash was varied linearly with the time between flashes (e.g. if Δt was doubled, so was the luminance of each

flash). We adopted this approach instead of the alternative (keeping individual flash luminance constant) because it rendered pursuit targets that appeared to have similar brightness regardless of Δt, and because we anticipated it would avoid changes in pursuit latency that would be a function of luminance rather than of the parameters of the apparent motion itself.

Each individual target flash was very brief. The duration increased with Δt, due to the extra time necessary to increase the luminance. For a Δt of 4 ms each flash lasted approximately 160μs. Each doubling of Δt doubled this duration, so that for a Δt of 64 ms each flash lasted approximately 2560 μs. The specifications of the display oscilloscope indicated that the phosphor will decay to 10% of its maximal level in 10μs to 1ms. The tracking target was brighter than the fixation point (see below for description of these targets). Photometer measurements revealed that the fixation target and tracking target had net luminances of approximately 1.6 and 25 cd/m^2, respectively. Because targets were small, roughly 0.2^o across, these luminances were bright but not dazzling. Experiments were performed in a dimly lit room. Due to the dark screen of the display, background luminance was beneath the threshold of the photometer, less than one mcd/m^2. Subsequent to an earlier review of this paper, an error was found in the program controlling the visual stimuli. The timing of the second flash in the sequence was often erroneous: the first two flashes would occur immediately following one another, with the specified Δt occurring only between subsequent flashes. This error was not visible to the naked eye, but could certainly have influenced some of our measurements of the effect of apparent motion on the initiation of pursuit, perhaps reducing the size of the observed deficits. All experiments were replicated following

correction of the error, using monkeys Na, Ka, and Mo. As all the same effects were observed, we have retained the original data and added the new data to our presentation.

Targets were presented in individual trials that began with the appearance of a fixation point 10° to either the right or left of straight-ahead gaze. The fixation point always had a Δt of 4 ms. The monkey was required to fixate this spot within 600 ms after its appearance and to maintain fixation within a 2° window of target position for 700 to 1100 ms. The fixation point was then extinguished and replaced 4 ms later with a tracking target that appeared eccentric relative to the fixation point and immediately began to move toward the position of fixation (Rashbass 1961). For example, a given trial might begin with the appearance of a fixation point to the left of center. When the fixation point disappeared, the target would appear to its left and move rightward. Because of the initial 10° offset of the fixation point, targets were able to traverse up to 35° before reaching the edge of the monitor. The duration of target motion varied from 700 to 2400 ms depending on the speed of the target. Quickly moving targets were extinguished when they neared the edge of the screen. In some later experiments, and for velocities faster than 16°/s, the target was not extinguished at the end of its trajectory. Instead, it stepped forward 2 to 4° and remained stationary for 600 to 1000 ms before being extinguished. This helped to minimize the decrease in sustained eye velocity that often occurred near the end of a trial.

Most experiments also included 'control trials', in which the tracking target appeared eccentric to the fixation spot and moved *away* from the fixation point towards the edge of the monitor that was closest to the fixation point. For all but the slowest velocities, the target neared the edge of the monitor quickly, at which point it stopped and

fixation was enforced for up to 1000 ms. These trials were not analyzed, but were intended to prevent the monkey from predicting the direction of target motion. In some later experiments, control trials were omitted. This had no discernable effect on pursuit within that experimental session, and no anticipatory eye acceleration was observed before the normal onset of pursuit.

Following the onset of target motion, the monkey was given 450 ms to bring his eyes from the initial point of fixation to the target, and was required to track the target with an accuracy of 3°. If the monkey maintained the required fixation and tracking throughout the trial, he was rewarded with a drop of juice. If fixation requirements were not met during a trial, the trial was immediately aborted. For some trials, particularly those with large values of Δx, the size of the fixation window was increased to as large as 9°, to allow the monkey to complete most trials successfully. Each experiment consisted of multiple repeats of a list of up to 132 types of trials, where each trial type presented a different stimulus. The trials were sequenced by shuffling the list and requiring the monkey to complete each trial successfully once. If he failed a trial, it was placed at the end of the list and presented again after all the other trials had been completed. After all trials had been completed once, the list was shuffled and presented again. Monkeys were allowed to work as long as they continued to complete most trials successfully, usually for 2000 to 4000 trials.

The wide range of possible parameters of apparent motion made it impossible to evaluate all parameters within a single experimental session. Instead, we varied different parameters on different days, in experiments designed to be complete along selected axes of the possible parameter space. Because each experiment type required slightly different

methods for design and data analysis, we outline separately the five basic classes of experiment reported here.

1) Experiments using a single target velocity and varying flash separation. All trials had the same target velocity of 18°/s, and up to 8 different values of Δt were used. In one later experiment we repeated this experimental design using a target velocity of 3°/s. The goal of this design was to collect large numbers of responses for each flash separation to allow the quantitative analysis of pursuit initiation shown in Figure 5. In some early experiments additional 'catch' trials were run at different velocities, but were not analyzed. Catch trials appear to have no influence upon the effects we observed and were not included in all experiments. The initial step of target position relative to the fixation point was set so as to increase the latency of the first saccade (Rashbass 1961). On each experimental day, prior to collection of data, step size was optimized so that saccades were rare during the first 400 ms of pursuit. Depending on the monkey, a step between 2 and 3° was ideal for target speeds of 18°/s. The absence of saccades during the rising phase of pursuit was crucial for the analysis of initial eye acceleration, described below. A drawback of this design is that for a constant apparent velocity, Δt and Δx vary together. It is thus not possible to determine if changes in pursuit initiation result from an excessive spatial separation or an excessive temporal separation.

2) Experiments using a single target velocity in which both target eccentricity and flash separation varied. These experiments were similar to those in (1)

above, except we varied the size of the initial step of target position, and observed the interaction of retinal eccentricity with the effects of flash separation. Within each experiment, the size of the step was randomly varied among 0.5, 3 and 7°. For steps of 0.5 and 7°, saccades were common during the first 400 ms of pursuit. When deficits were absent or small, the majority of responses nonetheless exhibited considerable pre-saccadic pursuit, with the first saccade occurring near the end of the rising phase of eye acceleration.

3) Experiments varying both target velocity and flash separation. Both apparent target velocity and Δt (and thus Δx also) were varied systematically. The goal of these experiments was to describe the combinations of Δx and Δt that produced normal initiation of pursuit, and if possible, to isolate independent temporal and spatial limits. The temporal limit would be defined as the maximum Δt for which normal pursuit is evoked, regardless of how small Δx is, and the spatial limit as the maximum Δx, regardless of Δt. As in (1) above, we attempted to optimize the initial step of target position so as to largely eliminate saccades during the rising phase of initiation. Unfortunately, the optimal step size depended strongly upon target velocity. It was thus not possible to eliminate early saccades at all velocities without introducing confounding effects from varying the step size. In early experiments (those using monkeys Da and Fi), we used the same starting eccentricity for all target velocities; the tracking target always appeared 3° to one side of the fixation spot. Because targets moving at faster speeds became less eccentric more quickly, the mean eccentricity in the first 100 ms of target motion was

different for different target velocities, as was the chance of early saccades. For all later experiments, we set the size of each target step so that mean image eccentricity during the first 100 ms of target motion was 1° on the same side of the fixation spot as the initial position of the moving target. Thus, more swiftly moving targets started further eccentric. Both methods of determining starting position provided similar results. The latter method used initial positions that reduced the occurrence of early saccades to some degree, though not nearly as much as if eccentricity had been optimized explicitly to do so. Although these experiments were designed to study pursuit initiation, deficits in pursuit maintenance were also sometimes observed and we took advantage of these data to examine how the maintenance deficits seen at a given Δt change with target velocity.

4) Experiments presenting two steps of target velocity. These experiments were designed to compare pursuit responses to a given apparent image motion presented either during fixation or during ongoing pursuit. These experiments included a) control trials in which we recorded the initiation of pursuit for apparent target motion that started at the position of fixation (with no position step) and b) experimental trials in which apparent target velocity changed after pursuit initiation. For the experimental trials, the initial target motion had a Δt of 4 ms so that stable sustained eye velocity was achieved within 400 ms after the onset of target motion. At 480 ms after the onset of target motion, the velocity of apparent target motion increased abruptly without any step of target position and, for most trials, Δt was also changed. Control trials

used the same range of Δt as did experimental trials. Thus, the single target velocity step of control trials and the second target velocity step of experimental trials produce nearly identical retinal image motions. In both, the target velocity step occurred at a time when the target image had been nearly stationary on the retina with a Δt of 4ms. In both the step produced a moving retinal image with a given apparent velocity, Δt, and Δx. Due to the lack of target position step, saccades before the end of the rising phase of pursuit were common for these experiments, although considerable pre-saccadic pursuit was nonetheless seen. A modification of this experiment was used to study sustained eye velocity during pursuit maintenance. For this modification only, a step of apparent target velocity at a given Δt was followed 480 ms later by a second step of the same size, with Δt held constant after the first step.

5) Experiments in which Δt was increased during the maintenance of pursuit. The goal of these experiments was to study the effect of Δt upon pursuit maintenance after eye velocity had reached target velocity. Pursuit was evoked with steps of apparent target velocity. In experimental trials, Δt was initially 4 ms but increased to a larger value after stable tracking had been achieved. In control trials, Δt was set to the same value when the target first began to move.

Data acquisition

Experiments were controlled and data were acquired by computer programs running on a UNIX workstation and a Pentium PC. The workstation provided a graphical

user interface for the design and control of the experiment, and the PC acted as a data-server and streamed the data over the local area network for storage on the UNIX file system. We obtained voltages proportional to eye velocity by analog differentiation of the eye position outputs from the search coil electronics (DC-25 Hz, -20 dB/decade) and we sampled voltages proportional to horizontal and vertical eye position and eye velocity at rates of 1000 samples/s per channel. In each file, we also recorded a series of codes to indicate the target motions we commanded, and we used these codes in the data analysis program to reconstruct horizontal and vertical target position and velocity.

Data analysis for the initiation of pursuit

Pursuit initiation was analyzed for experiment types (1) through (4) above. Eye velocity and position traces were initially viewed on a computer monitor and screened according to criteria that depended on the exact analysis to be done. The changes in pursuit initiation produced by apparent motion are illustrated using averages of the eye velocity response, often with eye velocity traces from individual trials superimposed. Our methods of averaging are described in more detail in a later section. Further quantification of the changes in pursuit initiation depended upon the type of experiment and the prevalence of early saccades. For experiments of type (1), the great majority of saccades were delayed until after the initiation of pursuit was over. This afforded the opportunity to observe the effects of apparent motion upon both peak initial eye acceleration and the latency of initial eye acceleration. For this analysis only, we smoothed the individual eye velocity traces by convolving them with a Gaussian having a standard deviation of 20 ms. For each trial we then differentiated, measured the peak eye acceleration, and estimated a value that we call "acceleration latency": the time when eye

acceleration reached 63% of its peak value. For the vigorous eye accelerations evoked by fast target velocities, measurements made using the 63% criterion were typically slightly more robust than similar measurement using the time to peak eye acceleration. In practice, we were interested in changes in latency, and these differed only slightly whether calculated using the peak of eye acceleration, or using the 63% point. In one experiment, when target velocity was 3°/s, we did in fact use the time to peak eye acceleration to calculate latency, as this measure was more robust in the presence of a low signal to noise ratio. We chose not to use the time of the actual onset of pursuit (when initial eye acceleration first began) as a dependent variable. Estimates of the actual onset of pursuit can be made reliably by human observers for target motions that evoke sufficiently crisp initiation of pursuit that eye velocity quickly exceeds measurement noise. However, human observers cannot make such reliable estimates for low target velocities or for parameters of apparent motion that evoke lower initial pursuit eye accelerations. Numerical algorithms suffer related drawbacks. Moreover, as we shall see, a consistent effect of apparent motion was to increase the latency to normal acceleration. Effects upon absolute latency were less consistent.

For all other experiments concerning the initiation of pursuit (2-4 above) saccades during the rising phase of pursuit were common. It was therefore impossible to make the acceleration based measurements, as peak acceleration was potentially obscured by a saccade. However, at least when Δt was small, and deficits absent to moderate, most early saccades occurred near the end of the rising phase of pursuit, at least 50-100 ms after initiation. We therefore chose to assess initiation by measuring eye velocity at a fixed time, after normal pursuit onset but before saccades occurred. We defined the

"normal" time of pursuit onset using the average eye velocity when Δt was 4 ms. For all trial types we then measured eye velocity at a fixed time following the normal onset. This method is illustrated in Figure 6. The measurement time was selected to fall during the rising phase of pursuit, as close as possible to the end of the open loop interval, and before the time of most saccades. The exact time ranged from 50-70 ms and depended upon the duration of the open loop interval of the monkey being studied. Minor errors in estimating either the duration of the open loop interval or the time of the onset of pursuit would not have had a major impact on this analysis, as the same measurement time was used for all values of Δt at a given apparent target velocity.

We discussed above three scalar measures of pursuit initiation: peak acceleration, acceleration latency and eye velocity at a fixed time. When a given measure was made, it was made for each individual trial of a given type. Averages and standard errors were then calculated. For experiments of type (3) above, responses to target velocities below approximately 4°/s suffered from a signal to noise problem. Large numbers of trials (at least 20-50) were needed to make accurate measurements of eye velocity at a fixed time. As these experiments employed a range of velocities and many trial types, it was often not possible to collect more than 20 trials of each type (some of which would have to be excluded because of early saccades, as described below). Measurements at low velocities were therefore sometimes quite variable, preventing us from analyzing pursuit for target speeds slower than 2°/s.

In examining the initiation of pursuit, we were primarily interested in changes in the pursuit trajectory, rather than in the absolute values of latency, eye velocity, or eye acceleration. Thus, the three measures described above are expressed in normalized

form. Peak acceleration is expressed as the proportion of the average peak acceleration seen for the same target velocity when Δt was 4 ms. The eye velocity measure is normalized by the average eye velocity at the same fixed time when Δt was 4 ms. Acceleration latency is expressed as the time shift relative to the average acceleration latency measured when Δt was 4 ms. An assumption of much of our analysis is that a Δt of 4 ms produces normal pursuit, and that the pursuit response to such targets would not have changed had we been able to decrease the temporal separation further. This appears likely for two reasons. First, with the exception of the highest apparent target velocities (32 to 45°/s), pursuit performance was not altered by doubling the temporal separation to 8 ms. For the highest target velocity of 45°/s, a Δt of 4 ms is probably only just acceptable, as doubling Δt to 8 ms does produce a small deficit. Second, in some later experiments, we were able to test performance at a Δt of 2 ms, revealing that it was identical to performance when Δt was 4 ms, even for target motion at 45°/s.

For all analyses, the onset of target motion was defined to be coincident with the first flash of the tracking target. However, no directional information is available until after the second flash. It might therefore appear that the onset of target motion should be defined as the time of the second flash, and that effects of varying Δt should be assessed after aligning the responses at this time. However, a simple example illustrates how aligning the data on the second flash would introduce artifacts. At many target velocities, pursuit initiation was identical when Δt was 4 ms and 16 ms. If we had aligned these responses on the second flash by shifting the response 12 ms left when Δt was 16 ms, then we would have found that pursuit initiation was earlier when Δt was 16 ms than when Δt was 4 ms. We thus opted not to shift the timing of the responses, even though it

is to be expected that initiation deficits at large values of Δt will be due at least partially to the delay in motion information until after the second flash.

Exclusion of trials with early saccades for analysis of the initiation of pursuit

In all analyses of pursuit initiation, some trials inevitably contained saccades that made the chosen measurement impossible. The analysis of acceleration described above was employed when saccades were rarely observed during the rising phase. However, the occasional saccade still fell within the rising phase. Similarly, the analysis of eye velocity at a fixed time was occasionally confounded by a saccade at or before that time. In such cases the trial was typically excluded from analysis. A sole exception was made in the analysis of acceleration. Some longer values of Δt produced initiation so delayed and slow that there were often saccades during the rising phase. Such trials were included (after interpolation of saccades, see below) so long as saccades were delayed by at least 400 ms following target motion onset. To the degree that linear interpolation of saccades is imperfect, measurements of the precise size of large initiation deficits will be imperfect.

Trials with saccades before or during the measurement interval were excluded not only because saccades obscure pursuit eye velocity, but also because saccades are known to enhance subsequent pursuit (Lisberger 1998). If we had included measures made after the first saccade in our analyses of the initiation of pursuit, then post-saccadic enhancement of pursuit might have created effects that resulted indirectly from the relationship between different targets and the latency of the first saccade. However, exclusion of trials with early saccades raises the concern that early saccades occurred primarily when pursuit was deficient, and that the exclusion of trials with early saccades

might therefore reduce the visibility of deficits. We spot-checked a handful of cases in which early saccades were common, comparing pre-saccadic pursuit when saccades were early in initiation to that when saccades were late. The magnitude of pre-saccadic eye acceleration was uninfluenced by the timing of subsequent saccades, and no consistent or statistically significant effects were seen.

In instances when the majority of responses contained early saccades, we did not attempt to analyze the data. For experiments using a range of apparent target velocities and values of Δt, the leftward pursuit of two monkeys (Fi and Ka) had to be discarded because early saccades were very common at slower apparent velocities. For experiments that varied the eccentricity of the moving targets, Monkeys El and Da were unable to provide sufficient usable responses. Some monkeys had very few early saccades (Mo and Na in both directions, and Ka in the rightwards direction), and were particularly useful in experiments in which eccentricity could not be optimized. We realize that the prevalence and latency of early saccades in response to step-ramp targets varies among publications from different laboratories and we attribute the delayed saccades and excellent pre-saccadic pursuit in many of our monkeys to the extensive experience they have with targets that could be tracked successfully with very few saccades.

Data analysis for the maintenance of pursuit

For analysis of the maintenance of pursuit, saccades were excised from each individual eye velocity trace, either by a user-supervised and verified semi-automatic algorithm or by using a cursor to point out the start and end of each rapid deflection of eye velocity. Each rapid deflection was replaced with a line segment that connected the

eye velocities before and after the excision. Eye velocity traces then were aligned on the onset of target motion, averaged, and filtered with a 25 Hz digital filter. This cutoff frequency reduced noise with no noticeable effects on the basic trajectory of either the initiation or maintenance of pursuit. For the maintenance of pursuit, our main documentation of the effects of changing the parameters of apparent motion consists of averages of eye velocity as a function of time. However, we will also show that average eye velocity traces are representative of single trial performance during both the initiation and maintenance of pursuit.

The analysis of pursuit maintenance necessarily includes epochs of pursuit that contain saccades. Nearly every pursuit response contained at least one saccade during maintenance. Experimental manipulations that impair pursuit maintenance further increase the prevalence of saccades, both in prior studies (Dursteler et al. 1987, Dursteler and Wurtz 1988) and in our data. It was thus necessary to analyze pursuit in a way that preserved as best as possible the eye velocity component produced by the pursuit system, but ignored the eye velocity component produced by the saccadic system. Inspection of our data showed relatively little change in smooth eye velocity before and after saccades during the maintenance of pursuit, implying that linear interpolation across the excised saccadic eye velocity is valid during the maintenance of pursuit. Saccades sometimes facilitated eye velocity during maintenance, but this effect was small. Another workable method is to excise each saccade, but to treat the missing time points as missing data during averaging. This approach essentially replaces each saccade with averaged data from other trials that do not have a saccade at that time. This approach only appears to avoid the necessity of interpolation. The replacement data may or may not be a good

estimate of the saccade-obscured pursuit *for that particular trial.* Averages of excised data are particularly unlikely to provide a good estimate of the excised pursuit if maintained pursuit eye velocity varies from trial to trial, as was often the case when maintenance was impaired. In fact, both methods in practice provide very similar results during maintenance. Still, the method of saccade replacement by linear interpolation seemed better suited to our purposes. It should be noted that the maintenance deficits we observe below are large, and could be neither produced nor obscured by any reasonable method of dealing with saccades.

Results

Figure 2 shows a typical pursuit response for a target that moved with an apparent velocity of 22°/s and a Δt of 16 ms. Although the stimulus consisted of sequential flashes of a stationary target at the times indicated by dots, both the eye position and velocity profiles appear normal (e.g. Lisberger and Westbrook 1985). Pursuit began about 100 ms after the onset of target motion: the eye accelerated rapidly towards target velocity, and maintained eye velocity settled near target velocity with only small fluctuations. The first saccade (arrows on the eye position and velocity traces) occurred more than 200 ms after the initiation of pursuit, after the end of the initial rising phase.

Pursuit initiation shows changes with increasing flash separation

In the first part of the paper, we analyze deficits in the pre-saccadic initiation of pursuit. In so doing, we explicitly avoid showing examples of deficits in the maintenance of pursuit, which are analyzed in the second part of the paper. Apparent motion had effects of three types on pursuit initiation: 1) increases in the latency to peak eye acceleration, 2) decreases in peak eye acceleration, and 3) unexpected increases in peak eye acceleration. The left column of Figure 3 illustrates an effect of the first type. Figure 3A shows ten single trial responses (thin traces) of monkey Ka to target motion with an apparent velocity of 16°/s and Δt of 4 ms. These traces are superimposed upon the average response for all trials of this type (bold trace). Figure 3B shows a similar plot for target motion at the same apparent velocity but with a (longer) Δt of 32 ms. The average responses in Figure 3A and B are similar in that both exhibit crisp initial eye acceleration, a small overshoot of target velocity, and a steady state gain of near unity. Comparison of the averaged and individual traces shows that the individual traces are well represented

by the averages. Superposition of the two averages of eye velocity (Figure 3C) reveals that peak initial eye acceleration was delayed when Δt was 32 ms, although the magnitude of peak eye acceleration appears similar. Note that the latency to the onset of pursuit appears little affected: it is the latency to normal eye acceleration that increased. Subsequent figures show examples where the onset of pursuit was also delayed. Effects of apparent motion on the latency of the onset of pursuit were generally less consistent than the effects on the latency to peak eye acceleration. We term this latter measure 'acceleration latency'.

In addition to producing increases in the acceleration latency, increases in Δt often produced decreases in peak eye acceleration. For example, Figure 3D shows responses of monkey Ka to target motion at an apparent velocity of 32°/s and Δt of 4 ms. Figure 3E shows a similar plot for data obtained when Δt was increased to 48 ms. Superposition of the average eye velocity traces for different values of Δt reveals a clear progression of deficits (Figure 3F). Increasing Δt from 4 to 24 ms caused an increase in acceleration latency accompanied by a small decrement in initial eye acceleration. A further increase of Δt to 48 ms (dashed trace) caused a larger increase in acceleration latency and a clear decrement in initial eye acceleration. For all 3 values of Δt, eye velocity eventually reached a sustained value that was close to target velocity. Note in Figure 3D and E that the averages made after linear interpolation across excised saccades provide a reasonable estimate of pursuit eye velocity during the period obscured by the saccades. Of course, there is no way of directly observing the underlying pursuit eye velocity during this period. Therefore, all subsequent quantitative analysis of pursuit initiation is limited to time periods that were saccade free.

Analysis over a finer grain of values for Δt revealed that as Δt was increased, initial eye acceleration at first *increased* and began to decrease only for still larger values of Δt. These effects are illustrated in Figure 4 using averages of eye velocity and acceleration. For the experiment summarized in Figure 4A, increases in Δt from 4 ms (bold traces) to 32 ms (fine traces) caused an increase both in acceleration latency and in peak eye acceleration. Further increases in Δt to 48 ms (dashed traces) caused the expected decrease in peak eye acceleration. For the experiment summarized in Figure 4B, peak eye acceleration increased as Δt was increased from 4 to 16 ms. Peak eye acceleration remained above normal at a Δt of 20 ms, and was reduced when Δt was 32 ms. The latency to peak acceleration increased when Δt was 20 ms or larger.

The increases in peak eye acceleration were not due to any effects of saccades, as all the above described data were collected under conditions that produced few saccades during the initiation of pursuit, and rare trials with saccades before the peak of acceleration were excluded from the analysis. Neither do the increases in peak eye acceleration result from any compensation for the longer latency of pursuit. This explanation assumes the pursuit system knows it is 'behind', and compensates to 'catch up'. This is unlikely, as the increase in acceleration was regularly observed within the open loop interval (60-80 ms), before visual feedback could have any impact. Further, the increase in acceleration cannot result from compensation for increased latency, as it occurred even when pursuit initiation was not delayed (e.g. Figure 4B, Figure 5, monkey Mo and Na). We therefore postulate that the increase in initial eye acceleration results because the relevant flash separations produce a larger than normal image velocity signal. This explanation is developed further in the discussion.

As Δt increased, changes in acceleration latency and peak eye acceleration followed different trajectories. We measured peak eye acceleration and the acceleration latency for each individual trial, as described in methods. The graphs in Figure 5 compare the progression of changes in these two measures as a function of Δt. Target velocity is held constant within each graph. Data are shown for four monkeys. Average peak eye acceleration (filled circles) is plotted as a fraction of that obtained when Δt was 4 ms. Average acceleration latency (open diamonds) is plotted as the time shift from when Δt was 4 ms. Sign conventions were chosen so that the horizontal dashed line shows normal performance and deficits are plotted as decreases on either y-axis. In the three examples in the left column, latency began to increase when Δt exceeded 16 ms and increased progressively as a function of Δt. Peak eye acceleration first increased, starting with values of Δt as low as 12 ms, and then declined below normal only for relatively large values of Δt. Statistically significant latency increases, peak acceleration increases, and peak acceleration decreases were observed in the experiments using Mo, Na, and Ka. The responses of monkey El are discussed below.

The three experiments shown in the left-hand column of Figure 5 were designed to reveal the typically small increase in eye acceleration that occurs over a narrow range of flash separations. These experiments also illustrate a more general finding. As Δt was increased, deficits in acceleration latency were produced prior to the production of deficits in the magnitude of eye acceleration (though not necessarily before the production of *increases* in eye acceleration). For the plots in the left column, the open symbols denoting acceleration latency are always below the filled symbols denoting peak acceleration. This pattern was consistently observed for all experiments and all monkeys,

with a single exception, illustrated in the lower right-hand panel. For rightward moving targets, monkey El showed the inverse pattern: as Δt increased, eye acceleration was significantly reduced at values of Δt that did not cause any increase in acceleration latency. We do not know why the changes observed in the rightwards pursuit of monkey El are so atypical. However, the rightward pursuit of monkey El was unusual in a number of other respects, and had an onset latency of 130 ms, nearly twice that of most monkeys and of monkey El's own leftward pursuit. The leftwards pursuit of monkey El shows the more typical pattern: deficits are observed in acceleration latency before any deficits are observed in peak eye acceleration. For the leftwards pursuit of monkey El, the lack of statistically significant increases or decreases in eye acceleration were probably due to an insufficient number of trials and to the limited range of values of Δt employed, as both effects were observed in other experiments using the same monkey (data not shown).

Spatial and temporal limits on the initiation of pursuit

The above described results reveal that apparent motion causes consistent deficits in pursuit, but do not reveal the cause of the deficits. At a given target velocity, Δt and Δx increase together. To ask whether the spatial or temporal separation between flashes is the limiting factor, we observed the effect of a given Δt at multiple target velocities. The same Δt is associated with large values of Δx at high velocities and small values of Δx at low velocities. Figure 6 shows the time course of average eye velocity during the initiation of pursuit at three apparent target velocities and three values of Δt. For a target speed of 32°/s (Figure 6A), deficits in the initiation of pursuit were present at values of Δt as low as 16 ms and became severe when Δt was increased to 32 ms. As target speed was

lowered, the deficit associated with each value of Δt was reduced. For a target speed of 16°/s (Figure 6B), a deficit was visible only when Δt was 32 ms (dashed trace). For a target speed of 8°/s (Figure 6C), the deficit was mild even when Δt was 32 ms. That the deficits associated with a given Δt are diminished as target velocity decreases indicates that they are related to the decreasing spatial separation.

These effects are quantified in Figure 7, which shows the effect of target speed on the magnitude of deficits in the initiation of pursuit for two values of Δt in 3 monkeys. In these experiments, it was not possible to optimize all trial types so as to minimize early saccades while maintaining the same starting eccentricity across velocities. As a result, peak eye acceleration often was obscured by saccades, especially for flash separations that produced increases in latency. To circumvent these problems, we measured average eye velocity at a fixed pre-saccadic time during the rising phase of pursuit (vertical dashed line in Figure 6) and normalized by the average eye velocity evoked at the same time, by the same target velocity, when Δt was 4 ms. Normalized eye velocities less than one indicate initiation deficits. This metric does confound the effects of increases in acceleration latency and decreases in eye acceleration, and indicates only the degree to which pursuit initiation is normal or abnormal without indicating the nature of the underlying deficit. However, small to moderate decreases in normalized eye velocity were caused primarily by latency deficits, as these appeared first.

Inspection of the data in Figures 7 reveals both spatial and temporal limits on the pre-saccadic initiation of pursuit. When Δt was 16 ms (open symbols), eye velocity was normal for target speeds up to 12-16°/s and then declined steeply. Because Δt was fixed at 16 ms, the deficits at higher target speeds must be due to an excessive Δx. In contrast,

when Δt was 64 ms (filled symbols), eye velocity wasn't normal even for the lowest target speeds. For such slow target speeds, the values of Δx associated with a Δt of 64 ms were sufficiently small to have evoked normal pursuit initiation when Δt was 16 ms. For example, Δx was identical when Δt was 64 ms at 2°/s and when Δt was 16 ms at 8°/s. Yet eye velocity is normal for the latter parameters and about half normal for the former. We therefore argue that the deficit in the former case cannot be due to Δx and must be due to the fact that Δt was 64 ms. In summary, although in all figures we express the flash separation in terms of Δt, the temporal separation is the limiting factor only for slow target velocities. For faster target velocities, deficits are actually produced by the associated Δx. The range of speeds over which each limit is operative is explored further below.

For values of Δt less than 32 ms, the disappearance of deficits when the target is slowed rules out a tempting explanation for these deficits: that they result from the delay in motion information until after the second flash. This explanation is unlikely for another reason. Latency deficits are often too large to be explained by the separation of the first two flashes. In Figure 6B, for example, a 16 ms increase in Δt, from 16 ms to 32 ms, delayed the initiation of pursuit by nearly 40 ms. In each of the graphs in the left column of Figure 5, the rate of increase in acceleration latency at high values of Δt exceeds the rate of increase in Δt.

To visualize simultaneously the spatial and temporal limits governing pursuit initiation, we measured eye velocity during the initiation of pursuit for a range of combinations of Δt and Δx, where apparent velocity is Δx/Δt. The symbols in Figure 8 plot normalized eye velocity as a function of Δt and Δx. The magnitude of initial eye

velocity is indicated by the size of the symbol, with filled symbols denoting eye velocities within 90% of normal. Although the plots from different monkeys are quantitatively different, there is a broad qualitative pattern. In each graph, the filled symbols denoting normal or nearly normal pursuit cluster in the lower left corner. The range of parameters that evoked nearly normal eye velocities can be exited by traveling either vertically or horizontally, indicating that normal initiation is bounded by both a spatial and a temporal limit. Traveling vertically within a graph keeps Δt constant, as in Figure 7, while traveling horizontally keeps Δx constant. Target velocity remains constant along the diagonal lines, at values indicated by the numbers along the top and right sides of each graph. All four monkeys tested with target speeds up to 45°/s showed a limit on pursuit initiation expressed primarily in terms of Δx (Figure 8C-F). At lower target velocities, pursuit faltered before this spatial limit was reached, indicating that pursuit initiation is also limited by Δt. The temporal limit is particularly clear in Figure 8B. Defined as the point at which eye velocity falls below 90% of normal, the spatial limit lay between 0.2 and 0.4° for five monkeys, and between 0.5 and 1° for the sixth (Fi) . The temporal limit lay between 32 and 64 ms. The plots are somewhat noisy, especially at low target velocities, because of the large number of trial types used in these experiments.

Deficits observed when Δx becomes too large are assumed to arise because the spatial integration ability of neural motion sensors is exceeded. Are the deficits observed when Δt becomes too large related to the temporal integration time of neural motion sensors? We concluded above that deficits seen when Δt was 32 ms or less were not due to the delay in motion information until the second flash, as they disappeared when the

target was slowed. However, this conclusion does not apply to the deficits observed when Δt is large, which persist at slow target velocities. In the extreme, delays in the arrival of motion information obviously must contribute: a monkey with a pursuit latency of 80 ms could not initiate normal pursuit when Δt is 96 ms. Still, there is some reason to believe that initiation deficits seen when Δt is large result in part from a failure of neural motion sensors. Figure 9 plots peak eye acceleration and acceleration latency as a function of Δt for monkey Ka at a target velocity of 3°/s. Little or no deficit is observed when Δt is 32 ms, while a large latency deficit is observed when Δt is 64 ms. Latency increased 55 ms while Δt increased only 32 ms. The deficit is 23 ms larger than expected if the latency increase were due solely to the additional 32 ms delay between the first and second flash. As Δx is 0.192° when Δt is 64 ms, just below the spatial limit of 0.2-0.4° seen for Ka in Figure 8, the additional 23 ms of delay are probably not the result of excessive spatial separation. This suggests that while a Δt of 32 ms is within the integration time of the neural motion sensors driving pursuit, a Δt of 64 ms produces deficits in part because it exceeds the temporal integration time. A similar argument can be based upon the deficits in eye acceleration seen in Figure 9. These deficits appeared when Δt was 64 ms or longer, corresponding to a Δx of 0.19°. At higher target velocities, a Δx of at least 0.58° was necessary to produce deficits in eye acceleration. Thus, it appears likely that, at least to some degree, deficits produced by large Δt's result because the stimulus exceeds the temporal integration abilities of neuronal motion sensors. These conclusions should, however, be viewed as tentative, in part because they rest upon the assumption that the spatial limit is similar across velocities. This assumption may be true only to a first approximation. Figure 9 shows data only for monkey Ka because only this

monkey produced sufficiently regular pursuit at low velocities to allow an analysis of eye acceleration in individual trials. However, similar effects were observed in the averaged eye velocity traces of other monkeys (data not shown).

The spatial limit is eccentricity dependent

In humans, the spatial limit governing the perception of short range apparent motion has been shown to increase with eccentricity (Braddick 1985). The spatial limit governing the direction selectivity of MT neurons shows a similar increase with eccentricity (Mikami et al. 1986). To determine if the spatial limit governing pursuit initiation was eccentricity dependent, we measured the effect of changing Δx on the initiation of pursuit for three values of initial target eccentricity. Target velocity was 18°/s. Different eccentricities were created using initial target position steps of different sizes. The three sets of traces in the left column of Figure 10 show averaged eye velocity as a function of time, and illustrate typical deficits. Flash separation is expressed in terms of Δt, but given the results described in previous figures it is presumed that, for Δt less than 32 ms, deficits arise from the associated value of Δx. When eccentricity was 0.5° (Figure 10A), deficits in the initiation of pursuit appeared when Δt increased from 4 ms (bold, solid trace) to 16 ms (fine, solid trace) and worsened when Δt was increased further to 24 ms (dashed trace). When eccentricity was 3° (Figure 10B), deficits were observed only when Δt increased from 16 ms to 24 ms. When eccentricity was 7° (Figure 10C), there was little deficit in the initiation of pursuit even when Δt was 24 ms.

Using the methods described earlier, we quantified the effects of eccentricity in three monkeys by measuring average eye velocity 50 ms after the normal time of initiation. This measurement time is indicated by the dashed vertical lines in Figure 10,

A-C. The histograms at the right of Figure 10 show how changes in flash separation affected the initiation of pursuit for targets presented at different eccentricities. Each panel represents a given eccentricity and contains three groups of histogram bars, one group for each monkey. The four bars within each group correspond to four values of Δt. All monkeys showed the same basic effects. When eccentricity was 0.5° (Figure 10D), initial eye velocity declined consistently as a function of Δt, starting when Δt increased from 4 to 16 ms. When eccentricity was 3° (Figure 10E), initial eye velocity did not decline until Δt was at least 24 ms. When eccentricity was 7° (Figure 10F), the only clear declines in initial eye velocity occurred when Δt increased from 24 to 32 ms. Thus, the effect of increasing the flash separation was reduced at larger eccentricities. Again, although flash separation is expressed in terms of Δt, most deficits are expected to be due to the spatial flash separation. Deficits first appeared at values of Δx around 0.29° (Δt = 16 ms) when starting eccentricity was 0.5°, and around 0.57° (Δt = 32 ms) when starting eccentricity was 7°.

Effect of imposing steps of apparent target velocity during ongoing pursuit

A number of previous papers have pointed out that image motion plays a dual role in pursuit. It must both a) engage pursuit by initiating the active transition from fixation to pursuit and b) provide the primary feedforward drive producing eye acceleration (Robinson 1965; Kawano and Miles 1986; Luebke and Robinson 1988; Morris and Lisberger 1985; Goldreich et al. 1992). The effects of apparent motion on the initiation of pursuit could arise either because the pursuit system takes longer to become fully engaged when a degraded motion signal is present, or because the motion signals driving eye acceleration are delayed and weakened. To distinguish between these two

possibilities, we compared pursuit initiation from fixation with pursuit responses to changes in target velocity, after pursuit had been engaged. Control trials were used to study initiation, and provided a single step of target velocity with different values of Δt. To allow comparison of pursuit initiation with responses to changes in target velocity, the onset of target motion was not accompanied by a position step. As with all the above experiments, Δt was 4 ms during fixation and was changed only when the target began to move. Experimental trials provided two steps of apparent target velocity. The first target velocity step retained a Δt of 4 ms, while the second step increased target speed and provided the Δt of interest. This design enabled the monkey to achieve nearly perfect tracking so that the image velocity produced by the second step was nearly equal to the change in target velocity. We were thus able to compare the response to a given image motion seen during fixation with the response to the same image motion seen during active pursuit. We expected one of two outcomes for this experiment. If apparent motion causes the initiation of pursuit to suffer because pursuit engagement is delayed, then responses to changes in target velocity should exhibit reduced deficits, as pursuit is already engaged. If deficits are due to degradation of the motion signals driving eye acceleration, then deficits in the responses to target velocity changes during pursuit should be identical to deficits produced in pursuit initiation. An assumption of this approach is that pursuit, once engaged by the first step, is not disengaged by the second step.

Figure 11A shows averages of eye velocity illustrating the effect of Δt on the response to a 30°/s target velocity step. At the time of the target velocity step, the animal was fixating the stationary target. As Δt progressed from 4 to 32 ms (trace weights

moving from solid to short dashes to long dashes), pursuit initiation became progressively more impaired. Figure 11B shows the same progression of deficits in response to a 30°/s step of target velocity that was imposed during maintained pursuit at 2°/s (i.e. from 2 to 32°/s). Every Δt that produced a deficit in the response from fixation produced a similar deficit in the response to a change in target velocity. Deficits in the response to the velocity step were not reduced by prior engagement of pursuit. Furthermore, the second step did not cause any decline in sustained eye velocity prior to the pursuit response for any of the values of Δt used. The absence of any decline argues that pursuit remained engaged when the second step was presented.

These and related data are quantified in Figure 12. The three graphs show data for 3 different monkeys and plot average eye velocity, measured 50 ms after the relevant step of target velocity, as a function of Δt. Different symbol types plot responses for different initial and final target velocities. Deficits in the response to 30°/s steps of target velocity were the same whether that step took velocity from 0 to 30°/s (filled circles) or 2 to 32°/s (open circles). Similar experiments were performed using target velocity steps of 10°/s. Again, deficits were very similar whether the steps took velocity from 0 to 10°/s (filled squares), from 2 to 12°/s (open squares), or from 20 to 30°/s (open diamonds). Prior engagement of the pursuit system did not diminish deficits. What we have referred to as 'initiation deficits' are not therefore deficits in the initiation of pursuit *per se*, but rather are deficits in the visuo-motor processing of image motion for the purpose of producing eye acceleration.

Figure 12 also addresses the assumption of some models of smooth pursuit eye movements: that the visuo-motor processing that produces eye acceleration occurs in

retinal coordinates (Goldreich et al. 1992; Krauzlis and Lisberger 1994; Ringach 1995). If deficits recorded at the initiation of pursuit result from the impairment of motion processing in retinal coordinates, then the deficits should be independent of target and eye velocity, and of the absolute spatial separation of the flashes. They should depend only upon the retinal flash separation. Figure 12 shows that this was indeed the case. When targets changed velocity, deficits were linked to the retinal Δx produced by the second step, and not to the spatial Δx. For example, all 10°/s velocity steps from the three different initial target velocities produced similar retinal image velocities and similar values of retinal Δx, and all three produced similar deficits at a given Δt. If the absolute Δx were the relevant factor, then deficits in the responses to steps that take target velocity from 20 to 30°/s should occur at values of Δt one-third those needed to produce deficits for steps of target velocity from 0 to 10°/s steps. Instead, deficits became apparent when Δt approached 20 ms regardless of the final target speed. These data also indicate that the underlying eye and target velocity have little effect on the magnitude of visuo-motor deficits produced by a given retinal flash separation. These conclusions might seem inevitable, but they are in contrast with the clear influence of extra-retinal factors on maintenance deficits, described below.

In two monkeys (Figure 12A, B), final eye/target speed did have a small effect on the magnitude of deficits at larger values of Δt: open diamonds are below the two square symbols when Δt is 32 ms. At least for monkey Mo (Figure 12B), this is probably because the gain of his pursuit maintenance was slightly less than one when target velocity was 20°/s. Image velocity was actually 12°/s when target velocity stepped from 20 to 30°/s, rather than the intended 10°/s, yielding a slightly larger retinal Δx.

Alternately, we present evidence below that deficits in pursuit *maintenance* do depend upon extra-retinal factors, are produced primarily at fast eye/target velocities and large flash separations, and involve deficits in processes other than visuo-motor drive. None of the stimulus parameters used produced maintenance deficits in these experiments. Nonetheless, when Δt was 32 ms, the slight increase in deficit size at the highest eye/target velocity suggests that the deficit in visuo-motor drive is compounded with further deficits that *are* related to extra-retinal factors. An extreme example of such a compound deficit can be seen in Figure 17, described later. For all other stimulus configurations presented in Figure 12, the consistency of deficit size despite changes in absolute target velocity implies that extra-retinal factors have negligible impact on deficits in visuo-motor drive.

Maintenance deficits were produced by large flash separations

All the deficits discussed so far have been deficits in pursuit initiation, with no concurrent deficits in pursuit maintenance. However, for some large flash separations, pursuit maintenance *was* impaired. For example, Figure 13 shows pursuit responses of monkey Na to 30°/s targets when Δt was 4 and 96 ms. When Δt was 4 ms (Figure 13A), the initiation of pursuit was brisk and sustained eye velocity reached target velocity. When Δt was 96 ms (Figure 13B), initial eye acceleration was both delayed and weak. Eye acceleration ceased before target velocity was reached, and the target was tracked with a combination of deficient pursuit and frequent saccades. To show that the averages of eye velocity are consistent with the responses in individual trials, the eye velocity responses from individual trials (fine traces) are superimposed on the averages (bold traces). Inspection of the individual traces, in which intervals where saccades were

excised have not been replaced with line segments, also shows that our method for analyzing eye velocity neither created nor obscured these deficits. Because saccades would confound any averages of eye position, we have superimposed the eye position traces from many individual trials in the bottom half of Figure 13. These traces reveal that the eye was consistently behind the target in Figure 13B, so that retinal image position was a few degrees eccentric, just as it was during the initiation of pursuit.

The most obvious explanation for the observed deficits in pursuit maintenance is that they, like deficits in pursuit initiation, result from a failure of the motion signals driving eye acceleration. If eye acceleration is weak, then target velocity cannot be reached during the course of the trial. A number of lines of evidence argue that this explanation is incorrect. First, maintenance deficits were sometimes observed despite considerable initial eye acceleration. In Figure 14A, target velocity was 32°/s and Δt was 48 ms. Had it been maintained, initial eye acceleration (prior to the saccade) would have been sufficient in most trials to bring eye velocity to target velocity. In fact, eye acceleration fails before target velocity is reached; eye velocity actually reaches a peak and then decays somewhat, both in the average (bold trace) and in most of the responses from individual trials (fine traces). Figure 14B shows averages of eye velocity from the same experiment when the value of Δt was 4, 32, 48, and 64 ms, revealing a progression of deficits in both the initiation and maintenance of pursuit. A mild maintenance deficit could be seen even when Δt was 32 ms. Though not shown, in this experiment a Δt of 64 ms produced deficits in initiation but *not* maintenance for target velocities of 8°/s or slower.

One might reason, in Figure 14A, that the presence of saccades is partially responsible for the decline in eye acceleration. However, saccades typically enhance post-saccadic eye velocity at the initiation of pursuit (Lisberger 1998). Even if saccades were disruptive rather than facilitory, eye acceleration would be expected to resume following the saccade, especially as the retinal Δx is less during defective pursuit maintenance that during the target motion that initiates pursuit. The most likely explanation for the data in Figure 14 is that maintenance deficits result from a failure of eye velocity memory to support eye velocity and to integrate eye acceleration commands. As discussed in the introduction, eye velocity memory is a postulated mechanism that integrates eye acceleration commands and maintains current eye velocity if no acceleration command is given. For a number of reasons, including the quick decline of eye velocity following target offset, eye velocity memory is presumed to be modulated with the engagement state of pursuit. The state of engagement of pursuit may in turn be modulated by the quality of the motion stimulus provided by the target.

The experiment shown in Figure 15 further bolsters the conclusion that deficits in the maintenance of pursuit result from a partial failure of eye velocity memory. Each of the two experiments shown consisted of three trial types. When Δt was 4 ms (solid traces labeled "4 ms"), initiation was brisk and the steady-state gain was near one. When Δt was 64 ms (Figure 15A, dashed traces) or 96 ms (Figure 15B, dashed traces), eye acceleration was weak at the initiation of pursuit and maintained smooth eye velocity was about half of target velocity. If Δt was initially 4 ms and was then changed to the longer value at the time indicated by the vertical arrows (solid traces labeled "4→64" and "4→96"), then eye velocity settled quickly into a maintenance deficit following the

increase in Δt. In both examples in Figure 15, the final eye velocity was very close to that obtained when the longer Δt was used from the outset. Thus, large values of Δt produced maintenance deficits even *after* eye velocity had reached target velocity, confirming that maintenance deficits result from a failure of eye velocity memory, and not simply from a failure of initial eye acceleration.

Deficits in the maintenance of pursuit are not in retinal coordinates.

When we examined deficits in the initiation of pursuit, we expressed the limits of normal eye acceleration in terms of Δt and the retinal Δx. It is natural to wish to do the same for pursuit maintenance, but it does not appear that the limits on normal maintenance can be expressed in these terms. Figure 16 shows the initiation and maintenance of pursuit for two monkeys when Δt was 4 or 64 ms and apparent target velocity was 16°/s (lower panels) or 32°/s (upper panels). When Δt was 64 ms, deficits in the maintenance of pursuit were present at an apparent target velocity of 32°/s (Figure 16, A and C), but were reduced or absent at 16°/s (Figure 16, B and D). These examples make a number of points. First, like many initiation deficits, maintenance deficits cannot result simply from an excessive Δt. Second, it is equally difficult to link maintenance deficits to a particular spatial limit, at least in retinal terms. In Figure 16, B and D, when target velocity was 16°/s, a Δx of 1° (associated with a Δt of 64 ms) produced impaired but still reasonable eye acceleration during initiation of pursuit. The same retinal Δx of 1° (also associated with a Δt of 64 ms) is achieved during the impaired pursuit of the 32°/s target (at the times indicated by arrows in Figure 16, A and C), yet there is little further eye acceleration towards target velocity. In general, any deficit linked solely to the retinal Δx should be reduced as the eye accelerates, facilitating further eye

acceleration. During maintenance deficits, just the reverse happens. Lastly, if we accept the conclusion argued above that the spatial and temporal limits of visuo-motor drive are expressed in retinal terms, then these examples illustrate that maintenance deficits do not result solely from a failure to convert retinal motion signals into eye acceleration commands. The retinal Δt and Δx of 64 ms and 1° are sufficient to produce considerable eye acceleration in Figures 15B and D. The failure of these same retinal parameters to produce eye acceleration in Figures 15A and C suggests that eye velocity memory is not properly integrating eye acceleration commands.

A final experiment further illustrates a number of these points. Figure 17 A and B show data for two monkeys. Pursuit target velocity was increased twice, first from 0 to 15°/s and then from 15 to 30°/s, while Δt was held constant for the duration of target motion. Neither velocity step was accompanied by a position step. When Δt was 4 ms (bold traces), both monkeys showed brisk eye acceleration in response to both the first and second 15°/s step of target velocity. When Δt was 60 ms in Figure 16A and 96 ms in Figure 16B (fine traces), the initiation of pursuit was delayed and showed clear deficits in eye acceleration. However, eye velocity neared or reached target velocity, implying that the apparent motion seen during the first step leads to a deficit in visuo-motor drive without a deficit in eye velocity memory. Because maintained eye velocity was close to target velocity, the second step of target velocity, to 30°/s, provided another 15°/s step of apparent image velocity, with the same Δt and retinal Δx as the first. Both monkeys showed little eye acceleration in response to this second step of target velocity. If one accepts that visuo-motor drive depends upon the retinal rather than absolute Δx, then visuo-motor drive is expected to be similar for the first and second step of target velocity.

That the observed acceleration is very weak after the second step argues that: 1) eye velocity memory is not operating normally, and/or 2) the visuo-motor commands for eye acceleration are being gated. Additionally, this experiment further illustrates that the effect of a given Δt on pursuit maintenance depends upon target velocity.

Taken together, Figures 13 through 17 strongly argue two points. First, maintenance deficits result primarily from a failure of eye velocity memory. Maintenance deficits persist under conditions where visuo-motor drive ought to be sufficient to accelerate the eye towards target velocity. Maintenance deficits can be produced even after eye velocity has reached target velocity, when no further eye acceleration is needed. We discuss below the likelihood that this failure of eye velocity memory is due to partial engagement of pursuit. A secondary contribution to maintenance deficits may arise if partial engagement gates visuo-motor drive, although our data do little to address this possibility. Second, the conditions that produce deficits in the maintenance of pursuit are not tied solely to the retinal image motion in retinal coordinates. The impact of apparent retinal image motion depends upon the absolute velocity of the target and/or eye.

Discussion

Pursuit of step ramp targets is generally described as having separate 'initiation' and 'maintenance' phases. While apparent motion does produce deficits in both pursuit initiation and maintenance, a full account of the deficits we have observed requires a more mechanistic description of pursuit. Behavioral (Young et al. 1968; Robinson 1971; Morris and Lisberger 1987), lesion (Newsome et al. 1985; Dursteler et al. 1987; Dursteler and Wurtz 1988) and modeling (Goldreich et al. 1992; Krauzlis and Lisberger 1994; Ringach 1995) studies argue that pursuit eye velocity is created by two mechanisms. The first is visuo-motor drive, which converts retinal image motion into commands for eye acceleration. The second is eye velocity memory, which integrates the eye acceleration commands into commands for eye velocity, and maintains those eye velocity commands until subsequent visual inputs provoke renewed eye acceleration, or until pursuit is disengaged. Each of these mechanisms contributes to both the initiation and maintenance of pursuit. The role of visuo-motor drive is minimized (though not eliminated) during maintained pursuit of constant velocity targets, but this would not be true for the majority of natural pursuit targets. In addition, several lines of evidence reviewed in the Introduction have suggested that the gain of visuo-motor drive and eye velocity memory are under on-line control by a mechanism governing pursuit engagement. Both visuo-motor drive and eye velocity memory may operate at full gain only when pursuit is maximally engaged. The level of engagement may depend upon both 'cognitive' factors such as motivation and expectation, sensory factors such as the speed and direction of the target and, we will argue, the quality of the visual motion. In the first part of the

Discussion, we will outline how our results fit with this more mechanistic view of the organization of the pursuit system.

Separable deficits in visuo-motor drive and eye velocity memory

We have reported deficits in the latency and magnitude of initial pursuit eye acceleration that depended upon retinal parameters such as the spatial separation of flashes on the retina and retinal eccentricity, and were independent of extra-retinal parameters such as eye velocity, target velocity, and the prior level of engagement of the pursuit system. We conclude that the deficits we have recorded at the initiation of pursuit are due to a failure of visuo-motor drive, presumably subsequent to the failure of apparent motion stimuli to evoke normal responses in the sensory end of the pathways that convert image motion into eye acceleration.

In contrast, the deficits we measured in pursuit maintenance cannot be attributed simply to a failure of visuo-motor drive and instead appear to result from a failure of eye velocity memory. A failure of visuo-motor drive alone is insufficient to explain the data in Figures 13 through 17. We suggest that the gain of eye velocity memory is influenced by the state of engagement of the pursuit system and that maintenance deficits result from a failure of highly degraded motion signals to fully engage pursuit. The idea that pursuit engagement may influence the gain of eye velocity memory has been suggested before, by Robinson (1986) and Krauzlis and Lisberger (1994).

Origin of deficits in visuo-motor drive

Cortical area MT is known to be a key part of the visuo-motor pathway driving eye acceleration, and there are a number of parallels between the factors influencing deficits in visuo-motor drive and those influencing the responses of cells in MT. These

parallels provide some support for the obvious interpretation that deficits in visuo-motor drive result from a failure of the relevant apparent motion stimuli to evoke normal responses in MT. First, deficits in visuo-motor drive were tied to the retinal Δx rather than the absolute or spatial Δx. Current data imply the same retinal coordinate frame for neurons in MT. Second, visuo-motor drive during the initiation of pursuit was able to withstand larger values of Δx when the target started more eccentrically. Cells in area MT with more eccentric, and therefore larger, receptive fields are also able to withstand larger values of Δx before losing directionality (Mikami et al. 1986). Third, as described below, there is general agreement between the maximum Δt and Δx that produce normal initiation of pursuit and the maximum Δt and Δx that evoke strongly directional responses in area MT. There is no such agreement for primary visual cortex. Thus, although the first parallel drawn above clearly applies to V1, and the second likely does, the third does not.

To allow comparison of our data with neural responses recorded in previous studies, we defined the spatial and temporal limits on pursuit as the maximum values of Δx and Δt that produced pursuit initiation within 90% of normal (Figure 8). The spatial limit on pursuit varied among monkeys from 0.2 to 0.5° for targets that appeared between 1.1 and 3.5° eccentric. For neural responses, we defined strong direction selectivity as a directional index greater than 0.8. Extrapolation along the curve used in Figure 5 of Mikami et al. (1986) to fit their neural recording data suggests that MT neurons have a spatial limit of 0.55° at an eccentricity of 2°. In contrast, the same figure shows that the spatial limit for V1 cells is only 0.1° at an eccentricity of 2°. These comparisons imply that pursuit initiation is dependent upon strongly directional responses in area MT but not

upon strongly directional responses in V1. Because both neural and pursuit responses degrade quickly once the spatial limits are exceeded, the qualitative conclusions drawn in this paragraph do not depend strongly on the precise criteria chosen to define the spatial limits.

Comparison of the effect of Δt on pursuit initiation and on responses in MT is more difficult. Figure 6 of Mikami et al. (1986) implies that neurons in MT maintain strong direction selectivity for values of Δt up to 90 ms. The latency to initiate pursuit was typically less than 90 ms, and the maximum Δt for normal pursuit initiation was of necessity less than this, falling between 32 and 64 ms. Measurements of the effect of Δt on initial eye acceleration afford a better opportunity for comparison, but were difficult to make at the low velocities required to remain below the spatial limit for normal pursuit initiation. The only experiment in which we were able to make these measurements is shown in Figure 9, and indicates that the temporal limit on normal acceleration was between 64 and 80 ms, in rough agreement with the temporal limits of responses of MT neurons.

Despite the agreement between the temporal and spatial limits for MT and for pursuit, a number of factors make it risky to compare our pursuit data with the available physiological data. 1) Mikami et al. (1986) recorded from cells with receptive fields more eccentric than our pursuit stimuli, requiring estimates made by extrapolation of linear fits. 2) Mikami et al. (1986) analyzed mean firing rate over the full 1000 ms duration of their stimulus while the initiation of pursuit would be driven by approximately the first 100 ms of the response. 3) Mikami et al. (1986) quantified responses in terms of the directionality of the responses. Their analysis was entirely

appropriate given the issues they considered, but does not directly address the question of how an estimate of target speed extracted from the population code in MT would change with Δx and Δt. To better compare the changes induced in MT responses and pursuit initiation, one would wish to pay particular attention to the initial 100 ms of the neural responses, and to observe the magnitude and time-course of a reconstruction of target speed from the population response in MT.

Such an approach is also needed to understand the presence of the different deficit types we observed in the visuo-motor drive for pursuit. Deficits in acceleration latency could conceivably result either from changes in the latency of MT responses, or from decreases in firing rates. Deficits in the magnitude of eye acceleration could result either from decreases in firing rate across the population of MT neurons, or from shifts in the population vector. Any of the deficits could be related either to decreases in the responses of neurons that prefer motion in the direction of target motion, or to increases in the responses of neurons with null directions that correspond to the direction of target motion.

Interestingly, the seemingly paradoxical facilitation of eye acceleration can be explained by a property of motion sensitive cells described by Mikami et al. (1986): cells tuned for lower speeds lose their directional selectivity at smaller values of Δx. This was true both for MT and V1. If we consider a population representation of speed within MT or V1, at a given target speed some values of Δx will suppress only the responses of cells with slower preferred speeds. This will effectively shift the peak of the population code to a speed higher than the veridical speed. If the population code is converted to commands for eye acceleration by a neural computation that depends on which cells are

firing most, then this shift in the population code would be construed as an increase in image speed.

Origin of deficits in eye velocity memory

Our interpretation of the deficits in the maintenance of pursuit is that pursuit is incompletely engaged when visual motion is insufficiently convincing, and that eye velocity memory does not therefore operate at full gain. Previous observations of deficits in the maintenance of pursuit in other contexts have ascribed such deficits to incomplete engagement, poor velocity memory, or both. These observations include: 1) a monkey who showed weak initiation of pursuit and poor tracking of upwards target motion with normal upward visual motion processing (Grasse and Lisberger 1992); 2) two monkeys with early-onset artificially-induced strabismus who had weak initiation and maintenance of pursuit for temporalward target motion, normal responses to temporalward image motion presented during nasalward pursuit, and normal direction selectivity and velocity tuning in visual area MT (Kiorpes et al. 1996); and 3) monkeys with unilateral lesions of visual area MST (Dursteler and Wurtz 1988), the frontal pursuit area (Lynch 1987; Keating 1991; MacAvoy et al. 1991), or the dorsolateral pontine nucleus (May et al. 1988). Our data extend these results by suggesting that pursuit engagement and the resulting recruitment of eye velocity memory are gated by visual motion and are sensitive to the quality of that motion.

Deficits in the maintenance of pursuit did not depend solely upon the retinal properties of the moving image, but were influenced by factors such as absolute target or eye velocity. We see two possible interpretations of this finding. 1) Engagement and the resulting gating of eye velocity memory may be influenced by extra-retinal signals

related to eye velocity or absolute target velocity. Such a mechanism might ensure that large values of Δt were not tolerated at high target velocities, perhaps as they imply a large spatial Δx. That the engagement of pursuit should involve extra-retinal parameters is not necessarily surprising. To detect a cessation of target motion (which typically results in the disengagement of pursuit), eye velocity would have to be compared to target velocity, not to retinal image velocity. 2) The degree of engagement of pursuit may be dependent only upon retinal features of the stimulus, but the gain of eye velocity memory may be nonlinear. When incompletely engaged, eye velocity memory may be more prone to 'leak' at higher velocities. Effects of incomplete engagement on pursuit maintenance would then be small at low eye velocities, but would become noticeable at high velocities. In fact, eye velocity memory does appear to be more prone to leaking at higher velocities even under nearly optimal conditions of target motion. For some monkeys small 'maintenance deficits' were observed for higher target velocities even when Δt was 4 ms (Figures 13, 14, 15 and 16). However, Δt's that produced large maintenance deficits at high apparent target velocities often produced perfectly normal, or even supra-normal maintenance at lower target velocities (Figures 15B, 16B). Thus, for this explanation to succeed, the gain of eye velocity memory would have to be very non-linear.

In addition to the impairment of eye velocity memory, there are two other classes of explanations for deficits in pursuit maintenance that we consider unlikely. 1) The prevalence of saccades during deficient pursuit maintenance disturbs pursuit, preventing normal maintenance. As discussed above, saccades potentiate subsequent smooth eye velocity, presumably by enhancing incomplete engagement (Lisberger 1998), and should

tend to ameliorate deficits in the maintenance of pursuit. In addition, severe deficits in initiation, accompanied by frequent saccades, were often followed by normal maintenance. Further, an explanation based on interference by saccades would also have difficulty accounting for the data in Figures 15 and 17. Thus, saccades appear to be a consequence rather than a cause of the deficits. 2) Target image eccentricity is different during the maintenance and initiation of normal pursuit. A given spatial flash separation produced larger deficits in visuo-motor drive for more foveal targets. As our pursuit targets started eccentrically, but were foveated during the maintenance of pursuit, this effect might have quelched visuo-motor drive as eye velocity neared target velocity. In practice, however, eye position lagged target position by a couple of degrees during deficient maintenance of pursuit, so that the actual retinal eccentricities of targets that failed to evoked eye acceleration during pursuit maintenance were similar to those of targets that evoked convincing eye acceleration at the initiation of pursuit (see Figure 13B). Furthermore, maintenance deficits could be observed when a step of apparent target velocity was presented in the absence of an initial position step (data not shown). Under such conditions the target image becomes progressively more eccentric during the initiation of pursuit. Lastly, this explanation cannot account for the data in Figures 15 or 17, nor can it explain why maintenance deficits were worse at higher target velocities, as in Figure 16.

A failure of processing in any number of cortical areas could produce the eye velocity memory deficits we observed. The presence of eye velocity memory deficits following lesions of visual area MST, which is thought to be the next level of motion processing for pursuit eye movements after area MT, suggests that the deficits we have

observed may result because the relevant apparent motion stimuli fail to evoke normal responses in MST. Due to the presence of extra-retinal signals, MST has previously been previously suggested as a site mediating corollary feedback of the type required for eye velocity memory (Newsome et al. 1988). Alternately, it is also possible that maintenance deficits result when weakened inputs from MT fail to properly excite neurons in the FPA or the DLPN, lesions of which may also lead to maintenance deficits.

Comparison with previous studies

Previous studies of pursuit of apparent motion in humans have found seemingly normal pursuit for values of Δt up to 150 ms, which produced large initiation deficits in our monkeys (Morgan and Turnbull 1978; Van der Steen et al. 1983; Schor et al. 1984; Fetter and Buettner 1990). However, these studies employed either continuously moving or low frequency periodic stimuli, and examined pursuit gain during steady-state tracking. Under these conditions, deficits in the latency and magnitude of visuo-motor drive are expected to have minimal impact. Deficient pursuit will be observed only when visuo-motor drive becomes very weak, or when eye velocity memory suffers. The studies that produced the largest tolerable Δt's (Morgan and Turnbull 1978, 150 ms; Van der Steen et al. 1983, at least 100 ms) did so at relatively low apparent target velocities (2°/s and 7.85°/s respectively). These values of Δt were at the limit of what produced normal pursuit maintenance in our monkeys at these velocities. The predictable nature of the targets used in these studies may also have contributed to the relatively normal performance at large values of Δt. Finally, our preliminary data (now shown in Chapter 3 of this Thesis) do not support the possibility that human visual processing is much more resistant to apparent motion than that of monkeys.

Comparison with perception of apparent motion

Comparison of pursuit and perception for apparent motion stimuli offers an opportunity to address the open question of whether the motion signals driving pursuit are identical to those that mediate perception. Baker and Braddick (1985) used random dot displays to probe the spatial limits of perception involving the 'short range' apparent motion process. They found that the maximum Δx increased with eccentricity and was approximately 0.2° and 1.3° for eccentricities of 1° and 8°. In reasonable agreement, the maximum Δx for normal pursuit initiation was approximately 0.2° and 0.5° for starting eccentricities of 0.5° and 7° (Figure 10). Comparison of the maximum Δt for pursuit initiation and for perception of short range apparent motion is more difficult, as pursuit necessarily suffers at any Δt that approaches the latency of pursuit. Nevertheless, we note that the maximum Δt for normal initial eye acceleration was 64-80 ms, in good agreement with the maximum Δt for perception of 40-80 ms.

Studies of short range apparent motion used random dot stimuli, and psychophysical performance was measured as the ability to discern the direction of motion. A better approximation to our discrete target is the bar-shaped target used by Newsome et al. (1986) in their evaluation of the perceptual limits of apparent motion. Unlike random dot stimuli, however, a single bar moves unambiguously in a given direction even at very large values of Δx. Newsome et al. (1986) therefore asked subjects to give their subjective impression of the smoothness of motion. The five subjects reported that smooth motion was absent when Δx exceeded 0.6 to 1.5°, for target velocities of 10-40°/s at an eccentricity of 5°. In reasonable agreement, the maximum Δx for pursuit was 0.5° for a starting eccentricity of 7°.

The broad agreement between the parameters of apparent motion that support pursuit and perception at least suggests common inputs to the two systems. However, there are some serious caveats to this conclusion. First, pursuit in humans may have somewhat different spatial and temporal limits than pursuit in monkeys. Second, our stimuli were different from those previously used to study perception. Lastly, the metrics used to study perception (subjective quality of motion, discrimination of direction) are not obviously parallel to the metric we used for pursuit (latency and magnitude of eye acceleration during pursuit initiation). A more detailed comparison necessarily awaits new experiments designed to study pursuit and perception in parallel.

References

Adelson., E.H., and Bergen, J.R. Spatiotemporal energy models for the perception of motion. J. Opt. Soc. Am. A. 2: 284-299, 1985.

Baker, C.J., and Braddick, O.J. Temporal properties of the short-range process in apparent motion. Perception 14: 181-192, 1985

Barlow, H., and Levick, W.R. The mechanism of directionally selective units in rabbit's retina. J. Physiol. Lond. 178: 477-504, 1965.

Barnes, G.R., and Asselman, P.T. Pursuit of intermittently illuminated moving targets in the human. J. Physiol. (Lond.) 445: 617-637, 1992.

Boussaoud, D., Desimone, R., and Ungerleider, L.G. Subcortical connections of visual areas MST and FST in macaques. Vis. Neurosci. 9: 291-302, 1992.

Braddick, O.J., and Baker C.L. Jr Eccentricity-dependent scaling of the limits for short-range apparent motion perception. Vision Res. 25: 803-812, 1985.

Braddick, O.J. Low-level and high-level processes in apparent motion. Phil. Trans. R. Soc. Lond. B290: 137-151, 1980.

Dursteler, M.R., and Wurtz, R.H. Pursuit and Optokinetic Deficits Following Chemical Lesions of Cortical Areas MT and MST. J. Neurophysiol. 60: 940-965, 1988.

Dursteler, M.R., Wurtz, R.H., and Newsome, W.T. Directional Pursuit Deficits Following Lesions of the Foveal Representation Within the Superior Temporal Sulcus of the Macaque Monkey. J. Neurophysiol. 57: 1262-1287, 1987.

Fettner, M., and Buettner U.W. Stimulus characteristics influence the gain of smooth pursuit eye movements in normal subjects. Exp. Brain Res. 79: 388-392, 1990

Fuchs, A.F., Robinson, F.R., and Straube, A. Participation of the caudal fastigial nucleus in smooth-pursuit eye movements. J. Neurophysiol. 72: 2714-2728, 1994.

Glickstein, M., Cohen, J.L., Dixon, B., Gibson, A., Hollins, M., Labossiere, E. and Robinson, F. Corticopontine visual projections in macaque monkeys. J. Comp. Neurol. 190: 209-229, 1980.

Goldreich, D., Krauzlis, R.J., and Lisberger, S.G. Effect of changing feedback delay on spontaneous oscillations in smooth eye movements of monkeys. J. Neurophysiol. 67: 625-638, 1992.

Gottlieb, J.P., MacAvoy, M. G., and Bruce, C.J. Neural responses related to smooth-pursuit eye movements and their correspondence with electrically elicited smooth eye movements in the primate frontal eye field. J. Neurophysiol. 72: 1634-1653, 1994.

Grasse, K.L., and Lisberger, S.G. Analysis of a naturally occurring asymmetry in vertical smooth pursuit eye movements in a monkey. J. Neurophysiol. 67: 164-179, 1992.

Groh, J.M., Born, R.T., and Newsome, W.T. How is a sensory map read out? Effects of microstimulation in visual area MT on saccades and smooth pursuit eye movements. J. Neurosci. 17: 4312-43330, 1997.

Judge, S.J., Richmond, B.J., and Chu, F.C. Implantation of magnetic search coils for measurement of eye position: an improved method. Vision Res. 20: 535-538, 1980

Keating, E.G. Frontal eye field lesions impair predictive and visually-guided pursuit eye movements. Exp. Brain Res. 86: 311-323, 1991.

Komatsu, H., and Wurtz, R.H. Modulation of Pursuit Eye Movements by Stimulation of Cortical Areas MT and MST. J. Neurophysiol. 62: 31-47, 1989.

Kiorpes, L., Walton, P.J., O'Keefe, L.P., Movshon, J.A., and Lisberger, S.G. Effects of early-onset artificial strabismus on pursuit eye movements and on neuronal responses in area MT of macaque monkeys. J. Neurosci. 16: 6537-6553, 1996.

Krauzlis, R.J., and Lisberger S.G. A Model of Visually-Guided Smooth Pursuit Eye Movements Based on Behavioral Observations. J. Comp. Neuro. 1: 265-283, 1994.

Langer, T., Fuchs, A.F., Scudder, C.A., and Chubb, M.C. Afferents to the flocculus of the cerebellum in the Rhesus macaque as revealed by retrograde transport of horseradish peroxidase. J. Comp. Neurol. 235: 1-25, 1985.

Lisberger, S.G., and Westbrook, L.E. Properties of Visual Inputs that Initiate Horizontal Smooth Pursuit Eye Movements in Monkeys. J. Neurosci. 5: 1662-1673, 1985.

Lisberger, S.G. Postsaccadic enhancement of initiation of smooth pursuit eye movements in monkeys. J. Neurophysiol. 79: 1918-1930, 1998.

Lisberger, S.G., and Fuchs, A.F. Role of primate flocculus during rapid behavioral modification of vestibuloocular reflex. I. Purkinje cell activity during visually-guided horizontal smooth pursuit eye movements and passive head rotation. J. Neurophysiol. 41: 733-763, 1978

Luebke, A.E., and Robinson, D.A. Transition dynamics between pursuit and fixation suggest different systems. Vision Res. 28: 941-946, 1988

Lynch, J.C. Frontal eye field lesions in monkeys disrupt visual pursuit. Exp. Brain Res. 68: 437-441, 1987.

MacAvoy M.G., Gottlieb, J.P., and Bruce, C.J. Smooth pursuit eye movement representation in the primate frontal eye field. Cerebral Cortex 1: 95-102, 1991.

May, J.G., Keller, E.L., and Suzuki, D.A. Smooth-pursuit eye movement deficits with chemical lesions in the dorsolateral pontine nucleus of the monkey. J. Neurophysiol. 59: 952-977, 1988.

Mikami, A., Newsome, W.T., and Wurtz, R.H. Motion Selectivity in Macaque Visual Cortex. II. Spatiotemporal range of directional interactions in MT and V1. J. Neurophysiol. 55: 1328-1339, 1986.

Morgan, M.J., and Turnbull, D.F. Smooth eye tracking and the perception of motion in the absence of real movement. Vision Res. 18: 1053-1059, 1978.

Morris, E.J., and Lisberger, S.G. Different responses to small visual errors during initiation and maintenance of smooth-pursuit eye movements in monkeys. J. Neurophysiol. 58: 1351-1369, 1987.

Newsome, W.T., Wurtz R.H., Dursteler M.R., and Mikami A. Deficits in visual motion processing following ibotenic acid lesions of the middle temporal visual area of the macaque monkey. J. Neurosci. 5: 825-840, 1985

Newsome, W.T., Mikami, A., and Wurtz, R.H. Motion Selectivity in Macaque Visual Cortex. III. Psychophysics and physiology of apparent motion. J. Neurophysiol. 55: 1340-1351, 1986.

Newsome, W.T., Wurtz, R.H., and Komatsu, H. Relation of cortical areas MT and MST to pursuit eye movements. II. Differentiation of retinal from extraretinal inputs. J. Neurophysiol. 60: 694-620, 1988.

Ringach, D.L. A tachometer feedback model of smooth pursuit eye movements. Biol. Cybern. 73: 561-568, 1995.

Robinson, D.A. The mechanics of human smooth pursuit eye movement. J. Physiol. Lond. 180: 569-591, 1965.

Robinson, D.A., Gordon, J.L., and Gordon, S.E. A model of the smooth pursuit eye movement system. Biol. Cybern. 55: 43-57, 1986.

Robinson, D.A. Integrating with neurons. Ann. Rev. Neurosci. 12: 33-45, 1989.

Rashbass, C. The relationship between saccadic and smooth tracking eye movements. J Physiol. (Lond) 159: 326-338, 1961.

Schor, C.M., Lakshminarayanan, V., and Narayan, V. Optokinetic and vection responses to apparent motion in man. Vision Res. 24: 1181-1187, 1984

Schwartz, J.D., and Lisberger, S.G. Initial tracking conditions modulate the gain of visuo-motor transmission for smooth pursuit eye movements in monkeys. Visual Neuroscience 11: 411-424, 1994

Shi, D., Friedman, H.R., and Bruce, C.J. Deficits in smooth-pursuit eye movements after muscimol inactivation within the primate's frontal eye field. J. Neurophysiol. 80: 458-464, 1998.

Tusa, R.J., and Ungerleider, L.G. Fiber pathways of cortical areas mediating smooth pursuit eye movements in monkeys. Ann. Neuro. 23: 174-183, 1988.

Tyler C.W. Temporal characteristics in apparent movement: omega movement vs. phi movement. Q. J. Exp. Psychol. 25: 171-181, 1973.

Ungerleider, L.G., Desimone, R., Galkin, T.W., and Mishkin, M. Subcortical projections of area MT in the macaque. J. Comp. Neurol. 223: 368-386, 1984.

Van der Steen, J., Tamminga, E.P., and Collewijn, H. A comparison of oculomotor pursuit a target in circular real, beta or sigma motion. Vision Res. 23: 1655-1661, 1983.

Watson, A.B., and Ahumada, A.J. Jr. Model of human visual-motion processing. J. Opt. Soc. Am. A. 2: 322-341, 1985.

Acknowledgements

Stephen G. Lisberger is an Investigator of the Howard Hughes Medical Institute. Mark M. Churchland was supported by a pre-doctoral fellowship from the Department of Defense. Research was supported by NIH grant EY03878. We acknowledge the efforts of Kay Logan, who completed a preliminary version of these experiments using now-outdated technology, but obtained many of the same results reported here. We thank Dr. J. Anthony Movshon, the members of the Lisberger laboratory, and an anonymous reviewer for insightful comments on the manuscript. Permission to reprint this manuscript was given by The Journal of Neurophysiology.

Figure 1. Representation of smooth and apparent motion in the space-time domain (A), and the frequency domain (B). A: Time is shown on the vertical axis, with downward movement along the axis reflecting the passing of time. Position along the horizontal meridian is plotted on the x-axis. B: Frequency domain representation of the same target motion as in panel A. Spatial and temporal frequency are plotted on the x- and y-axis with positive values plotted rightwards and upwards, respectively. The oblique solid line shows the relationship for real target motion at a given speed, while the two dashed oblique lines show 'replicas' that appear during sampled, or apparent, motion.

Figure 1

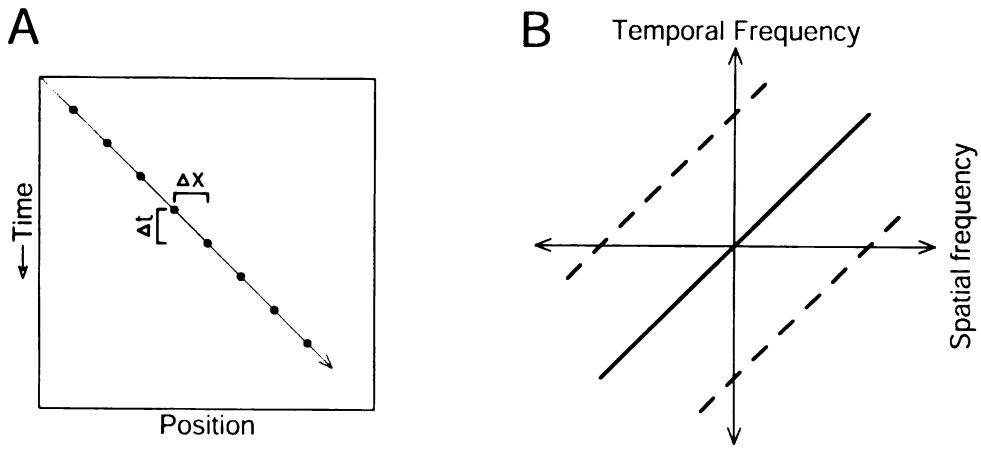
A
Time
Position
ΔX
Δt
B
Temporal Frequency
Spatial frequency

Figure 2. Single trial record showing a representative response to target motion at an apparent velocity of 22°/s, with a Δt of 16 ms. The top and bottom pairs of traces superimpose target (T) and eye (E) velocity and position, respectively. The dots on the target position trace indicate the time and position of each flash of the apparent motion target. The arrow on the eye position trace points out a saccade. The arrow on the eye velocity trace points out the (truncated) rapid upward deflection caused by the saccade. The traces begin 100 ms before the step-ramp of target motion, and about 1000 ms after the onset of the trial. Upward deflections of the traces indicate rightward motion.

Figure 2

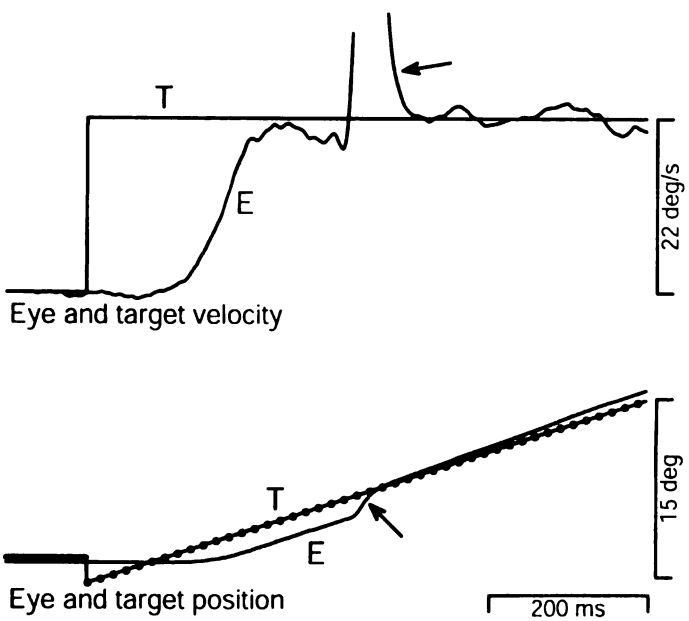
T
E
22 deg/s
Eye and target velocity
T
E
15 deg
Eye and target position
200 ms

Figure 3. Effect of varying □t on the time course of the initiation of pursuit in one monkey. In A, B, D, and E, the fine and bold traces show ten subsequent individual responses and averages of all 17-20 responses, respectively. A. Responses to apparent target velocity of 16°/s when Δt was 4 ms. B. Responses to apparent target velocity of 16°/s when Δt was 32 ms. C. The average responses from A and B are shown superimposed for comparison. The numbers next to each trace indicate the value of □t used to obtain that average. D. Responses to apparent target velocity of 32°/s when Δt was 4 ms. E. Responses to apparent target velocity of 32°/s when Δt was 48 ms. F. The average responses from D and E are shown superimposed for comparison, along with the average response when Δt was 24 ms. All traces begin at the onset of target motion. Traces for individual responses are interrupted during saccades. Both target motion and the pursuit response continued for 500-1000 ms after the portion of the response shown. These examples were drawn from experiments using multiple target velocities in monkey Ka, and not from the experiments shown in Figures 4 or 5. Although flash separation is indicated in terms of Δt, Δx and Δt change together for target motion at a constant speed.

Figure 3

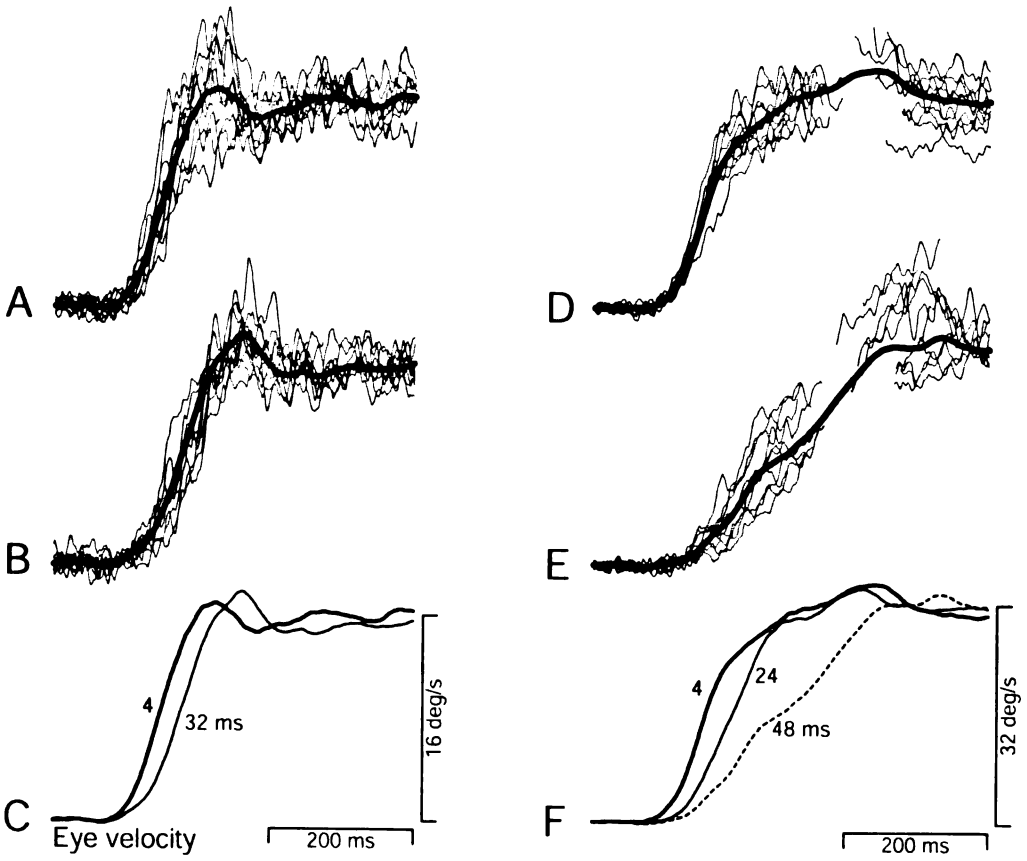
A
B
C
4
32 ms
16 deg/s
Eye velocity
200 ms
D
E
F
4
24
48 ms
32 deg/s
200 ms

Figure 4. Effect of varying Δt on the time course of average eye velocity and acceleration. Top and bottom groups of superimposed traces show average eye velocity and acceleration for multiple values of Δt. A. Responses of monkey Ka to an apparent target velocity of 16°/s. Numbers next to the eye velocity traces indicate the value of Δt. Data were taken from an experiment using a range of velocities. B. Responses of monkey Na to an apparent target velocity of 18°/s. Data were taken from an experiment using only one target velocity. For the data shown in both A and B, saccades occurred well after the peak of eye acceleration except for the longest values of Δt when they occurred just following the peak. Traces begin at the onset of target motion.

Figure 4

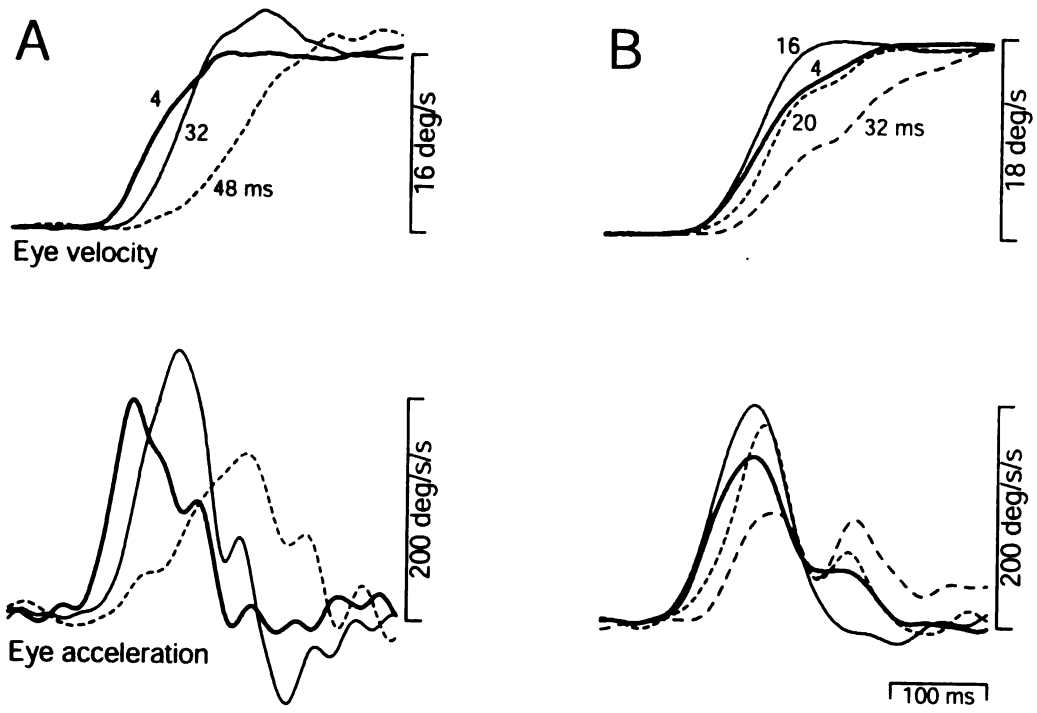
A
4
32
48 ms
16 deg/s
Eye velocity
B
16
4
20
32 ms
18 deg/s
200 deg/s/s
Eye acceleration
200 deg/s/s
100 ms

Figure 5. Separate effects of varying Δt on peak eye acceleration and acceleration latency for four monkeys. In each graph, filled circles plot peak eye acceleration and open diamonds plot acceleration latency as a function of Δt. Apparent target velocity was 18°/s for monkeys Mo, Na, and Ka and 16°/s for monkey El. Acceleration was normalized by the average value when Δt was 4 ms and is plotted relative to the left-hand vertical axis. Latency is shown as the time shift from the average value when Δt was 4 ms, and is plotted against the right-hand vertical axis. Values below the dashed line indicate decreases in acceleration and increases in latency. Error bars show the standard error of the mean and are omitted when smaller than the symbol. Asterisks indicate significant changes from the values at 4 ms (2-tailed t-test, $p<0.05$). Graphs for monkeys Mo, Na and Ka show responses to rightward target motion taken from experiments using a single apparent target velocity. Both directions are shown for monkey El, who exhibited an exceptional pattern of deficits in his rightward pursuit only.

Figure 5

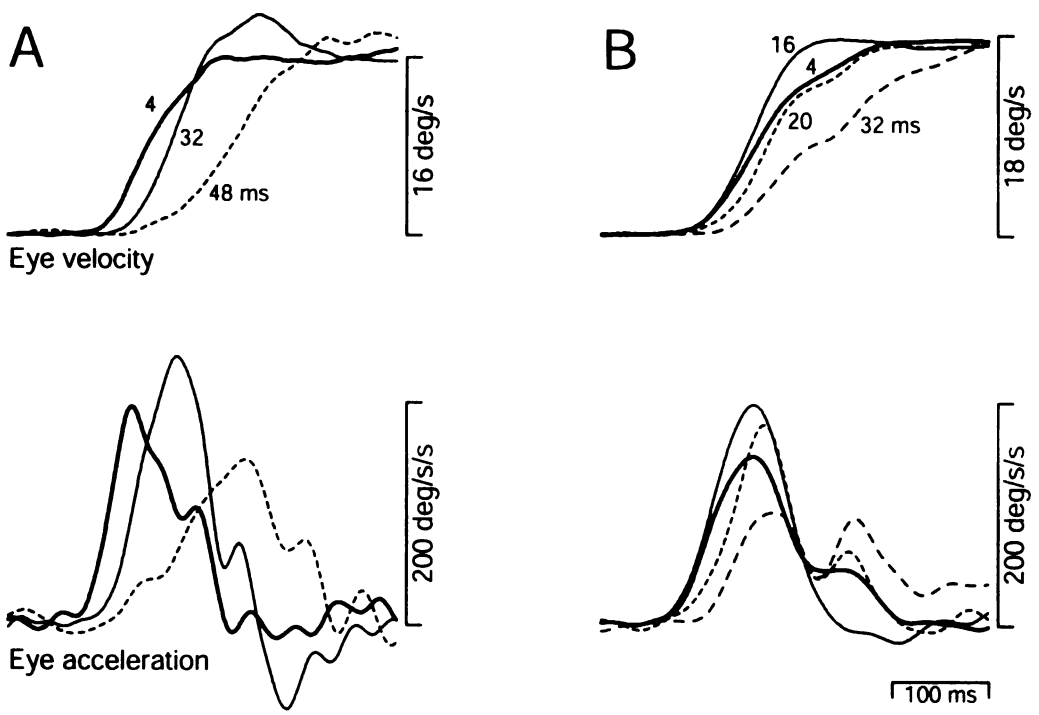
A
4
32
48 ms
16 deg/s
Eye velocity
200 deg/s/s
Eye acceleration
B
16
4
20
32 ms
18 deg/s
200 deg/s/s
100 ms

Figure 6. Average eye velocity traces showing how the effect of varying Δt depends on the apparent target velocity. Apparent target velocities were: 32°/s (A), 16°/s (B), and 8°/s (C). The different trace types show responses for different values of Δt: bold, 4 ms; fine, 16 ms; short dashes, 32 ms. Traces begin at the onset of target motion. To allow comparison of deficits, responses are scaled relative to the target velocity that evoked them. The vertical dashed line was placed 50 ms after the onset of pursuit when Δt was 4 ms, and illustrates how we selected a measurement time that was used to extract the eye velocity measure used in later figures. Data were obtained from monkey Mo in an experiment that used only three target velocities. Each average was constructed from at least 45 individual traces.

Figure 6

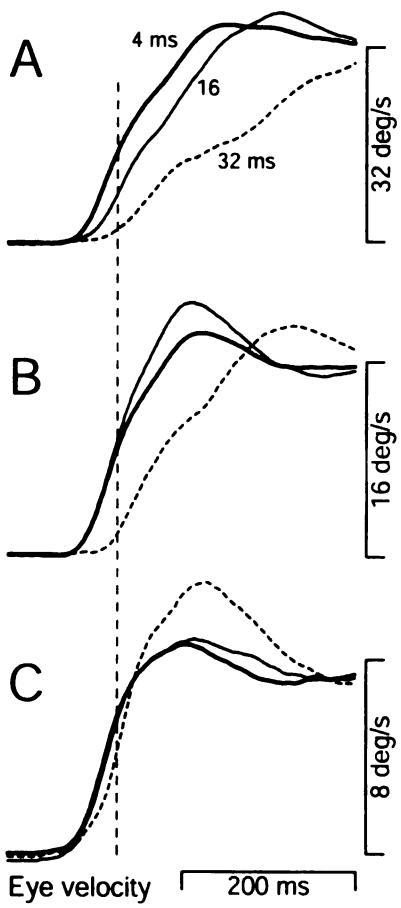

Figure 7. Effect of varying apparent target velocity on the initiation of pursuit at two values of Δt. The y-axis plots normalized average eye velocity measured 50 ms after the initiation of normal pursuit. The time of initiation of normal pursuit was measured when Δt was 4 ms, and was measured separately for each apparent velocity. The average eye velocity for a given Δt is normalized by the average eye velocity for normal pursuit; i.e. when Δt was 4 ms. The horizontal dashed line shows a normalized eye velocity of one, which would indicate that eye velocity was the same as when Δt was 4 ms. Values below the dashed line indicate deficits. Open and filled symbols show responses when Δt was 16 ms and 64 ms. Different symbol shapes show data for monkeys Mo (triangles), Na (squares), and Ka (circles). Error bars show the standard error of the mean. Overlapping error bars have been suppressed.

Figure 7

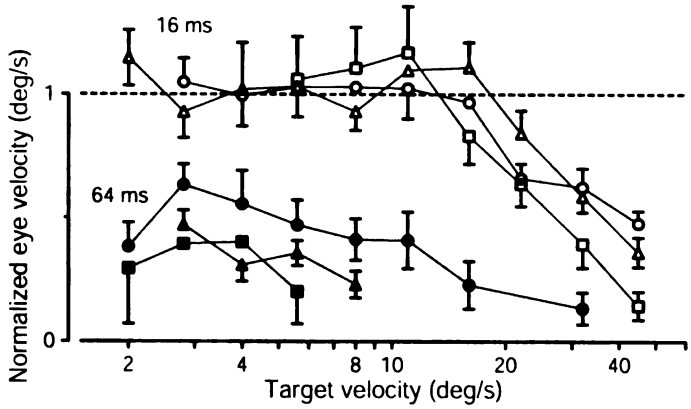
16 ms
64 ms
Normalized eye velocity (deg/s)
1
0
2
4
8
10
20
40
Target velocity (deg/s)

Figure 8. Temporal and spatial limits of apparent motion for the initiation of normal pursuit. Each graph contains one symbol for each combination of temporal separation (Δt) and spatial separation (Δx). The symbol type expresses mean eye velocity as a percentage of that evoked by targets of the same apparent velocity but with a Δt of 4 ms: large solid circles, eye velocity within 90% of normal; large open circles, eye velocity within 80-90% of normal; progressively smaller circles indicate progressively slower eye velocities as defined by the key in panel B. The diagonal lines correspond to fixed values of apparent target velocity, indicated by the numbers along the top and right edges of each panel. A,B: Experiments designed to tile a large range of possible values of Δt and Δx (Monkeys Da and Fi). C-F: experiments using a closer spacing of values of Δt and Δx over a more limited range, to allow a more complete sampling of the range where pursuit initiation becomes impaired (Monkeys El, Mo, Na, and Ka). Each point is based on the mean eye velocity in a 20-ms interval centered 70 ms after the initiation of normal pursuit for monkeys Da, Fi, and El, and centered 50 ms after the initiation of pursuit for monkeys Mo, Na, and Ka.

Figure 8

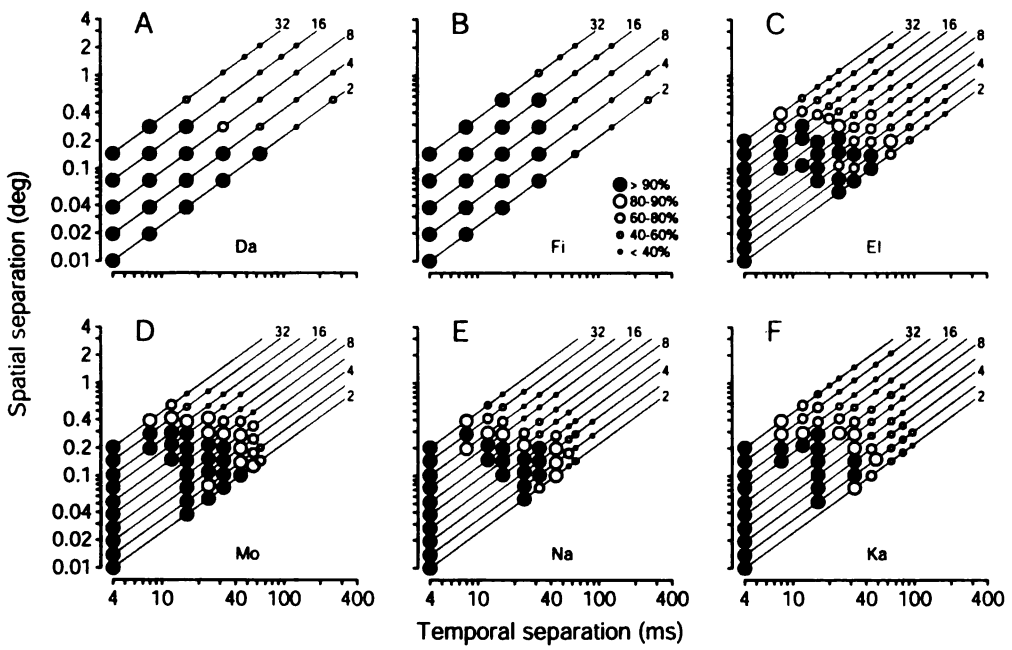
A
B
C
D
E
F
Da
Fi
El
Mo
Na
Ka
32
16
8
4
2
> 90%
80-90%
60-80%
40-60%
< 40%
Spatial separation (deg)
4
2
1
0.4
0.2
0.1
0.04
0.02
0.01
4
10
40
100
400
Temporal separation (ms)

Figure 9. Effect of varying Δt on the initiation of pursuit for a target velocity of 3°/s. Filled symbols show eye acceleration, normalized to the average value when Δt was 4 ms and plotted relative to the left-hand vertical axis. Open symbols show latency, calculated as the time to peak eye acceleration and plotted relative to the right-hand vertical axis as the time shift from the average value when Δt was 4 ms. Values below the dashed line indicate decreases in acceleration and increases in latency. Asterisks mark data points that differed significantly from the value when Δt was 4 ms (two-tailed t-test, $p<0.05$). Error bars show the standard error of the mean, and are omitted when obscured by the symbols. Data are from monkey Ka.

Figure 9

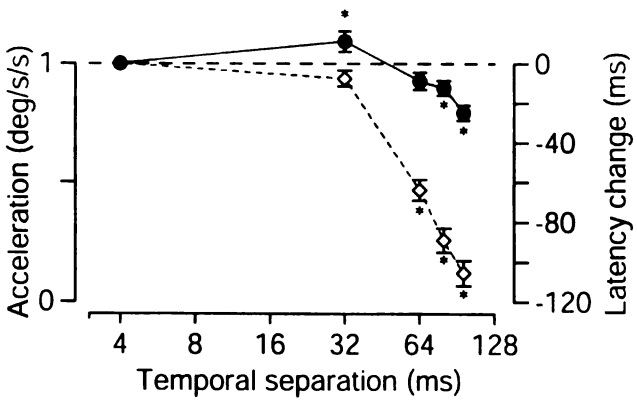
Acceleration (deg/s/s)
1
0
0
-40
-80
-120
Latency change (ms)
4
8
16
32
64
128
Temporal separation (ms)

Figure 10: Effect of starting target eccentricity on the initiation of pursuit to apparent motion. Each row of traces and bar graphs shows data for a single starting target eccentricity. A, D: 0.5°. B, E: 3°. C, F: 7°. A, B, C: Average eye velocity responses of monkey Na to apparent target velocity at 18°/s. Bold, fine, and dashed traces show responses when Δt was 4, 16, and 24 ms, respectively. Traces begin at the onset of target motion. Vertical dashed lines show the measurement time used to create the bar graphs, 50 ms after the initiation of pursuit when Δt was 4 ms. Each trace is an average constructed from at least 40 responses to a given apparent target motion. D, E, F: Bar graphs showing eye velocity, measured at the time of the dashed line, as a function of Δt for three monkeys. In each panel, the three groups of histogram bars show data from three monkeys. Each group of four bars summarizes the effect of Δt for a given monkey at one eccentricity. Numbers below each bar indicate the value of Δt used to obtain those data. Error bars show the standard error of the mean.

Figure 10

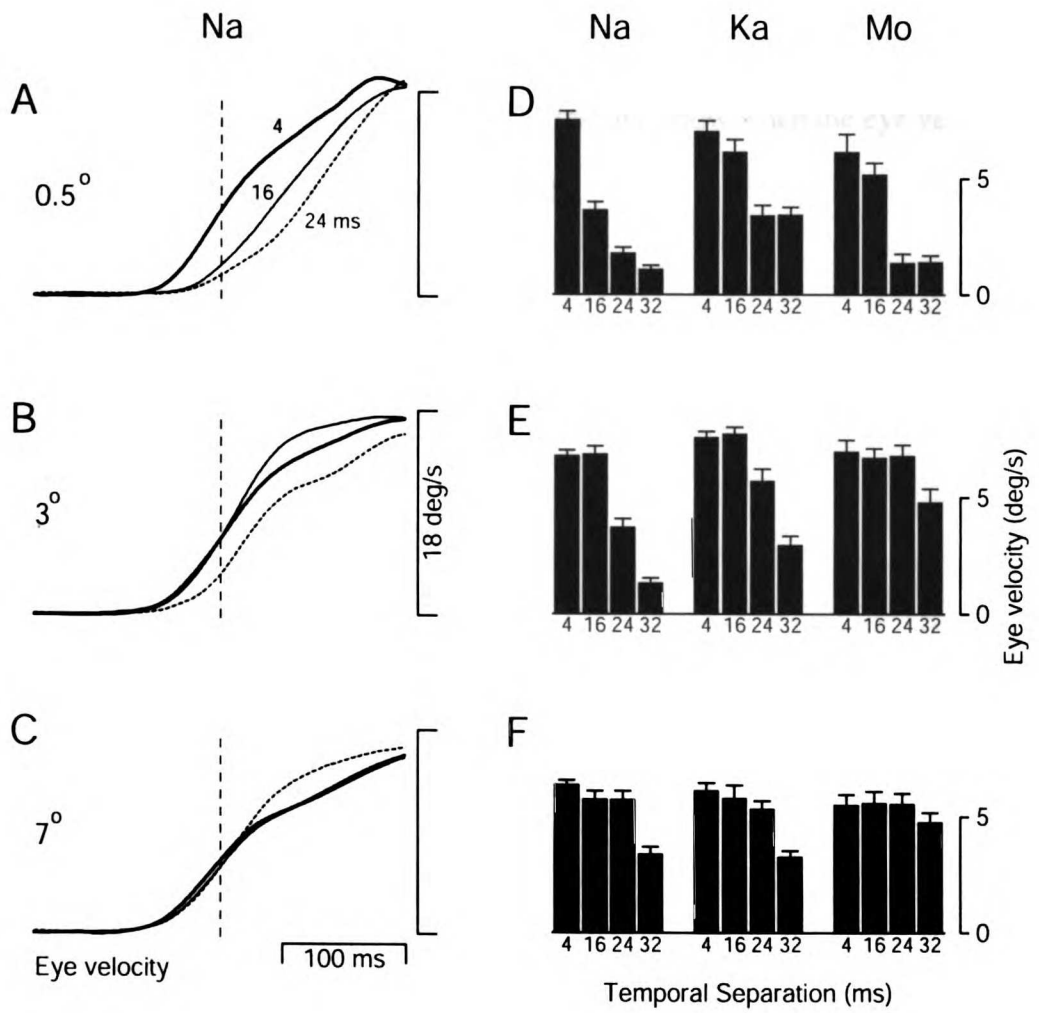
Na
Na
Ka
Mo
A
0.5°
4
16
24 ms
D
5
0
4 16 24 32 4 16 24 32 4 16 24 32
B
3°
18 deg/s
E
5
0
Eye velocity (deg/s)
4 16 24 32 4 16 24 32 4 16 24 32
C
7°
F
5
0
4 16 24 32 4 16 24 32 4 16 24 32
Eye velocity
100 ms
Temporal Separation (ms)

Figure 11. Effect of initial target velocity on responses to a 30°/s step of apparent target velocity using multiple values of Δt. A: Initial target velocity was 0°/s and the step took target velocity to 30°/s. B: Initial target velocity was 2°/s and the step took target velocity to 32°/s. Different trace types show average eye velocity for different values of Δt: bold traces, 4 ms; thin traces, 12 ms; small dashes, 16 ms; medium dashes, 24 ms; long dashes, 32 ms. The horizontal dashed lines mark 0°/s. Vertical dashed lines are placed 50 ms after the start of the response when Δt was 4 ms, and show when the eye velocity measurements plotted in Figure 12 were made.

Figure 11

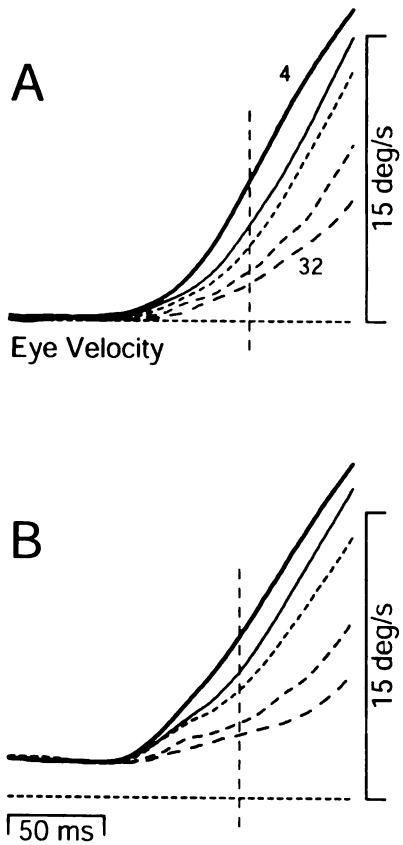

Figure 12. Quantitative analysis of the effect of initial target/eye velocity on the response to steps of target velocity as a functions of Δt. The three graphs show data from three monkeys. Each graph plots the normalized eye velocity response as a function of Δt for steps of apparent target velocity imposed both at the initiation and during maintenance of pursuit. Each response was normalized by dividing the mean eye velocity response by that for the same conditions when Δt was 4 ms. When steps of target velocity were imposed at the initiation of pursuit, we measured eye velocity 50 ms after the onset of the response when Δt was 4 ms. When steps of target velocity were imposed during the maintenance of pursuit, we measured the change in eye velocity by subtracting eye velocity 10 ms before the start of the response from that measured 50 ms after. Different symbols indicate different initial target velocities and velocity step sizes. Filled symbols plot responses to target steps imposed during fixation of a stationary target: 10°/s (filled squares) and 30°/s (filled circles). Open symbols plot responses to target velocity steps imposed during pursuit of a moving target: from 2 to 32°/s (open circles), from 2 to 12°/s (open squares), and from 20 to 30°/s (open diamonds). Error bars show the standard error of the mean.

Figure 12

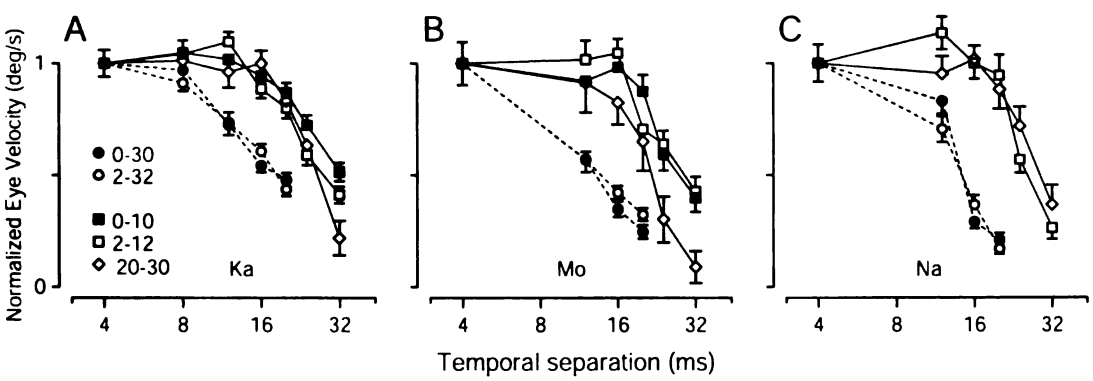
A
B
C
Normalized Eye Velocity (deg/s)
1
0
● 0-30
○ 2-32
■ 0-10
□ 2-12
◇ 20-30
Ka
Mo
Na
4
8
16
32
Temporal separation (ms)

Figure 13. Examples of the time course of eye velocity and position during apparent motion that caused deficits in the maintenance of pursuit. The top and bottom sets of traces show eye and target velocity and position when Δt was 4 ms (A) and 96 ms (B). Bold eye velocity traces show averages made after replacing saccades with straight line interpolations. Averages were made from 31 trials for A and 16 trials for B. Fine velocity and position traces show responses from 10 consecutive individual trials. In the individual eye velocity traces, the blank intervals indicate the times of saccades. The dots on the target position trace in B indicate the time and position of each flash of the apparent motion target. Data are from monkey Na.

Figure 13

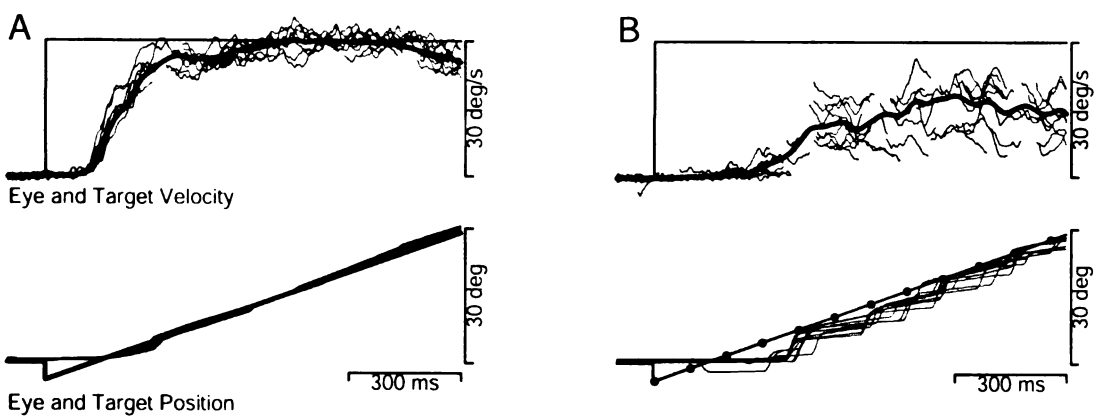
A
30 deg/s
Eye and Target Velocity
30 deg
300 ms
Eye and Target Position
B
30 deg/s
30 deg
300 ms

Figure 14. Effect of varying Δt on deficits in the maintenance of pursuit for target motion at 32°/s. A: Eye velocity traces showing responses when Δt was 48 ms. Fine traces show ten consecutive individual responses, with saccades replaced by blank intervals. Bold trace shows the average eye velocity after saccadic deflections of eye velocity had been replaced with straight line segments. B: Average eye velocity when Δt was 4, 32, 48 and 64 ms. Averages were computed from 10 to 15 trials taken from the same experiment on monkey Fi that produced Figure 8B.

Figure 14

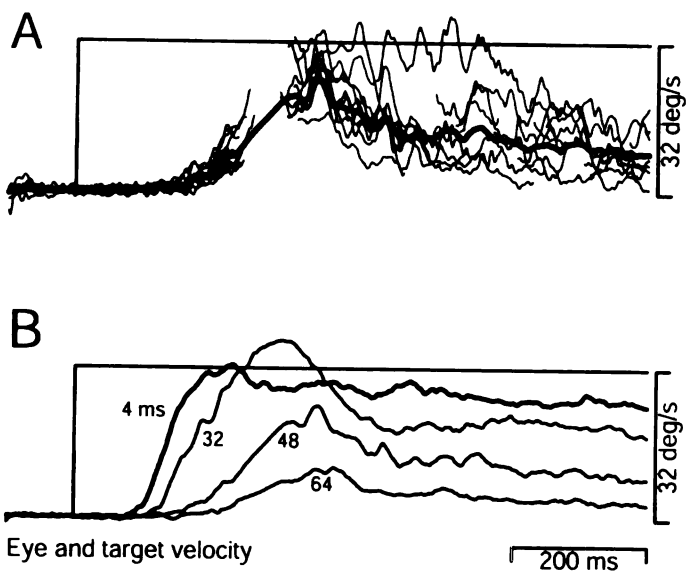

Figure 15. Demonstration that deficits in the maintenance of pursuit result from a failure of eye velocity memory. Each panel shows a step of target velocity and three averages of eye velocity. A: Responses of monkey Da when apparent target velocity was 32°/s. B: Responses of monkey Mo when apparent target velocity was 30°/s. Different line types show different sequences of Δt: bold traces, Δt was 4 ms throughout the trial; dashed traces, Δt was 64 ms (A) or 96 ms (B) throughout the trial; fine traces, Δt was initially 4 ms, then increased to 64 ms (A) or 96 ms (B) at the times marked by the arrows. Each average trace was computed from at least 15 trials.

Figure 15

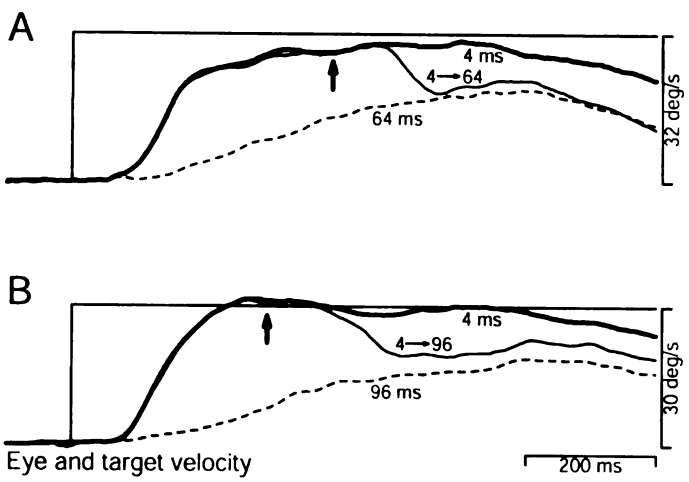
A
4 ms
4→64
64 ms
32 deg/s
B
4 ms
4→96
96 ms
30 deg/s
Eye and target velocity
200 ms

Figure 16. Examples demonstrating that during deficient maintenance of pursuit, eye acceleration is much less than expected given the residual retinal image motion. A, B. Results of an experiment using monkey El. For these panels, upward deflections represent leftward motion. C, D. Results of an experiment using monkey Da. The 4 panels shows averages of eye velocity for targets moving at apparent velocities of 32°/s (A, C) and 16°/s (B, D). Bold traces show responses when Δt was 4 ms and fine traces show responses when Δt was 64 ms. The arrows on the fine traces show the moments when image velocity (the difference of target and eye velocity) was 16°/s, so that the physical stimulus on the retina was the same at this point in the upper and lower panels. Each average trace was computed from about 15 trials.

Figure 16

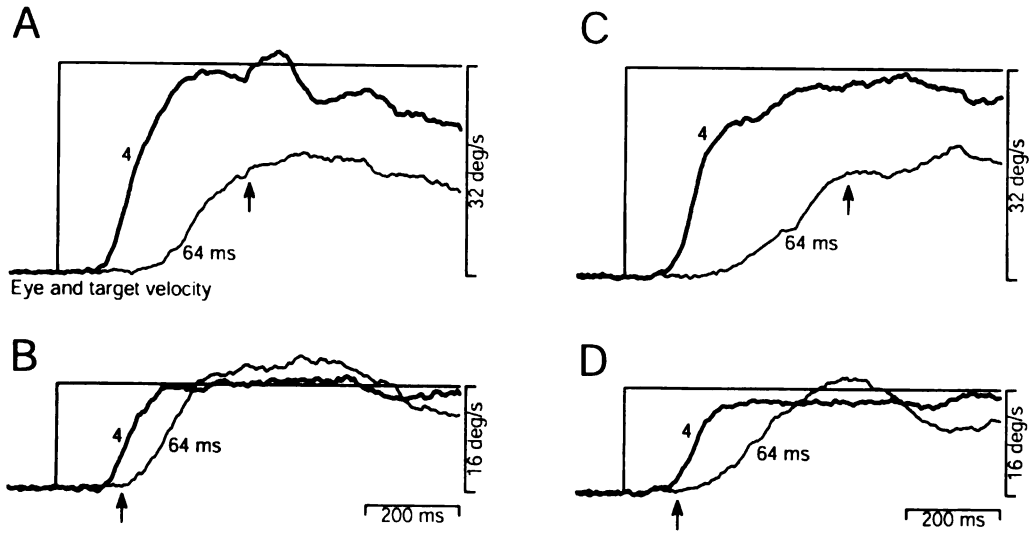
A
4
64 ms
32 deg/s
Eye and target velocity
C
4
64 ms
32 deg/s
B
4
64 ms
16 deg/s
200 ms
D
4
64 ms
16 deg/s
200 ms

Figure 17. Experiments demonstrating that the appearance of maintenance deficits does not depend solely upon the retinal image motion. Each panel shows average eye velocity for apparent target velocities that stepped first from 0 to 15°/s and subsequently from 15 to 30°/s. A: Responses of monkey Mo. B. Responses of monkey Na. Bold traces show average eye velocity when Δt was 4 ms. Fine traces show average eye velocity when Δt was 60 ms (A) or 96 ms (B). Each average was computed from 30 or more trials. Neither the first nor the second step of target velocity was accompanied by a step of target position.

Figure 17

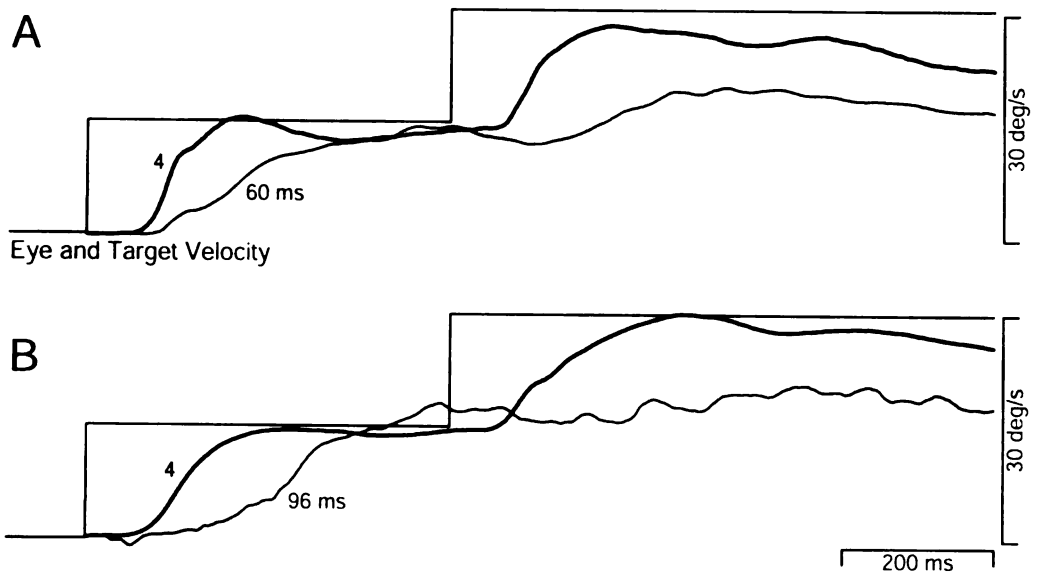

Chapter 3

Neural Basis of Illusory Changes in Speed Produced by Apparent Visual Motion

Mark M. Churchland and Stephen G. Lisberger

Abstract

We recorded behavioral, perceptual, and neural responses to apparent visual motion consisting of a sequence of briefly-illuminated stationary targets. It is generally thought that increasing the interval between flashes would degrade motion. Consistent with our previous findings, for a range of flash separations ocular smooth pursuit of apparent motion showed increased initial eye acceleration, relative to pursuit of smooth motion. The increased eye acceleration was appropriate for a target velocity greater than the actual velocity. Consistent with this, in humans such flash separations produced an increase in the perceived speed of the stimulus. To determine the neural basis of the illusory increase in speed, we recorded the response of single neurons in extastriate visual area MT of awake behaving rhesus monkeys. The flash separations associated with increased pursuit eye acceleration produced diminished responses, relative to smooth motion, in nearly all MT neurons. However, consideration of the population response revealed that neurons with slow preferred speeds were more affected than those with fast preferred speeds. As a result, the population response was shifted towards higher speeds. We constructed a simple decoding model based on opponent motion and vector averaging. When applied to the recorded neural responses, the model successfully predicts an increased estimate of speed the flash separations that produced increased eye acceleration. The model also accounts for the changes in pursuit latency produced by apparent motion, and for the decline in eye acceleration that occurs at larger flash separations. We tested a number of other decoding models which failed to account for one or more aspects of behavior. We conclude that apparent motion produces a number of changes in the neural estimate of speed, and that all such changes can be accounted for

if speed is estimated from the MT population response via a vector-average based upon opponent motion.

Introduction

It is often said that a particular sensory quantity is represented via 'population coding'. Inherent in this conception are the following ideas. First, the relationship between the sensory quantity and a neuron's response is not monotonic. Rather, neurons have roughly bell shaped tuning curves, centered on a preferred stimulus. Second, these tunings are relatively broad, so that a given stimulus excites a large proportion of neurons. Third, neurons are often tuned for multiple variables. Because of these properties, a single neuron can do little on its own to indicate the value of the sensory quantity. A neuron may fire at half its maximal firing rate because a) the sensory quantity is smaller than preferred, b) the sensory quantity is larger than preferred, or c) the sensory quantity is near the preferred, but the stimulus is sub-optimal in some other dimension. Estimating the sensory quantity therefore requires observation of multiple neurons with different preferred stimuli. Thus, the hallmark of population coding is not that *encoding* involves a population of neurons; this is true of virtually every way in which the mammalian brain represents the sensory world. Rather, it is that *decoding* depends on the response of the population. Therefore, to fully understand an instance of population coding we need to know both how responses are related to the sensory world, and how the sensory quantity of interest is subsequently estimated from the population response.

A number of methods for decoding a population response have been suggested by theoretical work (e.g. Salinas and Abbot, 1994; Pouget et al. 1998), and experimental studies have attempted to understand if and how these methods are used by the nervous system. In the case of visual cortex, much of the work has focused on the estimation of

orientation and the direction of motion from the responses of neurons in primary visual cortex (V1) and in the middle temporal area (area MT). Neurons in V1 and MT are tuned with respect to orientation and/or the direction of motion, and a natural assumption is that the decoding of V1 and MT responses provides the nervous system with estimates of orientation and direction. Three converging lines of evidence support this assumption. First, a number of visual illusions appear to depend upon changes in the response of orientation or direction tuned neurons. For example, Gilbert and Wiesel (1990) showed that the orientation tuning of V1 neurons was altered by surrounding stimuli in a manner consistent with the perceptual shift in orientation induced by such stimuli. The waterfall illusion and motion repulsion effects can also be explained by reference to the relative responses of neurons within a population (Tootell et al. 1995; Schrater and Simoncelli 1998). Second, the assumption is supported by a number of studies comparing psychophysical performance with the performance of individual MT neurons (Shadlen et al. 1996; Britten et al. 1992, 1996; Salzman et al 1990; Newsome et al. 1989). Third, a number of studies have observed behavioral responses evoked when multiple motion signals are present within area MT, and found them consistent with a population-based decoding mechanism (Salzman et al. 1992; Groh et al. 1997; Lisberger and Ferrera 1997; Kahlon and Lisberger 1999). The most complete of these approaches is that of Groh et al., who added a microstimulation-evoked signal to the ongoing response of MT. They then used pursuit eye movement as an index of the actual readout of direction extracted from MT. This approach allowed them to compare the predictions of two distinct direction-decoding schemes with the actual pursuit direction.

An obvious next step in the study of population codes and visual cortex would be to 1) record the response of a neural population to a set of stimuli, 2) apply different decoding schemes to this data, and 3) compare the results with perception or behavior evoked by the same stimulus set. In this paper we apply this strategy to the question of how the nervous system estimates the speed of visual motion. We record the responses of multiple MT neurons with varying preferred speeds. Using the same stimulus set, we record pursuit eye movements. It is natural to compare pursuit with the responses of MT neurons, as the visual motion signals that guide pursuit are known to depend in large part on area MT (Komatsu and Wurtz, 1989; Dursteler et al. 1988; Newsome et al. 1985). Furthermore, the close relationship between pursuit eye movements and stimulus speed (e.g. Lisberger and Westbrook 1985, Krauzlis and Lisberger, 1994) allows us to gauge the estimate of speed (presumably extracted from MT) that is used by pursuit. Our stimulus set is based upon apparent motion. The utility of apparent motion lies in its ability to create parallel changes in the responses of MT neurons (Mikami et al. 1996, Newsome et al. 1996) and in the response of the pursuit system (Churchland and Lisberger 2000). In particular, apparent motion creates an illusion of increased speed reflected in both perception and pursuit. We use the recorded MT population response as the input to different models for how speed could be decoded from the MT population response. These models were then tested by comparing their estimates of speed with the estimates of speed indicated by pursuit behavior. These comparisons reveal why apparent motion produces an increase in perceived speed, and provide constraints upon the mechanism by which speed is extracted from the population response of MT.

Methods

Behavioral and neural recording experiments were performed on two adult male rhesus monkeys (*macaca mulatta*) that were trained to fixate and pursue visual targets for juice reward. Monkeys were implanted with head restraints and scleral eye coils as described in the methods of the first chapter. Following initial training, monkeys were implanted with a stainless steel cylinder (Christ) placed over a 20 mm diameter circular hole cut in the skull. Details of anesthesia and post-surgical analgesia are as described in the methods of the first chapter. Neural recording experiments were then conducted. Following completion of these, pursuit behavior was recorded. For each experimental session, the monkey voluntarily exited his home cage and sat in a custom constructed primate chair. During the experimental session, the monkey sat in the chair with his head supported via the implant, which prevented any movement of the head. During the course of the experiment the monkey was rewarded with juice or water, according to his preference. Following each experiment (which lasted 2-4 hours) the animal was returned to his home cage. Methods had been approved in advance by the Institutional Animal Care and Use Committee at the University of California, San Francisco.

Behavioral and psychophysical experiments were performed on five human subjects who were unaware of the purpose of the experiments. During the experiments subject sat with their heads immobilized via a chin support, two forehead supports, and an elastic strap. Methods had been approved in advance by the Committee on Human Research at the University of California, San Francisco.

Stimulus presentation

Stimulus presentation was similar to that described in the methods section of Chapter 1. For experiments using monkeys, visual stimuli were presented using a 12-inch diagonal analog oscilloscope. The display was positioned 30 cm from the monkey so that it subtended a horizontal visual angle of 50° and a vertical visual angle of 40°. For experiments using humans, a 19-inch oscilloscope was placed at a distance of 50 cm, so that it subtended horizontal and vertical visual angles of 42° and 34°. For all experiments, the stimuli were square patches of moving dots. Patches contained on average 24 randomly spaced dots, bounded by an 8° square aperture, which was not itself visible. Individual dots were roughly 0.2° across, and their luminance was 1.6 cd/m^2. For pursuit experiments, the dots and their bounding aperture moved together across the screen. For psychophysical and recording experiments, the dots moved 'behind' the aperture: dots disappeared upon reaching the far edge, while new dots appeared on the near edge. Each single moving dot was in fact only apparently moving, and consisted of a sequence of briefly illuminated stationary dot flashes, with a consistent spatial separation (Δx) and temporal separation (Δt) between each flash. The sequence of flashes yields apparent motion with a speed given by $\Delta x/\Delta t$. When Δt and Δx were small (less than 20 ms and 0.25°), the impression was of a single dot moving smoothly and continuously. For larger flash separations, the motion became noticeably un-smooth. Speed, Δt, and Δx were the same for all moving dots within a patch. We therefore describe each patch stimulus in terms of the dot speed and Δt. Δx can then be calculated as speed*Δt, and it should be kept in mind that, for a given speed, changes in Δt are associated with changes in Δx. To maintain a constant mean luminance of the target, the

luminance of each dot flash was varied linearly with the time between flashes (e.g. if Δt was doubled, so was the luminance of each flash). Each individual target flash was very brief (160-2560 μs). The duration increased with Δt, due to the extra time necessary to increase the luminance. All dots within the patch were updated at virtually the same time; i.e. presentation of dots during a flash was essentially synchronous, with no dots being present until the next flash. The specifications of the display oscilloscopes indicate that the phosphor will decay to 10% of its maximal level in 10μs to 1ms.

Visual stimuli were presented in 'trials'. Each experiment consisted of a list of trials, each of which lasted a few seconds. The presentation order of the list was shuffled randomly, and each trial was presented once. After all trials had been completed, the presentation order was again shuffled and the process repeated. For some experiments, subjects were required to satisfy fixation constraints, or to respond within a particular time interval. If these requirements were not met, the trial was aborted, and was placed at the end of the presentation list, to be completed before the list was shuffled and repeated. For all experiments, such occurrences were rare.

Human Psychophysics

Human subjects viewed two patches of moving dots and were asked to report which patch appeared faster. Subjects were naive as to our hypothesis. At the beginning of each experiment, eye movements were recorded to verify that fixation requirements were being met. Following this initial verification, the eye tracking equipment was usually turned off. Tracking was turned off because it was often difficult to maintain a good lock on eye position for long periods of time, as subjects' heads occasionally moved slightly. The eye tracker (described in more detail below) emitted loud noises when a

lock was lost. Subjects found these noises distracting. Given the consistent fixation exhibited by subjects, we turned tracking off rather than interrupt the experiment to recalibrate the tracker.

Each trial began with the appearance of a stationary point in the center of the display. Subjects were asked to fixate this point visually throughout the entire trial. After 800 ms of fixation, a patch of dots (as described above) was presented centered 4.5° above the fixation point, for 300-450 ms (random duration). 300 ms following the offset of this first patch, a second patch appeared 4.5° below the fixation point, also for 300-450 ms. Following the offset of the second patch, subjects were given 1400 ms in which to press one of two buttons, indicating which patch appeared to move faster. One of the two patches, termed the 'standard' patch, always moved at 16°/s, and had a variable Δt, from 4-64 ms. The other patch, termed the 'comparator' patch, always had a Δt of 4 ms (i.e. it was effectively smooth motion) but had a variable speed from 11-24°/s. On half the trials (chosen randomly) the standard was the first patch, and the comparator was the second patch. For the other half, the standard was the second patch, and the comparator was the first. Subjects' responses were analyzed by calculating the percentage of trials for which the standard was judged to be faster than the comparator, as a function of the speed of the comparator.

Human Pursuit

Each pursuit trial began with the appearance of a fixation point. Following a 700-1100 ms interval, the fixation point was extinguished, and a rightwards-moving pursuit target appeared, offset 1-1.5° to its left. Pursuit targets were patches of dots, as described above. The offset situated the center of the pursuit target eccentrically on the retina

(though given its size it still overlapped the fovea). The size of the offset and the resulting eccentricity was customized for each subject, to reduce the occurrence of early saccades. Pursuit targets were patches of dots, as described above. Subjects were instructed to visually track the target as it moved across the display. All targets moved for 1000 ms before being extinguished, except for targets moving at 24 and 32°/s, which were extinguished after 800 and 600 ms when they neared the edge of the display. Eye movements were recorded using a Fourward Technologies Dual Purkinje Image Tracker (Generation 6.1). The auto-stage and focus servos were disabled to avoid introducing head position artifacts into the eye position signal. An eye velocity signal was calculated by analog differentiation of the eye position signal. A 25 Hz filter was associated with the differentiation.

Monkey Pursuit

Monkeys were trained to fixate a central point, and to track moving targets when the central point was extinguished. The details of the trials and stimuli were similar to those used for human subjects. Trials began with a fixation point, which was then extinguished and replaced by a rightwards-moving patch target that began centered 6.4° (monkey Mo) or 5.2° (monkey Q) to the left. These eccentricities were the average receptive-field eccentricity of cells recorded in each of the two monkeys. We had attempted to record from these eccentricities, so that pursuit stimuli centered at the same eccentricity would produce few early saccades. Eye movements were monitored using the scleral search-coil technique of Judge et al. (1980), and eye velocity was calculated via analog differentiation as described for human pursuit. Monkeys were rewarded with juice or water if eye position was within 3° of the fixation point and 6° of the center of

the pursuit target for the duration of the trial. We used the (somewhat larger than usual) 6° fixation window because of the 8° size of the tracking stimulus and because large Δt's produced poor pursuit for faster stimuli. In well-trained monkeys larger fixation windows do not decrease motivation or the quality of tracking.

Neural recordings

Single, isolated neurons were recorded from the middle temporal area (MT) of the brain of two awake monkeys. Monkeys were the same two that were used for the pursuit experiment. Neurons were recorded extracellularly with sharp, 1-3 MΩ, tungsten microelectrodes (Frederick Haer). The electrode location was determined by a guide tube inserted in a plastic grid (Crist), which was placed each day in the implanted cylinder. The guide tube was sharp, and following application of local anaesthetic (1% lidocaine) was pressed by hand through the dura. The vertical position of the electrode was controlled by a hydraulic microdrive (Kopf) mounted on a stage (Crist). The stage was secured to a cylinder extension (Crist) that also aligned the plastic grid. The voltage recorded by the electrode was amplified by a head-stage and amplifier (Dagan), band-pass filtered from 100 Hz to 10 KHz, and viewed on an analog oscilloscope. The voltage signal was also fed to an audio amplifier and speakers.

A trigger was applied to the incoming voltage, and all waveforms that exceeded the trigger were displayed on an oscilloscope. Two time/amplitude windows created by a dual window discriminator (Bach, DD15-1) were placed so as to surround the waveform produced by the cell to be isolated. A logic pulse, signaling the occurrence of an accepted spike, was produced whenever a triggered waveform passed through these windows. Using this method, it was possible to isolate the spikes of a single neuron,

even in the presence of similarly large spikes produced by nearby neurons, based on the shape of the spike waveform. Accepted waveforms were stored on a storage oscilloscope to verify that only one waveform shape was present, and that there was the expected refractory period between spikes. This latter criterion allows us to insure that two similar waveforms are not mistaken for a single unit.

The experiments to be performed on each cell lasted 20-30 minutes. Each isolated neuron was rated according to our level of certainty that perfect isolation was maintained throughout the recording period. Originally, we intended to restrict our analysis to neurons with perfect isolation. Much of our analysis is based on the speed-tuning of the recorded neurons. As neighboring neurons can have different speed-tunings, it was important to record from only one neuron at a time. However, we also analyzed a number of neurons whose isolation was imperfect. We considered isolation imperfect because we estimated that a) a spike from the isolated unit on rare occasions failed to fall within the windows that triggered acceptance, or b) a spike from another unit on rare occasions fell within the windows that triggered acceptance. Virtually all such imperfectly isolated units nonetheless showed tight, uni-modal speed-tuning. This is not surprising, as we estimate that missed-triggers and mis-triggers, though likely present, were uncommon for these isolations, and as nearby neurons tend to have similar speed tunings (Cheng et al. 1994), reducing the impact of imperfect isolation. We therefore saw no reason not to include these isolations in our analysis. The small contribution made by imperfectly excluded neurons is not expected to alter our interpretation.

Area MT was located based on 1) the well described response properties of MT cells, 2) the described response properties of cells in surrounding areas V4 and MST, and

3) the progression of white matter, gray matter, and lumen encountered prior to reaching MT. A successful penetration typically encountered the large-receptive-field directionally-selective cells of area MST, then encountered lumen, and finally emerged into MT. We wished to record from MT neurons with receptive fields near the fovea, at the lateral extent of MT. For monkey Q, the expected topography described above was not found when we moved to the lateral (foveal and peri-foveal) extent of MT. Instead, the peri-foveal part of MT was located directly below an area with small receptive fields and directionally non-selective cells. We presumed this area to be V4. The transition from this area to MT was distinguished not by lumen, but by a fovea-ward shift in receptive fields accompanied by the sudden presence of strong directional responses. Once in MT, virtually all cells were directionally selective. This landmark was less clear than lumen, which is unmistakable. Although we think it unlikely, it is possible that some of the neurons we recorded from monkey Q were, in fact, directionally selective V4 neurons near the V4/MT border.

Recordings were made during presentation of stimuli in individual trials. Each trial began with the appearance of a fixation point. A stimulus was introduced 800 ms later, was present for 500 ms, and was then extinguished. All stimuli were patches of moving dots, as described above. The fixation point was extinguished 300 ms later, and the animal was rewarded with a drop of juice. Monkeys were required to fixate throughout the trial with an accuracy of 4-5°. Actual fixation was typically much more accurate, with the exception that fast stimuli presented near the fovea evoked a small response that the monkey was unable to entirely suppress. Upon isolating a neuron, we first estimated its preferred direction. To do so we employed a list of 8 trials, each of

which presented motion in a different direction. Dot motion was presented within an 8° square window if the receptive field of the cell was known roughly, or within a larger window if it was not. Preferred direction was estimated subjectively from histograms of the responses to these eight directions. The receptive field of the neuron was then estimated. This was done either by using a list of trials that presented dot-patches at different spatial locations, or by manually moving a dot-patch to find the receptive field edges. For monkey Mo, receptive field eccentricity (measured as the distance from the fixation point to the center of the receptive field) varied from 5 to 8.9°, with a mean of 6.4° and a standard deviation of 1.1°. For monkey Q, eccentricity varied from 2.7 to 7.9°, with a mean of 5.2° and a standard deviation of 1.2°. Receptive fields sizes were of the same order as the 8° square patch stimulus. Following these preliminary analyses, we presented a list of 52 trials that presented apparent motion. Apparent motion stimuli were 8° square dot patches, as described in detail above. Each trial presented a patch of moving dots centered on the receptive field of the neuron. Dots moved in either the preferred direction of the neuron, or in the opposite, 'null', direction. The speed of motion was varied from 0°/s to 128°/s. All speeds were presented using a Δt of 4 ms. For all but the fastest speeds, this Δt should have produced motion that was effectively smooth from the standpoint of MT neurons. When the stimulus speed was 16°/s, we also employed Δt's of 12, 16, 20, 24, 32, 44, and 64 ms. When the stimulus speed was 32°/s, we also employed Δt's of 12, 16, 24, 32, and 44 ms. Trials were shown and data collected until histograms showed a reasonable signal to noise ratio, judged subjectively. This typically took 15-30 minutes.

Data Acquisition and Analysis

Experiments were controlled by a in-house software running on a UNIX workstation, as described in Chapter 1. Pursuit was analyzed, as described in Chapter 1, by calculating the peak eye acceleration during pursuit initiation, and the 'acceleration latency': the latency to reach 80% of the peak. For the eccentricities we used, saccades during the rising phase of pursuit were rare, and trials in which a saccade occurred before the end of the rising phase were excluded from analysis. Only saccades following the end of the rising phase were interpolated. An exception to this rule was made for responses to some targets with large flash separations. Such targets produced very delayed pursuit and weak initial eye acceleration, making saccades during the rising phase inevitable. Responses to such targets were included in the analysis after interpolation of the saccades (see Chapter 1 for details of saccade interpolation). For each target type, we were then able to calculate the average peak acceleration and average acceleration latency. As examples, we also show time-based averages of eye velocity. These averages were made by aligning individual trials, after saccade interpolation, on the onset of target motion. These averages slightly underestimate the magnitude of initial eye acceleration, due the small variability in the latency of pursuit.

For single neuron responses, we analyzed the data in a number of ways. We show examples in which the response of a neuron is plotted, as a histogram, as a function of time. These histograms had a bin width of 32 ms. For each neuron, we also calculate the mean and standard error of the spike rate over a 600 ms interval that begins with the onset of the stimulus and ends 100 ms after the onset of the stimulus. For many analyses, we analyze the responses of neurons in terms of their 'directional response', which we

define as the difference between the average spike rates evoked by motion in the preferred and null directions. For each neuron, we also abstract two scalar quantities: the limit of directionality and the preferred speed. The limit of directionality was estimated by plotting the directional response versus Δt, and fitting with a sigmoid (as in Figure 2). The limit of directionality was defined to be the Δt at the inflection point (the point of half-decline) of the sigmoid. The preferred speed was estimated by plotting the directional response versus speed, and fitting the data (as in Figure 6) using the following function:

$$G(s) = R_{\max}\left(e^{-\left[\frac{\log\left(\frac{s}{\mu_s}\right)}{\sigma_s + \varsigma \log\left(\frac{s}{\mu_s}\right)}\right]^2} - e^{-\left(\frac{1}{\varsigma^2}\right)}\right)$$

where R_{max} is the maximal firing rate, μ_s is the preferred speed (the peak of the function), s is the speed of the stimulus, σ_s is the tuning width and ζ is the skew of the cell, after the background firing rate has been subtracted. R_{max}, μ_s, σ_s, and ζ were varied to achieve an optimal least squared fit to the data.

Results

An increase in perceived speed

The general strategy of this chapter is to compare, for different parameters of apparent motion, the responses of MT neurons with pursuit responses. In doing so, we wish to use initial pursuit eye acceleration as a gauge of the pursuit system's estimate of target speed. We wish to assume that the changes in eye acceleration caused by changes in Δt are due to changes in the estimate of speed caused by the changes in Δt. For example, in chapter 1 we reported that initial eye acceleration was increased for some Δt's. We hypothesized that the increase results from an elevation of the neural estimate of speed used by pursuit. We argued for this hypothesis by arguing against the most obvious competing hypothesis: that the increase results from motor based compensation for longer pursuit latencies. We now report an experiment that demonstrates directly that the sensory estimate of speed in increased for some Δt's.

Human subjects were asked to make a perceptual judgement based on speed. The task is illustrated in Figure 1A. Figure 1B shows the performance of five subjects. As shown by the blue symbols, when the Δt of both patches was 4 ms, subjects made the perceptual judgment well. When the comparator moved at 11 or 14°/s, the 16°/s standard was usually judged to be faster (on average 97% and 82% respectively). When the comparator moved at 19 or 24°/s, the standard was rarely judged to be faster (on average 12% and 0.4% respectively). When the Δt of the 16°/s standard was increased (see below for exact Δt's), for 4 of the 5 subjects the psychometric function shifted to the right (red points and curves). The standard was judged to be faster more often as a result of the larger flash separation. This is most easily appreciated when both the standard and

comparator moved at 16°/s. The standard (with an increased Δt) was judged to be faster by four of the five subjects (50, 73, 80, 70, and 76% of the time, 50% being chance). The increase in the proportion of faster responses was significant for the four subjects that showed the effect ($p<0.01$ for each). Thus, a larger separation between target flashes created an illusory increase in speed.

The larger flash separations used to create the perceptual illusion were different for each subject. They were chosen based upon recordings of pursuit eye movements made immediately prior to the perceptual task. For the perceptual experiment, we chose a Δt in the range that had produced increased initial eye acceleration during pursuit of a 16°/s patch of dots. The chosen Δt varied from 32 to 64 ms (with corresponding Δx's of 0.51-1.0°), depending on the subject. Such an approach was necessary to keep the parameter space of the perceptual experiments tractable. One subject failed to show the perceptual illusion, at least for the flash separation we chose (inverted triangles). This subject also failed to show an increase in initial pursuit initiation at any of the temporal separations used (data not shown). Either this subject does not show the illusion (perhaps for both perception and pursuit) or we simply failed to find the most effective flash separation to demonstrate it. The latter is possible if the increase in pursuit acceleration were too small to be noticed given the limited number of trials performed, or occurred over a very limited range of flash separations.

MT neurons lose directionality as flash separation is increased

Action potentials of single MT neurons were recorded as described in Methods. Figure 2A shows the response of an MT neuron to motion at 16°/s. For a Δt of 4ms (which produced effectively smooth motion), the neuron was strongly directional,

showing a robust response to preferred-direction motion, and a suppression of baseline activity for null-direction motion. The response to preferred-direction motion decreased as the flash separation was increased. At the largest Δt (64 ms), the neuron completely lost the ability to signal the direction of motion. Figure 2C shows a similar set of histograms for a different neuron. Unlike the neuron above, this neuron continues to respond to preferred-direction motion even when Δt was 64 ms. However, when Δt was 64 ms, the neuron also responded to null-direction motion. Like the neuron above, this neuron lost the ability to signal the direction of motion. Figure 2B and D plot, as a function of Δt, the 'directional response', defined as the difference between the preferred-direction response and the null-direction response. The responses are averaged over a period from the onset of the stimulus, until 100 ms after its offset. Graphed this way, both neurons show a very similar effect: the directional response of each neuron remains near normal until a Δt of 20-24 ms (Δx of 0.32-0.38°), falls sharply around 32 ms (0.51°), and is near zero by 64 ms (1.0°). We define the 'directional limit' of each cell to be the Δt that corresponds to the half-decline point of the sigmoidal fit to the directional responses. Both cells in Figure 2 had a directional limit of 37 ms, corresponding to a Δx of 0.59°.

Figure 3 shows responses of the same two neurons as Figure 2, but to dot motion at 32°/s, rather than 16°/s. The overall pattern is similar: both neurons lost their directional response with increasing flash separation, though in different ways. Expressed in terms of Δt, he directional limit of the two cells was much smaller when dot motion was 32°/s (22 ms for the first cell and 16 ms for the two cells) than when dot motion was 16°/s (37 ms for both cells). These temporal separations correspond to

spatial separations of 0.70° and 0.51° for 32°/s, and 0.59° and 0.59° for 16°/s. Thus, for both neurons and both stimulus speeds, directionality was lost when Δx exceeded around half a degree. It thus appears that for these stimulus speeds, directionality is lost primarily because Δx becomes too large, and not because Δt becomes too large. These results are in keeping with the findings of Mikami et al (1986). Mikami et al. used oriented bars, rather than patches of dots, but also found that MT neurons ceased to fire in a directional manner as flash separation increased. They reported limits on both the maximum Δt and the maximum Δx that allowed directional firing. The latter was the primary limit for speeds above 16-32°/s.

As suggested by the examples in Figures 2 and 3, there was considerable heterogeneity in how the directional response was lost as flash separation was increased. To compare the responses of different neurons, for each neuron we computed the average spike rate from the onset of the stimulus until 100 ms after the offset. We then corrected these firing rates by subtracting, for each neuron, the baseline firing rate. Finally, we normalized the firing rate of each neuron so that the difference between the response to the preferred and null directions was one when Δt was 4 ms. Figure 4 plots, for a 16°/s stimulus, the resulting response for each MT cell to motion in both the preferred and null directions. Different colors indicate responses for different flash separations. When Δt was small (4 or 12 ms), the response to the preferred direction was larger than the response so the null direction, and the points plot on or near the top diagonal line. The points are distributed along the length of the line, reflecting variability in the response to the null direction. For motion in the null direction, some neurons showed strong suppression, while a few showed responses that were nearly half as large as those for the

preferred direction. For a Δt of 64 ms the difference in response between the two directions is greatly reduced, and the points plot closer to the lower diagonal line. Again, the points are distributed obliquely along the line. Some neurons showed large responses to both directions of motion, while others showed little or no response to either direction.

Figure 4 illustrates the considerable heterogeneity in the response to apparent motion, but also demonstrates that all neurons show a progressive loss in their directional response as Δt is increased. Figure 5 illustrates this progression, and shows the average response across the recorded neurons. Open and closed symbols plot the average response to the preferred and null directions as a function of Δt. For a stimulus speed of 16°/s, there was little change in the response until Δt exceeded 16 ms (Δx = 0.26°). For larger Δt's the difference between the two directions steadily declined: the preferred-direction responses became smaller and the null direction responses became larger. For a Δt of 64 ms (Δx = 1.0°), there was little difference in the average response to the two directions. For a stimulus speed of 32°/s, even a Δt of 12 ms (Δx = 0.38°) evoked a small change in the average response. Again, the difference between the two directions decreased steadily as Δt increased, with little difference observed for a Δt of 44 ms (Δx = 1.4°).

The effect of flash separation depends upon preferred speed

Responses of each cell were recorded, using a Δt of 4ms, to a range of different dot speeds. Figure 6C and F show the response of two MT neurons as a function of stimulus speed. We estimated preferred speed by taking the peak of the fit. The neuron in C had a preferred speed of 8.0°/s, while that in F had a preferred speed of 24°/s. As illustrated by the top and bottom rows of Figure 6, both neurons showed a decline in

directional firing as Δt was increased. However, the response of the neuron whose preferred speed was 8.0°/s dropped off more swiftly than did that of the neuron whose preferred speed was 24°/s. The limit of directionality was 20 ms (0.32°) for the former and 42 ms (0.67°) for the latter. In general, neurons with larger preferred speeds tended to have larger limits of directionality, as illustrated in Figure 7. The scatter plots in Figure 7 shows the considerable variability in the limit of directionality across neurons, and illustrates that there was a strong positive relationship between preferred speed and the limit of directionality for both stimulus speeds and both monkeys. For a stimulus speed of 16°/s, a regression analysis yielded slopes (expressed in terms of Δt) of 0.54 and 0.43 ms/°/s for monkeys Mo and Q. These effects were significant ($p < 10^{-7}$ and 10^{-2}). For a stimulus speed of 32°/s the directional limits, expressed in terms of Δt, were roughly half as large, and the resulting slopes roughly half as steep: 0.27 and 0.26 ms/°/s ($p < 10^{-5}$ and 10^{-2} for the two monkeys). The mean directional limits for monkey Mo were 40 ms for a stimulus speed of 16°/s and 24 ms for a stimulus speed of 32°/s. These temporal flash separations correspond to spatial flash separations of 0.64° and 0.77°, respectively. For monkey Q, the limits were 35 ms for 16°/s and 22 ms for 32°/s, corresponding to spatial flash separations of 0.59° and 0.69°. The limits for the two stimulus speeds are more similar when expressed in spatial terms than when expressed in temporal terms. This is in keeping with our earlier inference that, for these faster speeds, MT neurons lose directionality primarily because their spatial integration abilities are exceeded. Such an interpretation is also consistent with the correlation between preferred speed and the limit of directionality. Mikami et al. found that neurons with high preferred speeds tended to have larger maximum Δx's for which they maintained

directionality. If we accept that, for the 16 and 32°/s stimuli we used, spatial separation was the factor limiting the directional response, then neurons with faster preferred speeds ought to be able to withstand larger flash separations. Note that this is true even though we have chosen to express the flash separation in terms of Δt, as both Δt and Δx increase together for a given speed.

Figure 7 also shows distributions of preferred speeds for both monkeys. We recorded from cells with a wide range of preferred speeds: from 0.5 to 76°/s for monkey Mo and 2.5 to 61°/s for monkey Q. Plotted on the linear scale as shown, slow preferred speeds were most common. However, with bins of equal size on a logarithmic scale (not shown), preferred speeds in the 16-32°/s range appear most common. The sampling of preferred speeds was almost certainly biased to some degree by the search stimulus we used (typically 10-30°/s). From the point of view of the analysis in this thesis, the bias is acceptable. We are not interested in the responses of cells that do not respond to either our 16 or 32°/s test stimuli.

Population responses

The responses of an individual MT neuron do not reveal an obvious basis for the illusion of increased speed produced by apparent motion. Neurons became less responsive and less directional as Δt was increased. It therefore seems likely that the illusion may be due to changes manifested at the level of the population. The black symbols in the upper left panel of Figure 8 show the population response derived from the 73 neurons recorded in monkey Mo during stimulus motion at 16°/s with a Δt of 4 ms. The response of each cell is plotted against the vertical axis, and positioned on the horizontal axis according to the cell's preferred speed. Responses to preferred-direction

motion are plotted against positive values of preferred speed, while responses to null-direction motion are plotted against negative values of preferred speed. The inclusion in the population response of null-direction responses reflects our belief that neurons with preferred directions opposite the direction of motion may contribute to the estimate of speed. The response of each cell was normalized so that the directional response to the preferred speed was one. Responses greater than one are thus possible if there was some positive response to motion in the null direction. Baseline activity levels were subtracted, so that responses less than zero indicate suppression. As expected, for a Δt of 4 ms, most cells showed little response, or even suppression, for motion in the null direction. For preferred direction motion, most cells showed moderate to large responses. As expected, cells with preferred speeds near that of the stimulus (16°/s) responded most robustly.

The red symbols in the upper left panel of Figure 8 show the responses of the same 73 neurons to a 16°/s stimulus with a Δt of 32 ms. For motion in the preferred direction, the majority of red symbols plot slightly below the black symbols, while for the null direction, the majority of red symbols plot slightly above the black symbols. The centers of mass of the two population responses are shown by the vertical black and red lines. For a Δt of 32 ms, the center of mass is shifted leftwards, towards smaller speeds. This leftwards shift is due to the larger responses to the null direction of motion. The lower left panel of Figure 8 shows the same analysis for 34 cells recorded from monkey Q. Again, an increase in flash separation from 4 to 32 ms produces a shift in the center of mass towards slower speeds.

It has been suggested that neural estimates of motion may depend upon an opponent computation (Levinson and Sekuler 1975, Adelsen and Bergen 1985, Heeger et

al. 1999). The proposed opponency occurs between neurons with opposite preferred directions, and is thus expected to influence the neural estimate of direction. Such opponency could also influence the neural estimate of speed. The right panels of Figure 8 show 'opponent population responses' based on the directional response of the neurons we recorded. As described above, the directional response is the difference between the response to the preferred and null directions. The opponent population response is thus the difference between the right and left hand sides of the 'raw population response' shown in the left panels. Black and red symbols plot responses for Δt's of 4 and 32 ms respectively. As expected, the directional response of most cells is reduced for the larger flash separation. However, not all cells show the same reduction. Consistent with Figure 7, neurons that prefer slow speeds show a large reduction in directional firing, whereas neurons that prefer fast speeds respond almost as well to a Δt of 32 ms as to a Δt of 4 ms. As a result, the center of mass is located at a faster speed when Δt is 32 ms (red vertical line) than when Δt is 4 ms (black vertical line). A similar, though less profound shift of the center of mass was seen if one considered only responses to the preferred direction (i.e. the right hand side of the raw population response).

Note that in Figure 8, only responses to the preferred and null directions are shown. Had we recorded responses to many directions of motion, we would have been able to compute a complete representation of the population response, across all speeds and all directions. Instead, due to the limited time for which cells could be held (typically not more than 1 hour) we presented motion in only the preferred and null directions. Thus, the panels of Figure 8 show a slice though the population response along the preferred/null axis. As there was no noticeable or statistically significant interaction

between a cell's preferred direction and the response to apparent motion (data not shown), the preferred-direction responses of all cells are grouped together, on the right hand side of the plot, as if every cell preferred motion to the right. The null-direction responses are shown on the left-hand side. These are plotted as if they were the responses of different neurons, with opposing direction-tunings, though they are in fact the same neurons responding to the opposite-direction stimulus.

Comparison of neural responses and pursuit

The population responses shown in Figure 8 suggest that the estimate of stimulus speed used by the nervous system will change as a function of Δt. Can the shifts in the population account for the changes in pursuit initiation we observed in chapter one? In chapter one, we reported that, for the same actual target speed, initial pursuit eye acceleration varies as a function of Δt. As initial pursuit eye acceleration is typically closely tied to target speed, one strongly suspects that the changes in acceleration are due to changes in the neural estimate of target speed. To compare neural and pursuit responses, we recorded eye movements from both monkeys using the same moving dot patch stimuli used for the recording experiments. Figure 9A illustrates the pursuit task. Figure 9B shows the average pursuit responses of monkey Mo to a 16°/s stimulus with varying Δt. Increasing flash separations led to larger peak eye accelerations, and longer latencies to reach peak eye acceleration. For each individual trial, we computed peak eye acceleration during pursuit initiation. Figure 9C shows, for the responses of monkey Mo to a 16°/s stimulus, how peak eye acceleration (circles) changed as a function of Δt. Average peak eye acceleration is plotted as a percent of that when Δt was 4 ms (i.e. when the motion was nominally smooth). Eye acceleration changes little until Δt exceeds 20-

24 ms. Δt's of 32 and 44 ms produced significantly elevated eye acceleration. For a Δt of 64 ms, eye acceleration is no longer significantly above normal. For each trial we also computed the 'acceleration latency', defined as the latency to reach 80% of the peak eye acceleration. The choice of 80% is somewhat arbitrary, but is in the range that reduces the variability of the measurement (Churchland and Lisberger 2000). The average acceleration latency (triangles) is plotted as the change in latency from when Δt was 4 ms. The acceleration latency shows little change until Δt reached 24 ms, at which point it increases steadily. In keeping with the convention of chapter 1, increasing latencies are plotted downwards, so that deficits in either latency or acceleration plot below the dashed horizontal line. The results of experiments using a dot speed of 32°/s and of experiments using monkey Q are shown later in Figures 11 and 14. For both monkeys, the pattern of results is very similar to that reported in Chapter 1, in which we used single dot stimuli. As the flash separation passes a limit, peak acceleration first increases and then decreases, while the acceleration latency steadily declines. Within this overall pattern, there are clear quantitative differences between the two monkeys.

If the changes in pursuit eye acceleration result from changes in the neural estimate of target speed extracted from MT, then we ought to be able to account for the changes by extracting, for each Δt, an estimate of target speed from the recorded population response. There are many methods by which an estimate of target speed could be extracted. It has been previously argued that a vector-average based method can account for how target *direction* is estimated from MT (Groh et al. 1997). We have therefore chosen to use the vector-average method to estimate speed. The vector-average estimate is equivalent to taking the center of mass of the population response, as was

done in Figure 8. However, as that figure illustrates, the result of a vector-average computation depends upon how one expresses the population upon which the computation is based. The three most obvious candidates upon which to base a vector-average are 1) the raw population response, 2) the opponent population response, and 3) the response of the subset of the population that prefers the direction of motion (i.e. the right hand side of the raw population response). The equations below describe the vector-average based on each of these three population responses.

The standard vector-average is:

equation 1:
$$speed = \frac{\sum_i s_i R_i}{\sum_i R_i}$$

where s_i is the preferred speed of the i^{th} cell, and R_i is the cell's response. The sum is taken over cells with preferred directions aligned with the direction of motion (positive preferred speeds), and over cells with preferred directions aligned opposite the direction of motion (negative preferred speeds). When applied to the raw population response, the vector-average is expressed as:

equation 2, the raw vector-average:
$$speed = \frac{\sum_i s_i (R_i^{pref} - R_i^{null})}{\varepsilon + \sum_i (R_i^{pref} + R_i^{null})}$$

where s_i is the preferred speed of the i^{th} cell. As described above, rather than record from separate cells preferring opposite directions, we simply recorded both preferred and null direction responses from the same cells. Thus, each cell is included twice in the above equation, once for its preferred-direction response (R^{pref}) and once for its null-direction

response (R^{null}). We included one free parameter, ε, that prevented the denominator from nearing zero when responses are small.

When applied to the opponent population response, the vector-average is expressed as:

equation 3, the opponent vector-average: $$speed = \frac{\sum_i s_i (R_i^{pref} - R_i^{null})}{\varepsilon + \sum_i (R_i^{pref} - R_i^{null})}$$

Each pair of responses (R^{pref} and R^{null}) can be thought of as belonging to two cells forming an opponent-pair, with similar preferred speeds but opposite preferred directions. As described above, we approximated this situation by recording the response of each cell to both directions of motion.

When applied only to those neurons with preferred speeds aligned with the direction of motion, the vector-average is expressed as:

equation 4, the preferred-only vector-average: $$speed = \frac{\sum_i s_i R_i^{pref}}{\varepsilon + \sum_i R_i^{pref}}$$

where we consider only the responses to each neuron's preferred direction of motion.

When applying these methods for extracting target speed, we base them upon the actual recorded responses for the stimulus in question. Prior to extraction of the estimate of speed, the average response of each neuron was calculated as was done for Figure 8. The response of each neuron was averaged over the stimulus duration, and the baseline activity was subtracted. The average response was then normalized by the peak of the speed tuning (which was based upon the directional response), so that all neurons had

similar peak directional responses. This normalization is separate from the more global normalization created by the denominator of the vector-average.

The free parameter ε is included to account for the likelihood that the neural estimate of speed is based upon a computation involving incomplete normalization. An ideal vector-average will yield the same estimate regardless of how the overall responsiveness of the population is scaled. If every neuron fires at half its normal rate, the resulting vector-average will remain constant. The nervous system may not achieve such ideal constancy. By varying the value of ε, we are able to vary the degree to which the estimate of speed remains constant as neural responsivity drops. Figure 10 shows, for different values of ε, how the output of the models described in the equations above changes as a function of the strength of the input (i.e. the firing rates of the neurons). The horizontal blue line indicates perfect normalization (an ε of zero); the output remains constant despite the decreases in the input. The diagonal blue line indicates no normalization; the output decreases linearly with the input. The red lines correspond to the indicated values of ε. These values of ε create an incomplete normalization. Moderate decreases in the input are compensated for to a greater or lesser degree depending on the value of ε, but the output falls sharply to zero when the input becomes very small. In the subsequent simulations, we vary the value of ε to achieve the best fits to the data. This is the only free parameter used.

Figure 11 compares pursuit eye acceleration, measured for two stimulus speeds and for two monkeys, with the estimates of target speed produced by the three methods of estimation described by equations 2-4 above. Also shown is an estimate of speed produced by a pure weighted sum, with no normalization (i.e. the numerator of equation

2). The estimates of speed were made separately for each monkey are based upon the neurons recorded from that monkey. Like eye acceleration, estimates of speed are shown as percentages of the estimate of speed when Δt was 4 ms. The estimate of speed changes as a function of Δt, though not always in the same way in which peak eye acceleration changed. The weighted sum and raw vector-average estimates exhibit a steady decline with increasing Δt. These methods did not produce an increase in the estimate of speed for any Δt. The preferred-only and opponent vector-average estimates *did* produce increased estimates for the same Δt's that produced increased eye acceleration. These methods also produced reduced estimates of speed for the larger Δt's. For both pursuit and the estimates of speed, the pattern of changes was shifted towards smaller Δt's for the 32°/s stimulus speed.

The increases in estimated speed seen for the opponent vector-average and the preferred-only vector-average are due to the effect described in Figure 7 and manifested in Figure 8. Neurons with slow preferred speeds have smaller limits of directionality than do those with fast speeds. For some Δt's, the population is thus shifted towards faster preferred speeds. The increase in estimated speed is absent for the weighted-sum estimate. In the absence of normalization, reduced inputs cannot give rise to an increased output. The increase in estimated speed is absent for the raw vector-average. Any tendency towards an increase is counteracted by the rising response of neurons to the null direction of motion, as seen in Figure 8.

The decreases in the estimate of speed seen at larger Δt's occur for all methods, but for somewhat different reasons. The weighted sum is simply the numerator of the raw vector-average and opponent vector-average methods, and in the absence of

normalization the weighted sum decreases for larger Δt's, due to the decreased difference between the response to the preferred and null directions. The raw vector-average produces a reduced estimate of target speed for larger Δt's because of the increasing non-directional response. Many neurons begin to respond to both the preferred and null directions, and this non-directional component pulls the center of mass towards zero, as seen in Figure 8. For the opponent vector-average and the preferred-only vector-average, the reduction in the estimate of speed at large Δt's is due to the incomplete normalization provided by the parameter ε. As indicated by the weighted sum, for larger Δt's the overall response of the neurons is diminished. When normalization is imperfect, the output of the vector-average drops when the input becomes small (as in Figure 10).

The parameter ε had a strong influence on how the estimate of speed changed as a function of Δt. This was especially true for the opponent vector-average and the preferred-only vector-average. Figure 12 compares estimates made by the three vector-average methods, using different values of ε. For the raw vector-average the value of ε made little difference within this range. For the other two methods, larger values of ε led to declines in the estimate of speed that were both larger, and earlier with respect to Δt. Consequently, larger values of ε also led to smaller increases in the estimate of speed. The solid lines represent the values of ε that we considered to provide the best fits to the data, and that were used in the previous figure. The actual values of ε are indicated in the legend. The value is expressed in terms of the percentage of the denominator that ε contributes when Δt is 4 ms. For example, if the sum of firing rates in the denominator is 200, and the value of ε used was 10, then we express ε as 10%. Even for the same

method of estimation, the optimal values of ε were different for the two monkeys. Different values are expected, first because the actual readout of MT by the pursuit system of each monkey may differ slightly, and second because we recorded different distributions of preferred speeds for each monkey. The values of ε used were also slightly different for the estimates made when the stimulus speed was 32°/s, although the fits were very nearly as good if ε was constrained to be the same for the two speeds (data not shown). For 32°/s, the values used for the opponent vector-average method changed from 5 to 12% (Mo) and 24 to 26% (Q). For the preferred-only vector-average, the values changed from 0 to 9% (Mo) and 28 to 30%. The actual readout algorithm applied by the nervous system is presumably the same for each speed, and it might therefore appear that ε should be set to be the same for the two speeds. However, we have probably not recorded from the same distribution of preferred speeds sampled by the nervous system. Any mis-sampling is expected to differentially impact the readout for the two speeds, and it is thus expected that the optimal value of ε will differ slightly to compensate. At least for the opponent vector-average, the optimal values of ε changed only slightly between the two speeds, and if the same value was used for both, fits were nearly as good as those shown.

Time based models

The estimates of speed made by the above methods are based upon firing rates that were averaged over the 600 ms interval beginning at the onset of the target and ending 100 ms after its offset. Based on these averaged firing rates, the estimates of speed provided by the preferred-only and opponent vector-averages provide reasonable fits to the pursuit acceleration data. However, the pursuit system responds to the stimulus

within 100 ms, and continually updates its response based on the speed of the target image. Would estimates of speed extracted from the ongoing neural responses (on a millisecond by millisecond basis) show the appropriate changes with Δt? Furthermore, the timecourse of the neural estimate of speed may be different for different Δt's. This possibility is suggested by the changes in the acceleration latency seen in Figure 9. Larger Δt's delayed peak eye acceleration, suggesting that they may have likewise delayed the peak estimate of speed. We therefore constructed estimates of speed that were produced by the methods described above, but were computed each millisecond based on the time-varying neural responses. We wished to know a) if the models would still capture the changes in peak eye acceleration, and b) if the models could capture the changes in the latency to peak eye acceleration. We computed estimates of speed using both the preferred-only vector-average and the opponent vector-average. We did not compute estimates based on the raw vector-average, as in the prior simulations this method failed completely to account for increases in estimated speed.

The top row of Figure 13 shows, as a function of time, the directional response to a 16°/s target, averaged across the neurons recorded for each monkey. Larger Δt's produced not only reduced neural responses, but also longer latencies to reach the peak or plateau response. This was true for both monkeys. As in the analysis above, the response of each neuron was normalized so that all neurons had the same average directional response to their preferred speed. To smooth the spike-train of each neuron, we filtered using a simple exponential filter with a time-constant of 30 ms. This time-constant was chosen to be long enough to provide sufficient smoothing, but to be shorter than or equal to the estimated time-constant of pursuit. The filtering properties of pursuit

are not well known, but observation of the initiation of pursuit reveals that peak initial eye acceleration follows the absolute time of initiation by 30 ms or more. Models of pursuit eye movements have typically filtered image velocity signals by roughly this degree (Robinson et al. 1986, Krauzlis and Lisberger, 1994). A handful of neurons (4 from monkey Mo, and none from monkey Q) were excluded from this and subsequent analyses, because too few trials were collected to provide a low-noise estimate of their firing rate as a function of time.

The bottom row of Figure 13 shows the estimate of speed produced by the opponent vector-average, when applied to the time-varying response of the recorded neurons to a 16°/s stimulus. Inputs to the model were normalized and filtered as described above. The black trace shows the estimate of speed for a Δt of 4 ms. The left panel shows the output of the model when based on the neurons recorded from monkey Mo. Before the neurons respond to he stimulus, the estimate of speed is noisy, but centered around zero. After the neural response begins, the estimate of speed quickly climbs to a relatively stable value slightly above 16°/s. For Δt's of 32 and 44 ms (red and green traces) the estimate of speed is higher, and is reached later. For a Δt of 64 ms, the peak estimate of speed is lower than for 44 ms, though still slightly higher than when for 4 ms. The right panel shows the output of the model when based on the neurons recorded from monkey Q. The overall pattern of effects is qualitatively similar, though the increase in the estimate of speed is smaller and the estimate of speed is initially less noisy. In general, the estimate of speed prior to the onset of the neural response is noisy because the difference between the preferred and null direction responses ($R^{pref} - R^{null}$) fluctuates around zero. The parameter ε keeps the denominator of equation 3 from

nearing zero, and prevents the estimate of speed from approaching infinity as (R^{pref} - R^{null}) nears zero. However, unless ε was set to be large, moderate fluctuations of the estimate about zero were still present. These fluctuations were worse for monkey Mo, for whom we used a small value of ε.

To compare the magnitude and latency of the estimate of speed with the magnitude and latency of pursuit initiation, we extracted two quantitative measures from the estimate of speed. For each Δt, we computed the peak estimate of speed during the first 150 ms after the normal onset of the response (when Δt was 4 ms). We then calculated the latency to reach 80% of that peak. These measures are intended to be analogous to the peak eye acceleration and acceleration latency measurements made for pursuit. If the changes in pursuit eye acceleration are due to changes in the neural estimate of speed, then the peak and latency measures made for the two ought to change in the same way with Δt. As for pursuit, the measures of the estimate of speed are expressed relative to their values when Δt was 4 ms. The peak estimate of speed is expressed as a percentage of that when Δt was 4ms, and the latency is expressed as the change (in ms) from that when Δt was 4 ms. Figure 14 compares pursuit with the estimate of speed created by the preferred-only vector-average. Dotted and dashed lines correspond to estimates made using slightly different methodologies, described later. The peak estimate of speed is increased for many of the same Δt's that produced increased eye acceleration, and is reduced for most of the Δt's that produced decreased eye acceleration, although the magnitudes of the changes are not identical. The latency of the peak estimate of speed increases as Δt increases, though not to the same degree as did the acceleration latency of pursuit. For the largest Δt's, the change in the latency of

pursuit is underestimated by 50-100 ms. The parameter ε was set by hand for each monkey and each speed to produce the best fit. The parameter had a large effect on the peak estimate of speed (similar to that described in Figure 12), but little effect on the latency measure. Expressed relative to the denominator when Δt was 4 ms, the values of ε used were 5 and 5% (monkey Mo, 16 and 32°/s) and 39 and 40% (monkey Q, 16 and 32°/s).

Figure 15 compares pursuit and the estimate of speed computed using the opponent vector-averages. The peak estimate of speed is increased for the same Δt's that produced increased peak eye acceleration. For the larger Δt's where peak acceleration was reduced, the peak estimate of speed is likewise reduced. Quantitative agreement is generally excellent, although for a 32°/s stimulus with a 44 ms Δt (Δx = 1.4°, the largest tested), the estimate of speed was considerably more diminished that was eye acceleration; pursuit was more resistant to apparent motion than predicted. This was true for both monkeys. Both pursuit and the estimate of speed exhibited latency increases as Δt was increased. The quantitative agreement was generally good, although when the stimulus speed was 32°/s and Δt was 44 ms, the estimate of speed was so reduced that no reliable estimate of latency could be extracted for comparison with that of pursuit. As with the preferred-only vector-average, the parameter ε had a large effect on the peak estimate of speed, but little effect on the latency measure. The values used were 9 and 13% (monkey Mo, 16 and 32°/s) and 29 and 40% (monkey Q, 16 and 32°/s). These values are similar to those used for the non-time-based version of the model. For both the preferred-only and opponent methods, fits were very nearly as good if the same value

of ε was used for both speeds, but much worse if the same value was used for both monkeys.

Different MT neurons can have very different latencies (58-120 ms for Mo, 50-105 ms for Q). These latencies were computed based on the latency of the directional component of the response. Some neurons gave earlier, non-directional responses to the target onset. Given the 20 ms latency of the pursuit response to microstimulation of MT (Komatsu and Wurtz), only a small proportion of MT neurons have latencies short enough to account for the latency of pursuit. Monkey Mo had a pursuit latency of 85 ms, but only 17% of the cells we recorded from Mo had latencies less than 65 ms. Monkey Q had a pursuit latency of 80 ms, though only 44% of the neurons we recorded from Q had latencies less than 60 ms. Pursuit may be selectively driven by the shortest-latency neurons, or may be driven by neurons of all latencies. In estimating speed from the neurons we recorded, we therefore faced three choices. We could 1) include only those neurons with latencies short enough to account for the pursuit latency, 2) include all neurons regardless of latency, or 3) include all neurons, but artificially align the responses, if each had the same short latency. The first possibility is impractical, as few of the neurons we recorded had latencies short enough, especially for monkey Mo. The second possibility appears the most natural, while the third has the advantage of basing the estimate of speed upon a population of neurons that all begin responding at the same time, which may be the case for the actual neural estimate of speed. We constructed estimates of speed using both the second and third methods. The dashed and solid lines in Figures 14 and 15 represent estimates computed using, respectively, the natural latencies of the neurons and the artificially corrected latencies. In practice, the results of

the two methods proved very similar. Although the absolute latencies of the estimate of speed differed between the two methods, the changes in latency for different Δt's were very similar. The average response traces and estimates of speed shown in Figure 13 were based upon the artificially corrected latencies.

Discussion

Effect of apparent motion on individual MT neurons

The experiments and analysis in this chapter sought to 1) describe the effect of apparent motion on the responses of individual MT neurons, and 2) examine the population response and potential explanations for the changes in pursuit initiation we first documented in Chapter 1. The first of these goals confirmed many of the findings of Mikami et al. (Mikami et al, 1986a, 1986b). We found, as did they, that MT neurons lose directionality with increasing flash separation, and that this loss was often partly due to an increase in the null-direction response. Our results argue that, for stimulus speeds above 16°/s, the response-limiting factor is primarily the distance between successive flashes. Again, this is consistent with their findings that a spatial limit was operative for higher speeds. Our results give an average value for the spatial limit of 0.77° (Mo) and 0.69° (Q) for the 2.7-8.9° receptive field eccentricities we recorded. This estimate is consistent with that of Mikami et al. From Figure 8 of Mikami et al (1986b) the mean limiting Δx in the eccentricity range of 2-8° appears to be about 0.9°. However, Mikami et al. appear to have found somewhat more cells with large spatial limits than we did. The largest limits of directionality we observed corresponded to Δx's between 1 and 1.5°. Mikami et al report a fair proportion of cells with spatial limits of 2-5°. These differences could result from differences in our stimuli. A single bar unambiguously moves in a given direction no matter what the Δx, while the direction of a patch of dots moving within an aperture becomes increasingly ambiguous at large Δx's, due to aliasing. Our results also replicate the finding of Mikami et al. that the maximum spatial interval

that evoked a directional response was on average larger for neurons with faster preferred speeds.

Our replication strengthens some of the conclusions of Mikami et al. Our stimulus has some practical advantages over that used by Mikami et al. These authors held the luminance of each flash constant, a method that aided some aspects of their analysis, but introduced a potential artifact into others. The lower mean luminance at larger Δt's could contribute to the decline in directional firing. By holding the overall luminance of each flash constant, we eliminate the possibility of such an artifact. Our dot patch stimulus is also more spatially homogeneous than the single moving bar used by Mikami et al. This homogeneity eliminates the possibility that response reductions result because larger flash separations cause the stimulus to miss the most responsive part of the receptive field. Our replication, using a complementary stimulus, thus demonstrates that the effects of apparent motion are due to general properties of MT, and not to particulars of the stimulus presentation. We also performed analyses that extended the results of Mikami et al., such as those in Figures 4, 5 and 8. These analyses yield additional information about the changes in MT responses caused by apparent motion, and suggest how these changes might affect downstream computations. It was also important that we make our own recordings from MT because to properly compare pursuit and neural responses, both should be recorded from the same animal, using the same stimulus. Given the effect of eccentricity on both the pursuit and neural responses to apparent motion (Churchland and Lisberger 2000, Mikami et al. 1986b), we wished to record from neurons with receptive fields near where the pursuit stimulus was presented.

Neural basis of an illusion of increased speed

Using human subjects, we demonstrated that apparent motion can lead to an increase in perceived speed. This finding supports our assertion that increases in pursuit eye acceleration are produced because apparent motion increases the estimate of speed used by pursuit. Such an effect appears paradoxical: why should a degradation of motion lead to an increase in the perceived speed? Our neural recordings and analysis reveal the likely basis of this increase in apparent speed. Larger flash separations reduce the response of MT neurons. However, this reduction is not homogeneous: cells with slower preferred speeds show the largest response reduction. The net effect is that for some values of Δt, the balance between slow-preferring cells and fast-preferring cells is shifted towards the latter. Thus, the positive correlation between preferred speed and limit of directionality forms the basis of the illusion. However, the correlation alone in not sufficient: only some methods for estimating speed from the population response reproduce the illusion.

When the opponent vector-average is used to estimate target speed from the MT population response, the resulting estimate undergoes changes that parallel the changes in pursuit initiation. The estimate of speed is elevated for those Δt's that increased initial eye acceleration, and is decreased for those Δt's that reduced initial eye acceleration. Furthermore, the latency of the estimate increases for larger Δt's, paralleling the increased latency of initial eye acceleration. In summary, virtually all of the apparent-motion-induced changes in pursuit initiation are accounted for if one assumes that those changes are subsequent to changes in the neural estimate of speed, and that the estimate

of speed is extracted from the MT population response via an opponent vector-average computation.

The other methods for estimating speed all fail to account for at least one aspect of pursuit behavior. The weighted sum and raw vector-average models fail to produce an increase in estimated speed for the relevant Δt's. They former fails because total neural activity drops steadily with increasing Δt, and the latter because non-directional responses pull the center of mass towards zero. The preferred-only vector-average produces the desired increase in estimated speed, but fails to account for the large changes in latency seen at larger Δt's. This is because even though the latency of the directional component of the MT response is greatly increased for large Δt's, the absolute latency of most neurons is only slightly increased. Many neurons still respond with relatively short latencies, but this early response is equally large for motion in both the preferred and null directions. The preferred-only vector-average is based upon the response of those neurons with preferred directions aligned with the direction of motion, and does not distinguish between the directional and non-directional components of the response. Thus, for large Δt's, the estimate of speed made by the preferred-only vector-average is based largely on the non-directional responses. For the same reason, the preferred-only vector-average does not show a large decrease in the estimate of speed, even for the largest Δt's. Even if there were no directional component of the response, the preferred-only vector-average would extract a positive estimate of speed from the non-directional component.

The failure of the raw and preferred-only vector-averages to account for some of the changes observed in pursuit initiation does not necessarily mean that they are

incorrect descriptions of how speed is estimated by the nervous system. Speed could be estimated by a computation analogous to the raw vector-average, if one postulates that the increases in eye acceleration have another source, unrelated to the method for estimating speed. Alternately, a preferred-only type method could be used by the nervous system, if one assumes that the large increases in latency are due to another effect. However, in the absence of appealing alternate explanations for the unaccounted for effects, we conclude that the neural estimate of speed is probably not extracted using a raw or preferred-only vector-average type computation.

Even the opponent vector-average, which appears to be the most promising of the methods we tested, shows some quantitative failures. These were observed primarily for the higher stimulus speed of 32°/s. For a Δt of 44 ms, the model overestimates the magnitude of the decreases in eye acceleration. The opponent vector-average predicts a nearly zero estimate of speed, due to the almost complete lack of directional firing. In contrast, eye acceleration is reduced by about half, although with large latency increases. Why does eye acceleration eventually reach half of normal when there is almost no directional response in MT? The likely explanation is that for these long latencies, pursuit is no longer operating in open loop. Small initial eye accelerations reduce the speed of the stimulus on the retina, reducing the retinal Δx, and potentiating both the response in MT and further eye acceleration. Eye acceleration is thus larger than expected, because the flash separation of the stimulus is smaller than intended. Thus, we do not think that the underestimate of eye acceleration reflects a failure of the opponent vector-average method. Rather, it probably reflects the improper comparison of neural

responses driven by a constant retinal stimulus with long-latency pursuit responses that are driven by a changing retinal stimulus.

If changes in the MT population response produce an illusion of increased speed from the standpoint of pursuit, then one suspects that the perceptual illusion of increased speed could also be traced to MT. A number of prior studies have demonstrated the importance of MT in the performance of a perceptual task based on direction discrimination (Shadlen et al. 1996, Britten et al. 1992 1996, Salzman et al 1990, 1992, Newsome et al. 1989). However, these studies involved highly trained monkeys, and it is still unclear if the monkeys' success on the task is related to perception, or simply constitutes a trained motor response. Given our results, area MT certainly could be the neural basis of the perceptual illusion. However, neurons in other cortical areas may also show a correlation between preferred speed and the limit of the directional response. We feel confident in asserting that MT is the basis of the elevated pursuit response because of the known link between MT and pursuit, and because of the accurate prediction of pursuit by a model based directly on MT responses. We believe it is still an open question if the perceptual illusion is the result of changes in the MT population response, although this certainly seems likely.

The bases of many visual illusions and effects have been attributed to MT or V1, and recordings have often supported these attributions (Gilbert and Wiesel 1990, Grosof et al. 1993, Tootell et al. 1995, Quian et al. 1994, Quian and Anderson 1994, Stoner and Albright 1992). The ability of apparent motion to pass for real motion (when Δt and Δx are small enough) is itself an illusion, the basis of which is the fact that V1 and MT neurons can respond to apparent motion as if it were real (Adelsen and Bergen 1985,

Mikami et al 1986a). To this body of work we add our explanation of the illusion of increased speed. The illusion of increased speed has some disadvantages from a practical standpoint. It is a relatively weak illusion, and occurs for a limited range of stimulus parameters. This latter feature is also advantage, however, as it allows comparison of when the illusion is present, and when it is expected given the neural responses. The close agreement between observation and expectation supports the conclusion that the changes in the population response are the basis of the illusion. Our approach also has the advantage that we are comparing behavioral evidence of the illusion with neural responses in the same awake animal. Unlike many illusions, the source of the illusion of increased speed cannot be observed when recording from any single neuron. The basis is clear only when one considers the relative response of multiple neurons. For this reason it becomes clear that understanding the illusion requires a theory about how neural responses are decoded. In actuality, such a theory is required to understand almost any illusion. For the explanations of many illusions, the hypothesized decoding mechanism may not be made explicit, especially if it is clear that any reasonable method would produce the same illusion. However, confusion can arise when the issue of decoding is not explicitly considered. A good example is the case of Mach-bands (see Pessoa 1996 for a review), which are often said to be produced by lateral inhibition in the retina. In the absence of an understanding of how the rest of the brain interprets the retina, it is not clear why Mach-bands are produced for some stimuli but not others, or for that matter why they are not ubiquitous. In general, assumptions about readout mechanism should be made explicit before a neural effect is deemed the basis for a perceptual effect.

Other explanations for the illusory increase in speed

The neural responses we recorded provide an explanation for the illusory increase in speed, the root of which is the correlation between neurons' preferred speed and the robustness of their response to apparent motion. Are there other possible bases for the illusion? For example, it is intuitively plausible that each dot appears to be stationary from the moment it is flashed until the moment the next dot appears, at which point its speed could appear nearly infinite. Might such intervals of very high estimated speed be the basis for the illusory increase in speed? This explanation suffers from a number of flaws. First, it probably greatly overestimates the temporal resolution of the visual system. For the faster of the two speeds we used (32°/s) the illusion was maximal for flash separations of 16 ms (Mo) and 12 ms (Q). It is unlikely that the visual system is capable of resolving such motion into intervals of zero and near-infinite speed. Certainly no evidence of this is seen in the responses of MT neurons. Furthermore, even if such resolution were possible, the net speed would still be the same. In fact, if one makes the reasonable assumption that that there is some saturation in the ability of the visual system to estimate speed (or in the ability of pursuit to respond to the estimate of speed) then this explanation actually predicts a smaller net estimate of speed. Lastly, we have previously reported (Churchland and Lisberger, 2000) that the range of Δx's for which eye acceleration is increased depends upon eccentricity. The effect of eccentricity is consistent with our explanation, as Mikami et al. found that the spatial limit of MT neurons is larger for more eccentric receptive fields. It is not clear how the effect of eccentricity could be accounted for by an alternation between stationary and infinite estimates of speed.

Another explanation is offered by Castet (1995). Castet also found that apparent motion can appear faster than smooth motion, and suggested the following explanation. In the frequency domain, apparent motion introduces combinations of temporal and spatial frequency that were not present in the original smooth motion. These "replicas" or "aliases" of the original frequency content could excite motion sensors tuned to speeds both faster and slower than that of the stimulus. Given certain assumptions about the sensitivity of the visual system, the excitation of fast-tuned sensors could dominate for slow stimulus speeds. In essence, this alias-based explanation proposes that the non-directional motion signals introduced by apparent motion bias the speed estimate towards higher speeds when the actual speed is low. This effect would disappear or invert when the actual speed is high. Appropriately, Castet found that the illusion he studied was restricted to slow stimuli: the illusory increase disappeared for speeds of 8°/s and above. However, we *did* observe an illusion of increased speed for faster stimulus speeds. For pursuit, an increase in eye acceleration was observed for both 16 and 32°/s targets, the latter of which is near the top of the range of speeds that can be accurately pursued. Conversely, in the first chapter we did not observe still larger increases in eye acceleration for target velocities slower than 16°/s. Our results thus conflict with a central prediction of the alias-based explanation; the illusion does not disappear or invert as target speed is increased. Nor does it grow for slower speeds. Furthermore, the aliasing-based explanation does not seem to be born out by the recorded neural data. For example, in Figure 8 some neurons with speeds faster than that of the stimulus showed a slight increase in firing rate for a Δt of 32 ms, but just as many showed a slight decrease. For the opponent population response, the shift of the center of mass to higher speeds is

due to decreased responses from slower-tuned neurons, not to increased responses from faster-tuned neurons.

Why did Castet find, contrary to our results, that the illusion of increased speed was absent for higher speeds. First, it is possible that the illusion studied by Castet at slow speeds *is* produced by the aliasing-based mechanism he proposes, and is only superficially similar to the illusion we report for moderate to fast speeds. This interpretation is supported by the larger size of his illusion (some of his subjects reported as much as a doubling of perceived speed). It also likely that Castet simply failed to evoke the illusion for higher stimulus speeds because he did not use Δx's above 0.26°. For a speed of 16°/s, we found that the effect appeared primarily for Δx's above 0.38-0.51°.

Theoretical advantages of the opponent population response

Of the methods tested, we found that the opponent vector-average produced the estimate of speed that best accounted for our data. Why might the nervous system adopt such a strategy? Although MT neurons are tuned for speed and direction, they may also respond to other aspects of the stimulus. Such responses can add a non-directional component to the population response. The blue trace in Figure 16 illustrates an ideal population response. The red trace in Figure 16 illustrates the effect of adding a non-directional component to a strong directional component. An ideal read-out computation would extract the same speed for both the red and blue responses. The green trace in Figure 16 illustrates the effect of adding a non-directional component to a very weak directional component. It is probably desirable, when there is little or no directional response, to extract an estimate of speed near zero. The opponent vector-average

accomplishes both of these goals, while the standard and preferred only vector-averages do not. The opponent vector-average is formally identical to 1) computing the average response in the null direction (an estimate of the non-directional component), then 2) subtracting this baseline from the response of each cell, and 3) performing a standard vector-average. In much the same way that normalization allows accurate estimation when the population response is scaled, the opponent computation allows accurate estimation when there are changes in the un-tuned component of the response. The nervous system may employ opponency because some common stimulus features (e.g. increased overall luminance, or ongoing local luminance changes within the moving object) may drive MT in a non-directional manner.

Although we have chosen to use the opponent vector-average to extract an estimate of speed from the population response, we do not wish to claim that it is the best method from a theoretical standpoint, or the only plausible method from an empirical standpoint. We have used it because it is simple, easily understood, and biologically reasonable. Other methods, such as the optimal linear estimator (Baldi and Heiligenberg 1988, Pouget et al. 1998, Salinas and Abbott 1994) have some theoretical advantages over the vector-average. The vector-average uses weights based on the preferred speed of each neuron. The optimal linear estimator effectively introduces a correction into these weights to account for such factors as the uneven sampling of preferred speeds and the often asymmetric speed tuning of MT neurons. If the optimal linear estimator were based upon and normalized by the opponent population response (at which point it would no longer be linear), we expect that it could account for the changes in pursuit we observed. In general, we expect that a number of reasonable methods for estimating

speed from the population response could account for our data, so long as they incorporate an opponent computation. For example, Pouget et al. (1998) have proposed a decoding method using recurrent connections that yields a second population code with more desirable properties, which can then be read via any reasonable algorithm such as vector averaging. Their method could be adapted to estimate speed from our population data, and might successfully account for our data if either the feed-forward or recurrent connections provided appropriate inhibition between opposing directions of motion. Another obvious candidate is a winner-take-all algorithm. A pure winner-take-all algorithm, in which the estimate is based on the most active neuron, is not particularly realistic. However, an approximation that considers only the most active neurons would reproduce the observed increase in estimated speed. However, some additional mechanism would have to be proposed to account for the decreases in preferred speed.

Implications of incomplete normalization

We included a free parameter, ε, in the denominator of the equation describing the vector-average. The effect of ε is to prevent complete normalization, especially when directional responses are small. For the opponent vector-average, the values of ε that produced good fits were fairly large (9-40% for the time-based model). Such values imply that the nervous system incompletely normalizes for overall firing rate when estimating speed. Incomplete normalization could lead to an underestimation of speed for stimuli that evoke weak responses. Some psychophysical experiments suggest that the nervous system *does* underestimate speed when responses are weaker. Humans underestimate speed both for low-contrast stimuli (Stone and Thompson, 1992), and for

chromatic stimuli that produce weaker MT responses (Seidemann et al. 1999, Dougherty and Wandell 1999).

It is also possible that the degree of normalization achieved by the nervous system varies systematically, perhaps as a function of the likelihood that the stimulus is stationary. We found a handful of neurons in MT that actually preferred a stationary stimulus, and were inhibited by motion in any direction (at least for the speeds above 0.5°/s we used). Interestingly, although such neurons show little response to motion at 16 or 32°/s when Δt is 4 ms, their response grows with Δt. Included in a vector-average, such neurons would contribute nothing to the numerator, and could substitute for the parameter ε in the denominator. The vector-average would then effectively use a low value of ε when motion is convincing (allowing for complete normalization) and a large value when motion is not convincing (creating incomplete normalization). Unfortunately, we did not record from enough of these neurons to be able to include them in our simulations, and we have no reason to believe that the nervous system makes use of these neurons in the manner proposed above. We nonetheless find such a strategy intriguing because of its potential utility.

Neural instantiation of a vector-average?

In the case of pursuit, a scalar representation of target speed (or of the resulting pursuit command) appears to be present in the dorso-lateral pontine nuclei (DLPN). Lesions of the DLPN impair pursuit (May et al. 1988) and many neurons in the DLPN show monotonic increases in firing over a range of target speeds (Suzuki et al. 1990). This scalar representation is imperfect at the level of the individual neuron, most of which respond appropriately over a limited range of speeds, but is present in the sum of

activity over multiple neurons. Area MT sends both direct and indirect projections to the DLPN and other nuclei of the pons (Brodal 1978, Glickstein 1980, Ungerleider et al. 1984, Boussaoud et al. 1992). It appears likely that these connections embody a decoding algorithm that converts the MT population code of speed into a scalar code. It is not hard to see how such projections could embody a weighted sum. However, the normalization used by the vector-average algorithm (and probably by most other plausible decoding algorithms) also requires division. A number of methods by which neurons could accomplish division have been proposed. In theory, a sufficiently large network of neurons with sigmoidal input/output relationships can approximate any smooth function (Hornik et al. 1989, Cybenko 1989), including division, although such a method might prove practically inefficient. Shunting inhibition is often said to be capable of instantiating division in a more straightforward manner (Torre and Poggio 1978, Hildreth and Koch 1987, Borg-Graham et al. 1998). A balanced input of excitation and inhibition can also emulate division by increasing the conductance of the post-synaptic neuron without contributing net excitation or inhibition (Larry Abbott, personal communication). Regardless of the method used, our results suggest that the approximation to division may be rather crude, as the normalization used to estimate speed appears to be quite incomplete.

References

Adelson., E.H., and Bergen, J.R. Spatiotemporal energy models for the perception of motion. J. Opt. Soc. Am. A. 2: 284-299, 1985.

Baldi, P. and Heiligenberg, W. How sensory maps could enhance resolution through ordered arrangements of broadly tuned receivers. Biol. Cybern. 59: 313-318, 1988.

Barlow, H., and Levick, W.R. The mechanism of directionally selective units in rabbit's retina. J. Physiol. Lond. 178: 477-504, 1965.

Borg-Graham L.J., Monier C., and Fregnac Y. Visual input evokes transient and strong shunting inhibition in visual cortical neurons. Nature 393: 369-73, 1998

Boussaoud, D., Desimone, R., and Ungerleider, L.G. Subcortical connections of visual areas MST and FST in macaques. Vis. Neurosci. 9: 291-302, 1992.

Britten K.H., Shadlen, M.N., Newsome, W.T., and Movshon, J.A. The analysis of visual motion: a comparison of neuronal and psychophysical performance. J. Neurosci. 12: 4745-4765, 1992.

Britten K.H., Newsome, W.T., Shadlen, M.N., Celebrini, S., and Movshon, J.A. A relationship between behavioral choice and the visual responses of neurons in macaque MT. Vis. Neurosci. 13: 87-100, 1996.

Brodal P. The cortico-pontine projection in the rhesus monkey. Origin and principles of organization. Brain 101: 251-283, 1978.

Castet, E. Apparent speed of sampled motion. Vision Res. 35: 1375-1384, 1995.

Chance, F.S. and Abbott, L.F. Divisive inhibition in recurrent networks. Network: Comput. Neural Syst. 11: 119-129, 2000.

Cheng, K., Hasegawa, T., Saleem, K.S., and Tanaka, K. Comparison of neuronal selectivity for stimulus speed, length, and contrast in the prestriate visual cortical areas V4 and MT of the macaque monkey. J. Neurophysiol. 71: 2269-2280, 1994.

Churchland M.M. and Lisberger S.G. Apparent motion produces multiple deficits in visually guided smooth pursuit eye movements of monkeys. J Neurophysiol. 84: 216-235, 2000.

Cybenko, G. Approximation by superpositions of a sigmoidal function. Mathematics of Control, Signals, and Systems 2: 303-314, 1989.

Dougherty, R.F., Press, W.A., and Wandell, B.A. Perceived speed of colored stimuli. Neuron 24: 893-899, 1999.

Dursteler, M.R., and Wurtz, R.H. Pursuit and Optokinetic Deficits Following Chemical Lesions of Cortical Areas MT and MST. J. Neurophysiol. 60: 940-965, 1988.

Gilbert C.D. and Wiesel T.N. The influence of contextual stimuli on the orientation selectivity of cells in primary visual cortex. Vision Res. 30: 1689-1701, 1990

Glickstein, M., Cohen, J.L., Dixon, B., Gibson, A., Hollins, M., Labossiere, E. and Robinson, F. Corticopontine visual projections in macaque monkeys. J. Comp. Neurol. 190: 209-229, 1980.

Goldreich, D., Krauzlis, R.J., and Lisberger, S.G. Effect of changing feedback delay on spontaneous oscillations in smooth eye movements of monkeys. J. Neurophysiol. 67: 625-638, 1992.

Groh, J.M., Born, R.T., and Newsome, W.T. How is a sensory map read out? Effects of microstimulation in visual area MT on saccades and smooth pursuit eye movements. J. Neurosci. 17: 4312-43330, 1997.

Grosof D.H., Shapley R.M., and Hawken M.J., Macaque V1 neurons can signal 'illusory' contours. Nature 365:550-552, 1993.

Heeger, D.J., Geoffrey, M.B., Demb, J.B., Seidemann, E., and Newsome, W.T. Motion opponency in visual cortex. J. Neurosci. 19: 7162-7174, 1999.

Hildreth E.C. and Koch C. The analysis of visual motion: from computational theory to neuronal mechanisms. Ann. Rev. Neurosci. 10: 477-533, 1987

Hornik, K., Stinchcombe, M., and White, H. Multilayer feedforward networks are universal approximators. Neural Networks 2: 359-366, 1989.

Judge, S.J., Richmond, B.J., and Chu, F.C. Implantation of magnetic search coils for measurement of eye position: an improved method. Vision Res. 20: 535-538, 1980

Kahlon, M. and Lisberger, S.G. Vector averaging occurs downstream from learning in smooth pursuit eye movements of monkeys. J. Neurosci. 19: 9039-9053, 1999.

Komatsu, H., and Wurtz, R.H. Modulation of Pursuit Eye Movements by Stimulation of Cortical Areas MT and MST. J. Neurophysiol. 62: 31-47, 1989.

Krauzlis, R.J., and Lisberger S.G. A Model of Visually-Guided Smooth Pursuit Eye Movements Based on Behavioral Observations. J. Comp. Neuro. 1: 265-283, 1994.

Levinson, E., and Sekuler, R. Inhibition and disinhibition of direction-specific mechanisms in human vision. Nature 254: 692-694, 1975.

Lisberger, S.G., and Westbrook, L.E. Properties of Visual Inputs that Initiate Horizontal Smooth Pursuit Eye Movements in Monkeys. J. Neurosci. 5: 1662-1673, 1985.

Lisberger, S.G. and Ferrara, V.P. Vector averaging for smooth pursuit eye movements initiated by two moving targets in monkeys. J. Neurosci. 17: 7490-7502, 1997.

May, J.G., Keller, E.L., and Suzuki, D.A. Smooth-pursuit eye movement deficits with chemical lesions in the dorsolateral pontine nucleus of the monkey. J. Neurophysiol. 59: 952-977, 1988.

Mikami, A., Newsome, W.T., and Wurtz, R.H. Motion Selectivity in Macaque Visual Cortex. I. Mechanisms of Direction and Speed Selectivity in Extrastriate area MT. J. Neurophysiol. 55: 1308-1327, 1986.

Mikami, A., Newsome, W.T., and Wurtz, R.H. Motion Selectivity in Macaque Visual Cortex. II. Spatiotemporal range of directional interactions in MT and V1. J. Neurophysiol. 55: 1328-1339, 1986.

Morris, E.J., and Lisberger, S.G. Different responses to small visual errors during initiation and maintenance of smooth-pursuit eye movements in monkeys. J. Neurophysiol. 58: 1351-1369, 1987.

Newsome, W.T., Wurtz R.H., Dursteler M.R., and Mikami A. Deficits in visual motion processing following ibotenic acid lesions of the middle temporal visual area of the macaque monkey. J. Neurosci. 5: 825-840, 1985

Newsome, W.T., Mikami, A., and Wurtz, R.H. Motion Selectivity in Macaque Visual Cortex. III. Psychophysics and physiology of apparent motion. J. Neurophysiol. 55: 1340-1351, 1986.

Newsome, W.T., Wurtz, R.H., and Komatsu, H. Relation of cortical areas MT and MST to pursuit eye movements. II. Differentiation of retinal from extraretinal inputs. J. Neurophysiol. 60: 694-620, 1988.

Pessoa, L. Mach Bands: how many models are possible? Recent experimental findings and modeling attempts. Vision Res. 36: 3205-3227, 1996.

Pouget, A., Zhang, K., Deneve, S., and Latham, P.E. Statistically efficient estimation using population coding. Neural Comp. 10: 373-401, 1998.

Qian N., Andersen R.A., and Adelson E.H. Transparent motion perception as detection of unbalanced motion signals. I. Psychophysics. J Neurosci 14: 7357-7366, 1994.

Qian N. and Andersen R.A. Transparent motion perception as detection of unbalanced motion signals. II. Physiology. J Neurosci 14: 7367-7380, 1994.

Ringach, D.L. A tachometer feedback model of smooth pursuit eye movements. Biol. Cybern. 73: 561-568, 1995.

Robinson, D.A. The mechanics of human smooth pursuit eye movement. J. Physiol. Lond. 180: 569-591, 1965.

Robinson, D.A., Gordon, J.L., and Gordon, S.E. A model of the smooth pursuit eye movement system. Biol. Cybern. 55: 43-57, 1986.

Rashbass, C. The relationship between saccadic and smooth tracking eye movements. J Physiol. (Lond) 159: 326-338, 1961.

Salinas, E. and Abbott, L.F. Vector reconstruction from firing rates. J Comp. Neuro. 1: 89-107, 1994.

Salzman, C.D., Britten, K.H., and Newsome, W.T. Cortical microstimulation influences perceptual judgements of motion direction. Nature 346: 174-177, 1990.

Salzman, C.D., Murasugi, C.M., Britten, K.H., and Newsome, W.T. Microstimulation in visual area MT: effects on direction discrimination performance. J. Neurosci. 12: 2331-2355, 1992.

Seidemann E., Poirson A.B., Wandell, B.A. and Newsome, W.T. Color signals in area MT of the macaque monkey. Neuron 24: 911-917, 1999.

Schrater P.R. and Simoncelli, E.P. Local velocity representation: evidence from motion adaptation. Vision Res. 38: 3899-3912, 1998.

Shadlen, M.N., Britten, K.H., Newsome, W.T. and Movshon, J.A. A computational analysis of the relationship between neuronal and behavioral responses to visual motion. J. Neurosci. 16:1486-1510, 1996.

Shi, D., Friedman, H.R., and Bruce, C.J. Deficits in smooth-pursuit eye movements after muscimol inactivation within the primate's frontal eye field. J. Neurophysiol. 80: 458-464, 1998.

Stone, L.S. and Thompson, P. Human speed perception is contrast dependent. Vision Res. 32: 1535-1549, 1992.

Stoner G.R. and Albright T.D. Neural correlates of perceptual motion coherence. Nature 358: 412-414.

Suzuki D.A., May JG, Keller E.L., and Yee R.D. Visual Motion Response properties of Neurons in Dorsolateral Pontine Nucleus of Alert Monkey. J Neurophys. 63: 37-59, 1990.

Tootell R.B., Reppas J.B., Dale A.M., Look R.B., Sereno M.I., Malach R., Brady T.J., Rosen B.R. Visual motion aftereffect in human cortical area MT revealed by functional magnetic resonance imaging. Nature 375: 139-141, 1995

Torre V. and Poggio T. A synaptic mechanism possibly underlying directional selectivity to motion. Proc. R. Soc. London Ser. B 202: 409-16, 1978.

Tusa, R.J., and Ungerleider, L.G. Fiber pathways of cortical areas mediating smooth pursuit eye movements in monkeys. Ann. Neuro. 23: 174-183, 1988..

Ungerleider, L.G., Desimone, R., Galkin, T.W., and Mishkin, M. Subcortical projections of area MT in the macaque. J. Comp. Neurol. 223: 368-386, 1984.

Watson, A.B., and Ahumada, A.J. Jr. Model of human visual-motion processing. J. Opt. Soc. Am. A. 2: 322-341, 1985.

Acknowledgements

We are grateful to Nicholas Priebe, who assisted with pilot recording studies, and to Ken Miller, Philip Sabes, and William Newsome for helpful comments on analysis and presentation. Research was supported by the Howard Hughes Medical Institute, and by NIH grants R01-EY03878 and T32-EY07120.

Figure Legends

Figure 1. Human judgment of the speed of apparent motion. **A**. Illustration of the task. Subjects fixated a central spot (indicated by the cross) throughout each trial. A patch of moving dots appeared briefly above fixation (top panel). A second patch then appeared briefly below fixation (bottom panel). Subjects pressed one of two buttons to indicate which patch was moving faster. **B**. Symbols plot the proportion of responses in which the 16°/s standard patch was judged faster, as a function of the speed of the comparator patch. Blue symbols plot, for each of five subjects, responses when both patches had the same 4 ms Δt, and were thus identical apart from speed. Red symbols plot responses when the comparator patch had a Δt of 4 ms, and the standard patch had a Δt of 32-64 ms. The exact separation depended on the subject. The red and blue lines show sigmoidal least-square fits.

Figure 1

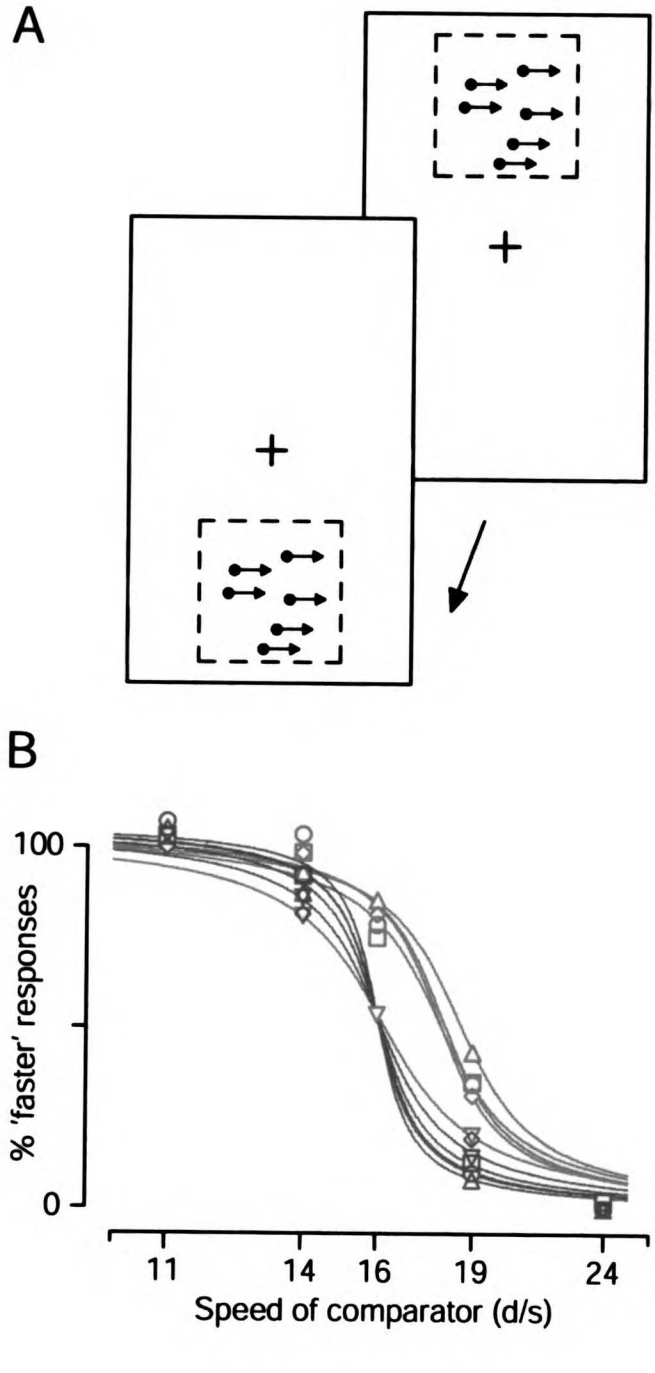
A
B
100
0
% 'faster' responses
11
14
16
19
24
Speed of comparator (d/s)

Figure 2. Responses of two MT neurons to apparent motion at 16°/s and of varying Δt. **A.** Histograms showing firing rate as a function of time for one MT neuron (bin width of 32 ms). Upwards plotted histograms show the response to stimulus motion in the neuron's preferred direction. Downwards plotted histograms show the response to motion in the null direction. The arrows provide a scale: their length indicates a firing rate of 100 spikes/s. Stimulus duration was 500 ms, and is indicated by the sequence of dots above each histogram. The locations of the dots indicate the timing of the flashes. The five pairs of histograms show the response for five different Δt's, indicated by the labels above. **B.** The directional response of the neuron in A, plotted as a function of flash separation. The fit is sigmoidal, with the inflection point at 37 ms. **C.** Histograms showing the response of a second MT neuron, for the same stimuli as in A. The arrow length indicates a firing rate of 50 spikes/s. **D.** The directional response of the neuron in C, plotted as a function of flash separation. The inflection point of the sigmoidal fit is at 37 ms. The two cells had preferred speeds of 13.1°/s (top) and 8.2°/s (bottom).

Figure 2

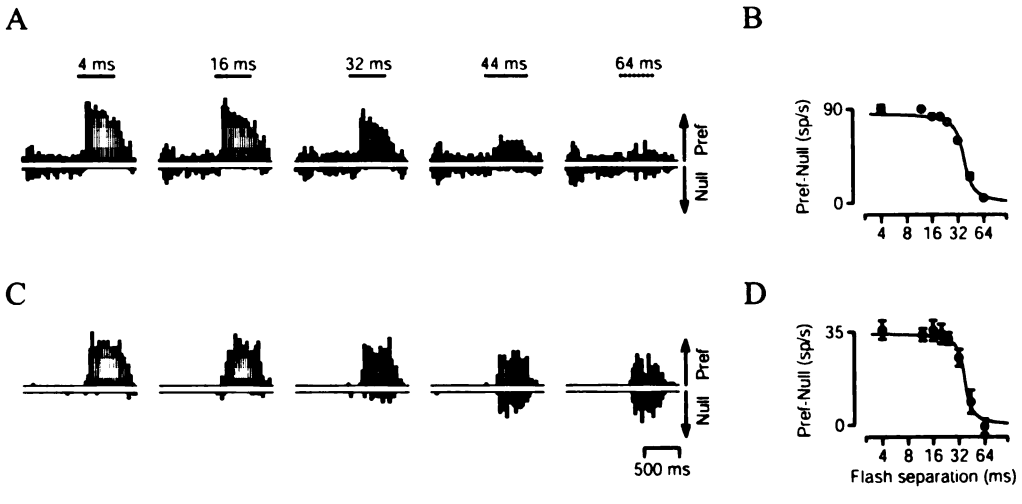
A
4 ms
16 ms
32 ms
44 ms
64 ms
Pref
Null
B
Pref-Null (sp/s)
90
0
4 8 16 32 64
C
Pref
Null
500 ms
D
Pref-Null (sp/s)
35
0
4 8 16 32 64
Flash separation (ms)

Figure 3. Responses of two MT neurons to apparent motion at 32°/s and of varying Δt. Responses are from the same two neurons shown in Figure 2, and the same histogram scalings are used. **A**. Histograms showing the response of the first neuron to preferred and null directions of motion, at 32°/s, for each of 4 Δt's. **B**. The directional response of the neuron in A, plotted as a function of flash separation. The inflection point of the fit is at 22 ms. **C**. Histograms showing the response of the second neuron for the same stimuli. **D**. The directional response of the neuron in C, plotted as a function of flash separation. The inflection point of the fit is at 16 ms.

Figure 3

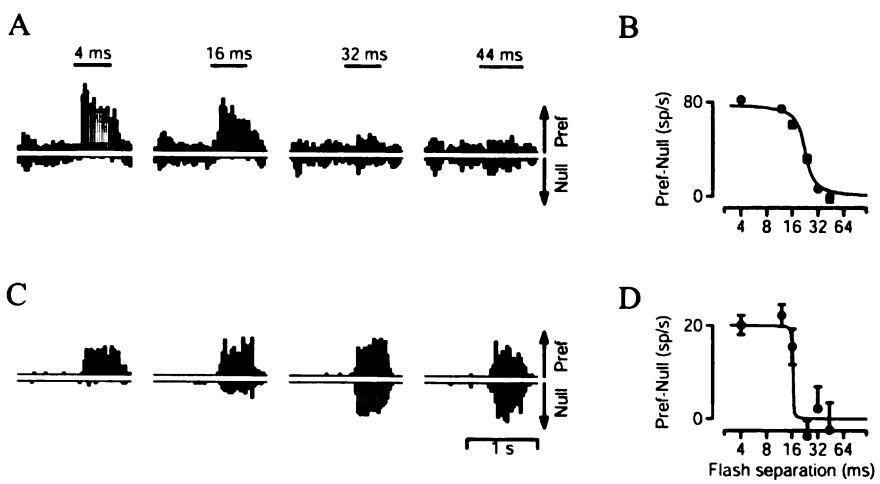
A
4 ms
16 ms
32 ms
44 ms
Pref
Null
B
Pref-Null (sp/s)
80
0
4 8 16 32 64
C
Pref
Null
1 s
D
Pref-Null (sp/s)
20
0
4 8 16 32 64
Flash separation (ms)

Figure 4. Scatterplot showing the response of all 107 MT neurons recorded in both monkeys. Each symbol plots, for one neuron, the response to motion in the preferred direction versus the response to motion in the null direction. The stimulus speed was 16°/s. Different colored symbols plot the response for different Δt's, as indicated in the legend. Points plotting below zero on either axis indicate suppression below baseline firing. The response of each neuron was normalized so that, for a Δt of 4 ms, the difference between the response to the preferred and null directions was one. Therefore, the points corresponding to a Δt of 4 ms plot along the upper black diagonal line, whose slope and y-intercept are both one. The lower black line has a slope of one and a y-intercept of zero, and indicates a lack of difference in the response to the two directions. Nine cells, which had very high or low preferred speeds, showed no reliable difference in their response to the two directions of motion at 16°/s, even when Δt was 4 ms, and were excluded from this analysis.

Figure 4

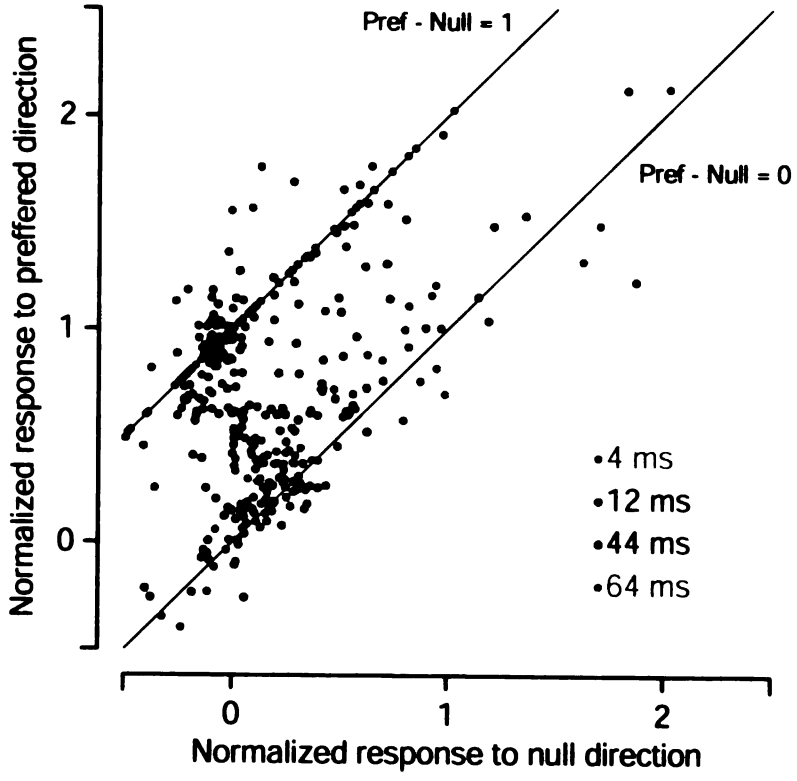
Pref - Null = 1
Pref - Null = 0
•4 ms
•12 ms
•44 ms
•64 ms
Normalized response to preffered direction
Normalized response to null direction
0
1
2
0
1
2

Figure 5. Plots showing average preferred-direction and null-direction responses. Data for monkeys Mo and Q are shown in the left and right columns. Data for stimulus speeds of 16 and 32°/s are shown in the top and bottom rows. Open symbols plot the average preferred-direction response. Closed symbols plot the average null-direction response. Error bars show the standard error of the mean. Averages across cells were based on the normalized, baseline corrected, average firing rate of each cell, calculated as for Figure 4. Prior to averaging, each cell was normalized so that its directional response to the presented speed (16 or 32°/s depending on the plot) was 100% for a Δt of 4 ms. Neurons that showed no reliable difference in response to the preferred and null directions for one of the two stimulus speeds (i.e. neurons with very fast or slow preferred speeds) were excluded from the analysis of that speed. For monkey Mo, 9/73 neurons showed an insufficient response for 16°/s, and 14/73 showed an insufficient response for 32°/s. For monkey Q, 1/34 neurons showed an insufficient response for 32°/s.

Figure 5

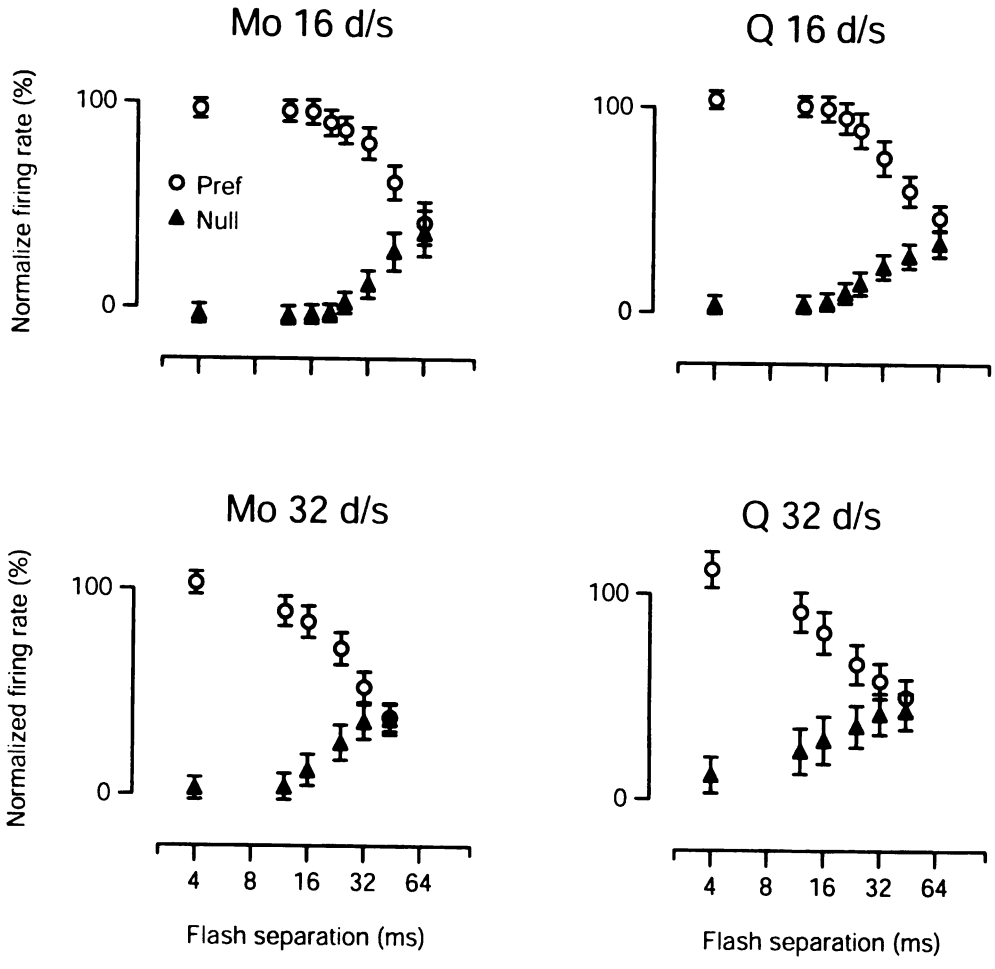
Mo 16 d/s
Q 16 d/s
Mo 32 d/s
Q 32 d/s
Normalize firing rate (%)
Normalized firing rate (%)
100
0
Pref
Null
4
8
16
32
64
Flash separation (ms)

Figure 6. Responses of two MT neurons with different speed tunings. **A**. Histograms showing the response of one MT neuron to a 16°/s stimulus for different Δts. Upwards plotted histograms show the response to stimulus motion in the neuron's preferred direction. Downwards plotted histograms show the response to motion in the null direction. The arrows provide a scale of 100 spikes/s. **B**. The directional response of the neuron in A, plotted as a function of flash separation. The inflection point is at 20 ms. **C**. The speed tuning of the same neuron; the directional response is plotted as a function of stimulus speed. The peak of the fit is at 8.0°/s. **D**. Histograms showing the response of a second neuron to the same stimuli as in A. The arrows provide a scale of 100 spikes/s. **E**. The directional response of the neuron in D, plotted as a function of flash separation. The inflection point is at 42 ms. **F**. The speed tuning of the same neuron. The peak of the fit is at 24°/s.

Figure 6

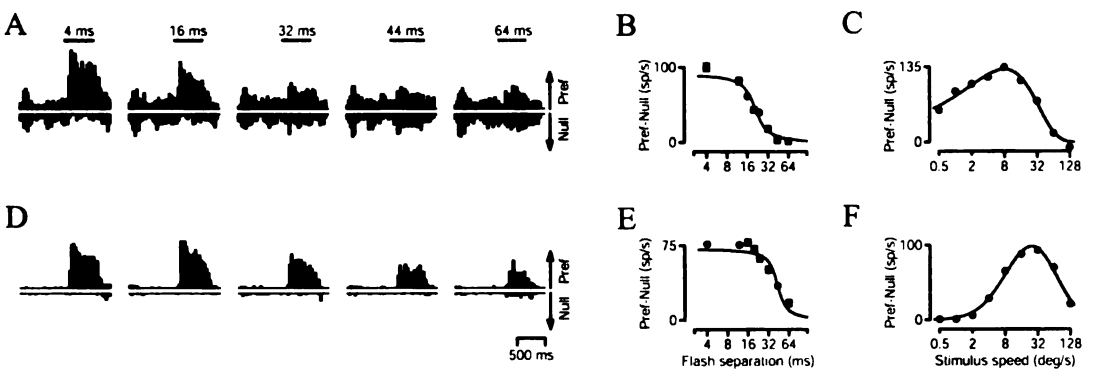
A
4 ms
16 ms
32 ms
44 ms
64 ms
Pref
Null
B
Pref-Null (sp/s)
100
0
4 8 16 32 64
C
Pref-Null (sp/s)
135
0
0.5 2 8 32 128
D
Pref
Null
500 ms
E
Pref-Null (sp/s)
75
0
4 8 16 32 64
Flash separation (ms)
F
Pref-Null (sp/s)
100
0
0.5 2 8 32 128
Stimulus speed (deg/s)

Figure 7. Scatter-plots showing the relationship between preferred speed and the limit of directionality. Each open symbol corresponds to one cell. The limit of directionality was calculated as described in the text, as the inflection point of sigmoidal fits such as those shown in Figure 6 B and E. Data are shown for monkey Mo (left column) and monkey Q (right column). The limit of directionality was measured separately for stimulus speeds of 16°/s (top row) and 32°/s (bottom row). Shown at the top of each column is the distribution of preferred speeds. Shown at the right of each panel is the distribution of the limit of directionality. As in Figure 5, neurons were excluded from the analysis of a given speed if their directional response to that speed was so weak that the limit of directionality could not be calculated.

Figure 7

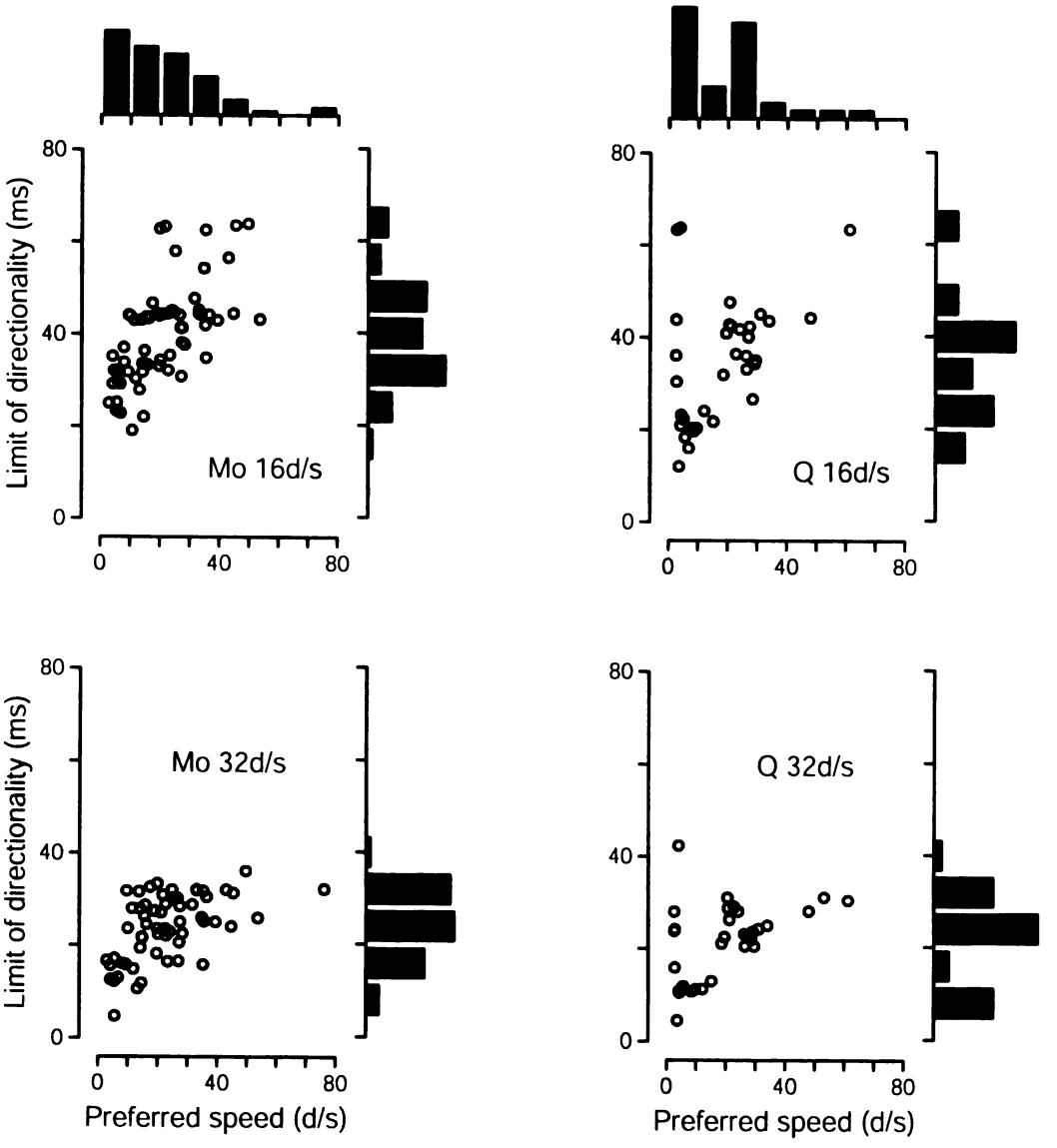
Limit of directionality (ms)
80
40
0
Mo 16d/s
Q 16d/s
Mo 32d/s
Q 32d/s
0
40
80
Preferred speed (d/s)

Figure 8. Population responses of MT neurons for a 16°/s stimulus and two Δt's: 4 ms and 32 ms. Each point corresponds to one neuron, and plots its response to a 16°/s stimulus against its preferred speed. The top and bottom rows show data for monkey Mo (73 neurons) and Q (34 neurons) respectively. The panels in the left column plot the 'raw population response'. Responses to motion in each neuron's preferred direction are plotted on the right-hand side (positive preferred speeds) and responses to motion in the null direction are plotted on the left-hand side (negative preferred speeds). Each cell is thus plotted twice. The panels in the right column plot the 'opponent population response'. Each point plots the directional response: the difference between the responses to the preferred and null directions. For both columns, the response of each cell has been normalized by the peak of the fit to the speed tuning data, so that its directional response to its preferred speed is one when Δt is 4 ms. Vertical black and red lines show, for Δt's of 4 and 32 ms, the centers of mass of the population.

Figure 8

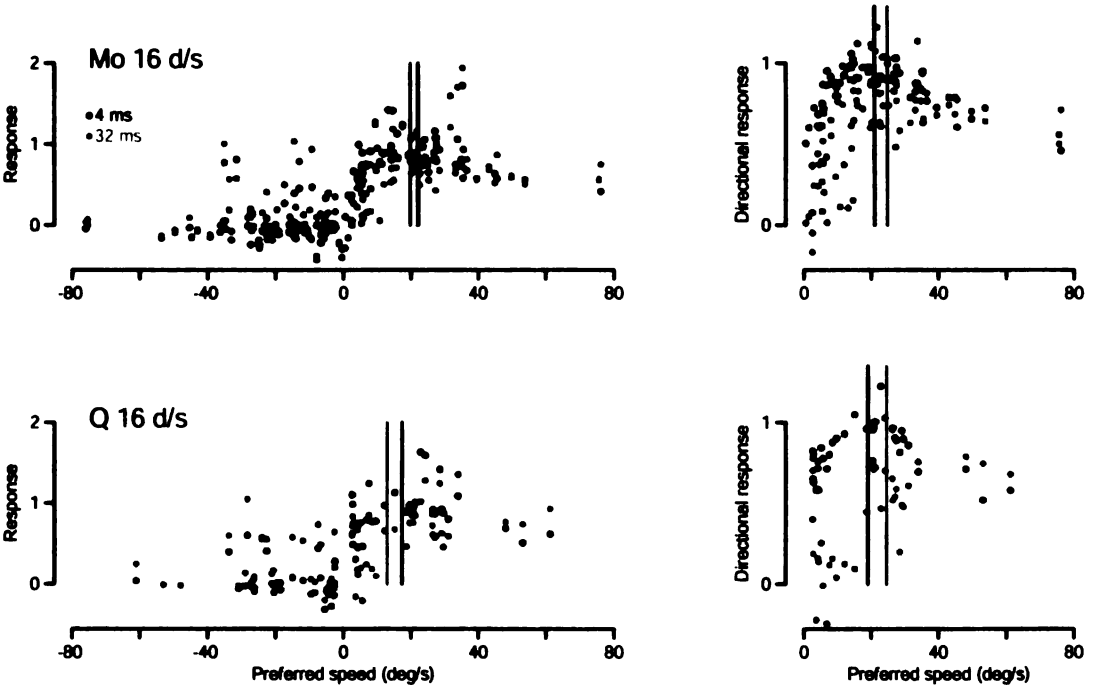
Mo 16 d/s
•4 ms
•32 ms
Response
Directional response
Q 16 d/s
Response
Directional response
Preferred speed (deg/s)
Preferred speed (deg/s)

Figure 9. **A**. Illustration of the pursuit task. The monkey initially fixated a point (crosshairs). The fixation point was then extinguished and replaced by a dot-patch target that appeared to its left and immediately began to move rightwards. The starting position of the center of the dot patch relative to the fixation point was set to be equal to the average receptive field eccentricity of the MT neurons recorded in that monkey (6.4° and 5.2° for Mo and Q respectively). **B**. Pursuit responses of monkey Mo to a 16°/s target with varying Δt. The top and bottom sets of traces plot average eye velocity and acceleration as a function of time. Traces begin at the time the patch target appeared and began to move. Different colors plot responses for different Δt's, as indicated in the legend. **C**. The average peak eye acceleration evoked by a 16°/s target (circles) and the average acceleration latency (triangles) are plotted as a function of Δt. Eye acceleration is plotted as a percentage of that when Δt is 4 ms, for which motion was effectively smooth. Latency is plotted as the change from the latency when Δt was 4 ms. Longer latencies are plotted downwards. Thus, for both acceleration and latency, symbols below the dashed line indicate deficits relative to the pursuit evoked when Δt was 4 ms. Error bars show the standard error of the mean.

Figure 9

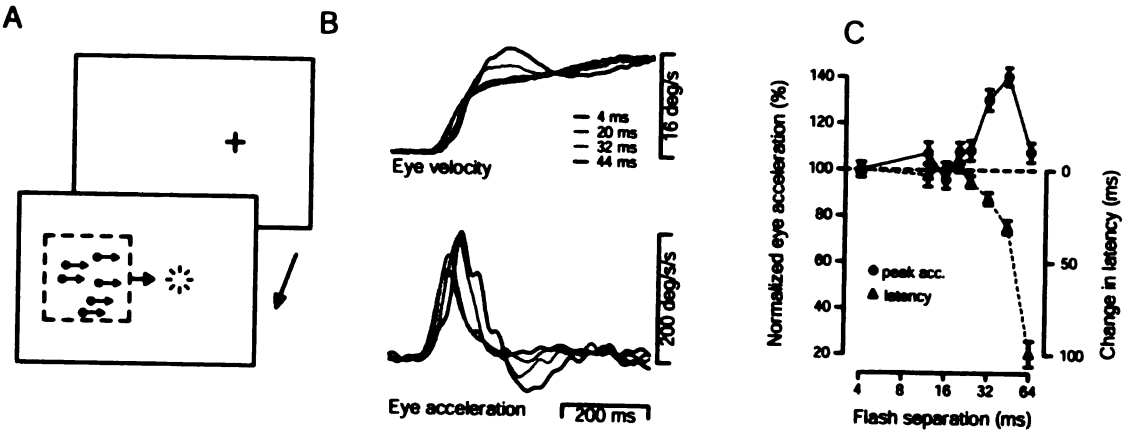
A
B
C
4 ms
20 ms
32 ms
44 ms
16 deg/s
Eye velocity
200 deg/s/s
Eye acceleration
200 ms
Normalized eye acceleration (%)
peak acc.
latency
Change in latency (ms)
Flash separation (ms)

Figure 10. Illustration of the impact of the parameter ε on the normalization provided by the vector-average methods. The output of the normalization is plotted as a function of the input. If there is no normalization, then the output decreases as a function of the input (diagonal blue line). If ε is zero, normalization is perfect, and for all non-zero inputs the output is the same (horizontal blue line). The three red lines show the input/output function for different values of ε. The values shown provide differing degrees of incomplete normalization. The value of ε is expressed as a percentage of the denominator when the input is at 100%.

Figure 10

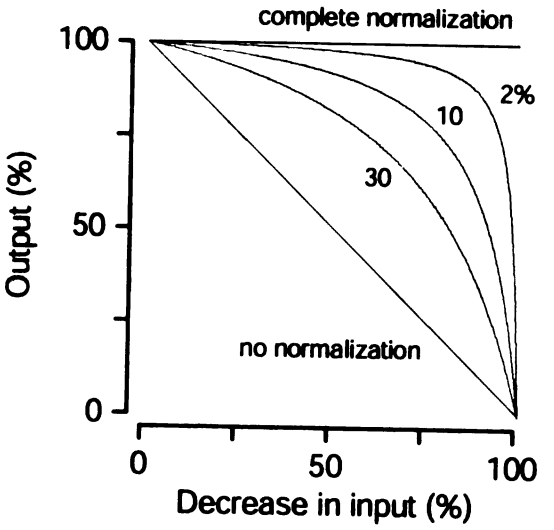
complete normalization
100
2%
10
30
50
Output (%)
no normalization
0
0
50
100
Decrease in input (%)

Figure 11. Comparison of pursuit responses with estimates of speed calculated from the population response. All quantities are plotted as a function of Δt. Open black symbols show mean peak pursuit eye acceleration, calculated as for Figure 9. For a target speed of 16°/s the eye acceleration of monkey Mo was significantly increased for Δt's of 32 and 44 ms ($p<10^{-7}$ for each). The eye acceleration of monkey Q was significantly increased for Δt's of 20, 24 and 32 ms ($p<0.05$ for each) and decreased for larger Δt's ($p<10^{-9}$ for each). For a target speed of 32°/s the eye acceleration of monkey Mo was significantly increased for Δt's of 16 and 24 ms ($p<0.03$ for each), and decreased for larger Δt's ($p<10^{-4}$ for each). The eye acceleration of monkey Q was significantly increased for a Δt of 12 ms ($p<0.005$) and decreased for Δt's 24 ms or larger ($p<10^{-7}$ for each). Colored traces show estimates of target speed extracted via four methods: three versions of the vector-average (VA) and a weighted sum, as indicated in the legend. These methods were applied, for each speed and Δt, to the recorded population response of the relevant monkey. Like the pursuit acceleration data, the estimates are shown in normalized form, as a percentage of the estimated speed when Δt is 4 ms. Error bars show the standard error of the estimates, computed based on the standard error of the firing rate of the neurons providing the input to the estimation.

Figure 11

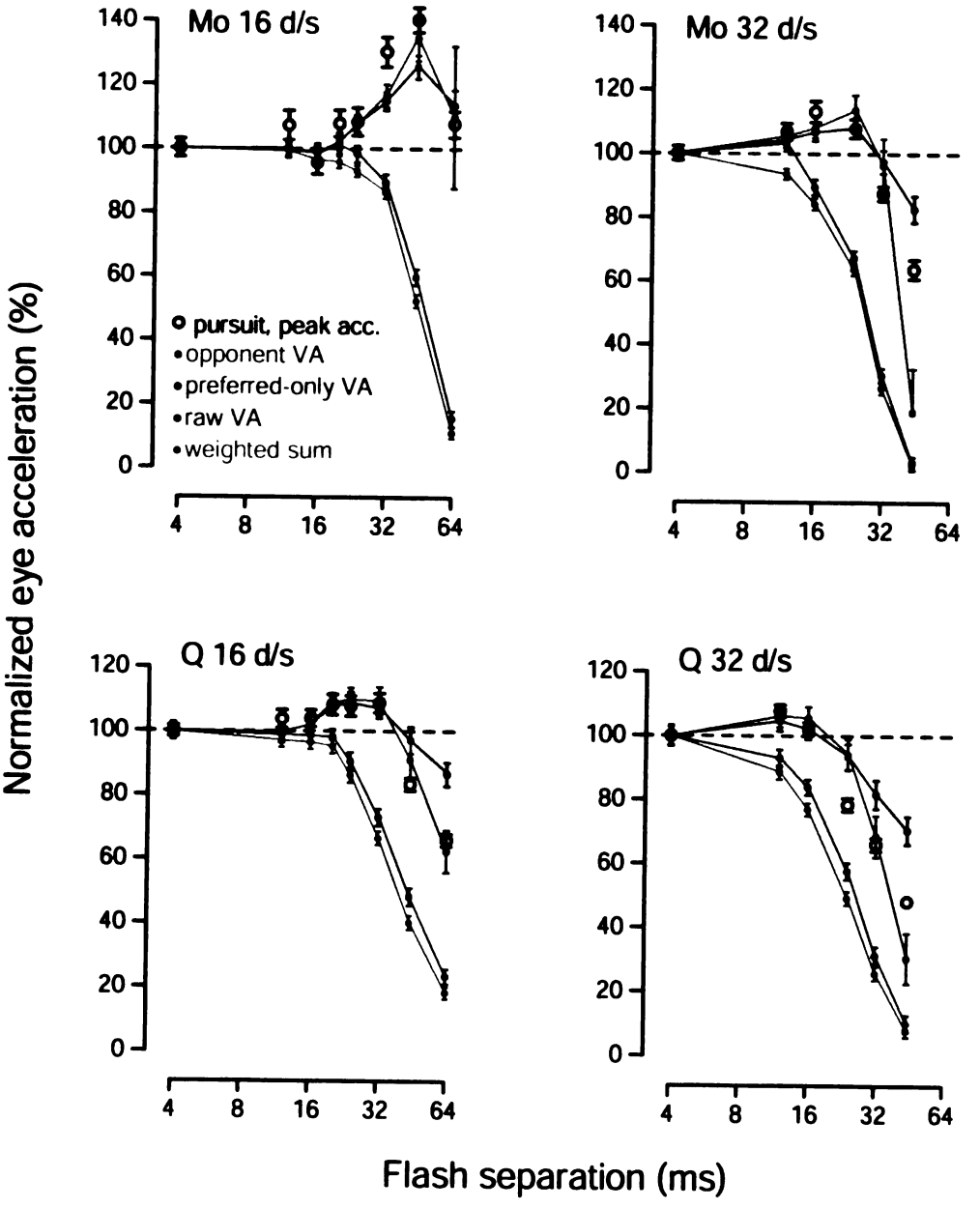
Mo 16 d/s
Mo 32 d/s
Q 16 d/s
Q 32 d/s
pursuit, peak acc.
opponent VA
preferred-only VA
raw VA
weighted sum
Normalized eye acceleration (%)
Flash separation (ms)
140
120
100
80
60
40
20
0
4
8
16
32
64

Figure 12. The influence of the parameter ε upon the behavior of the three vector-average models. All graphs plot pursuit data and speed estimates, as described in Figure 11, for a stimulus speed of 16°/s. The top and bottom rows show data for monkeys Mo and Q, respectively. From left to right, the three columns show estimates made by the raw vector-average, the preferred-only vector-average, and the opponent vector-average. The three colored traces within each panel show estimates using different values of ε, as indicated by the legends.

Figure 12

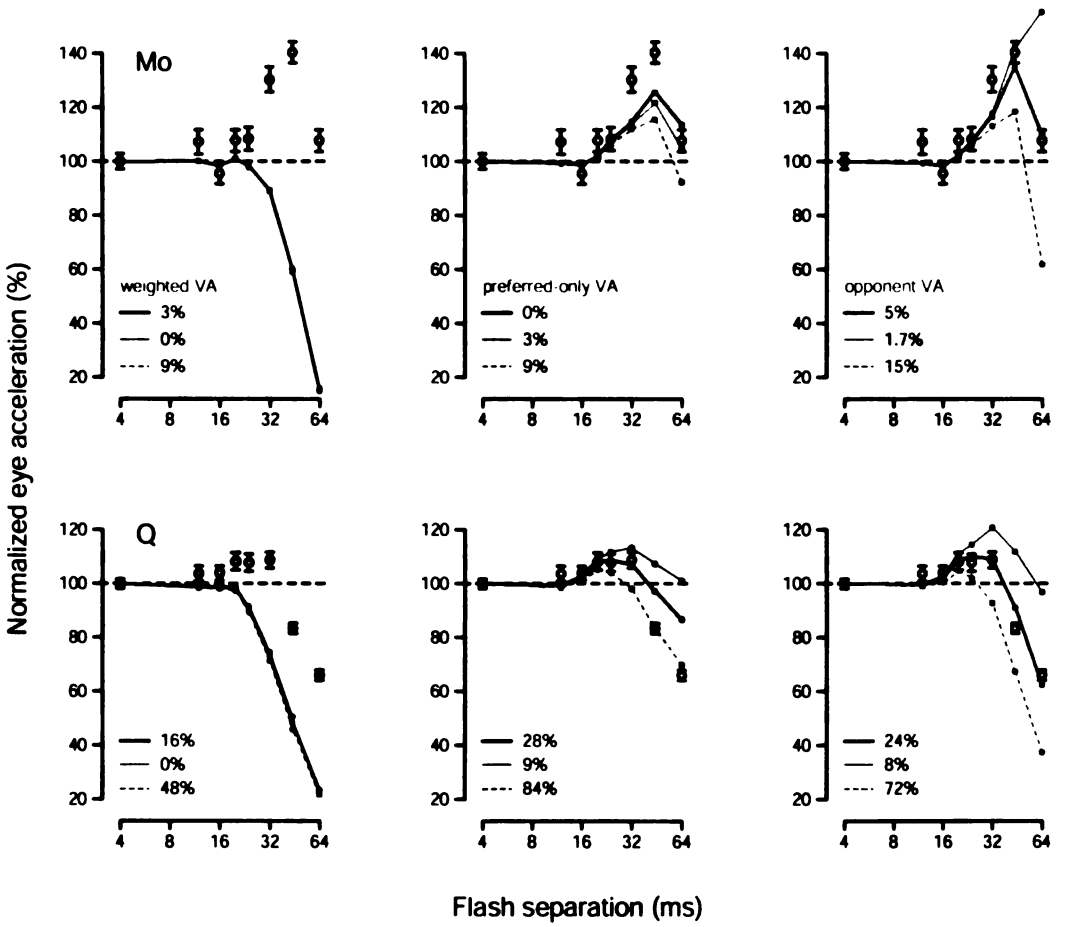
Mo
weighted VA
3%
0%
9%
preferred-only VA
0%
3%
9%
opponent VA
5%
1.7%
15%
Q
16%
0%
48%
28%
9%
84%
24%
8%
72%
Normalized eye acceleration (%)
Flash separation (ms)

Figure 13. Top row: directional firing rates as a function of time, averaged over all neurons recorded for monkey Mo (left column) and Q (right column). The latency of every neuron was artificially set to be 100 ms, so that for the purposes of the average all neurons responded to the stimulus as the same time. Before averaging, spike-trains were filtered with an exponential filter with time-constant 30 ms. The amplitude of each spike-train was also normalized by the peak of the fit to the speed tuning data, so that each neuron's directional response to its preferred speed was the same for a Δt of 4 ms. Different colored traces correspond to different values of Δt, as indicated. Bottom row: estimates of speed calculated using the opponent-based vector-average, shown as a function of time for both monkeys. Latencies were aligned and spiketrains filtered and normalized as for the averages above. The model was constructed to have a latency of 100 ms, so the target can be thought of as appearing at the start of each plot. As with the top panels, different colors plot estimates for different Δt's. For monkey Mo, these anayses were based on 69 of the total 73 cells recorded. Four cells had firing rates that were so noisy that they were excluded, though they were included in previous versions of the model, which averaged firing rate across the entire stimulus interval. For monkey Q, all neurons were included.

Figure 13

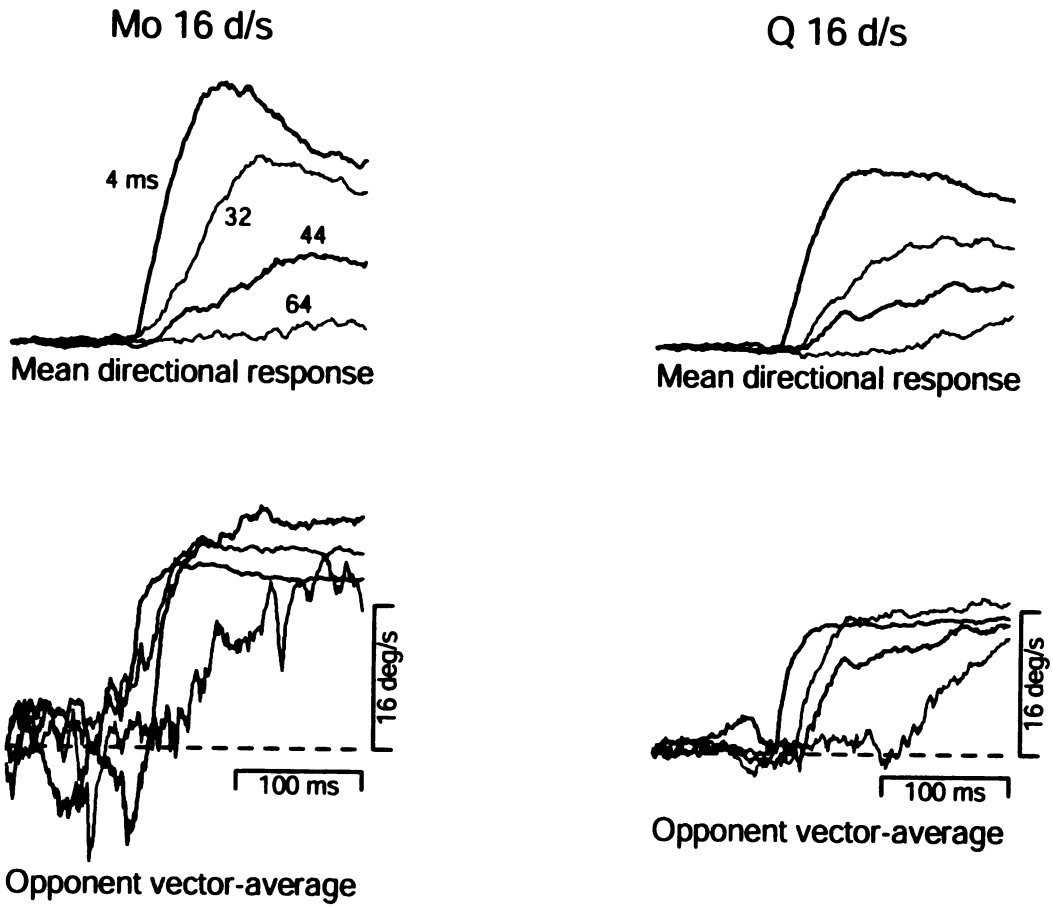
Mo 16 d/s
4 ms
32
44
64
Mean directional response
16 deg/s
100 ms
Opponent vector-average
Q 16 d/s
Mean directional response
16 deg/s
100 ms
Opponent vector-average

Figure 14. Comparison of pursuit with the time-based version of the preferred-only vector-average model. Open symbols correspond to pursuit performance, and the colored traces to model performance. Circles and triangles plot, respectively, average peak acceleration and acceleration latency for each Δt, computed and plotted as in Figure 9. Green and cyan traces show, respectively, the peak estimate of speed (plotted against the left vertical axis) and the latency of the estimate of speed (plotted against the right vertical axis). These quantities were calculated as described in the text, and like pursuit are shown relative to their values when Δt was 4 ms.

Figure 14

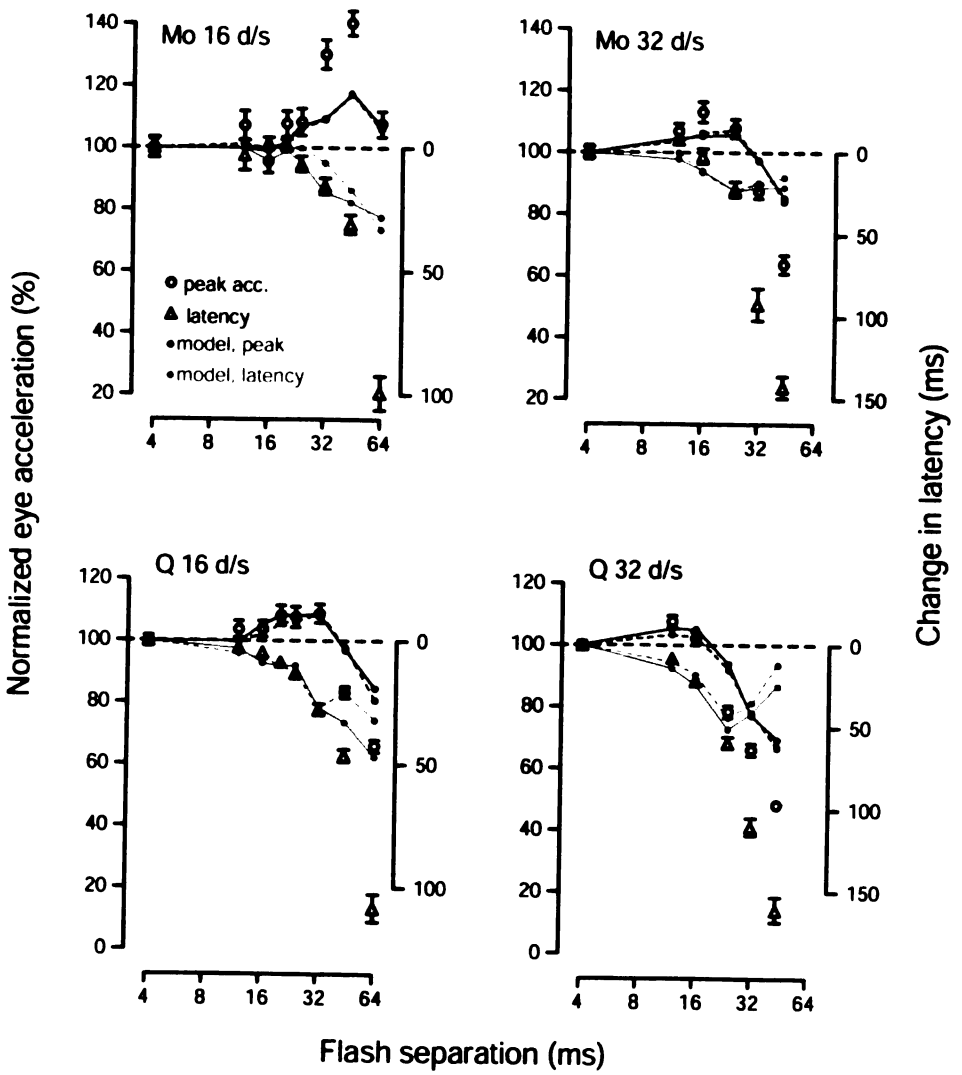
Mo 16 d/s
Mo 32 d/s
Q 16 d/s
Q 32 d/s
peak acc.
latency
model, peak
model, latency
Normalized eye acceleration (%)
Change in latency (ms)
Flash separation (ms)
4
8
16
32
64

Figure 15. Comparison of pursuit with the time-based version of the opponent vector-average model. Open symbols correspond to pursuit performance, and the colored traces to model performance. Circles and triangles plot, respectively, average peak acceleration and acceleration latency for each Δt. Red and pink traces show, respectively, the peak estimate of speed (plotted against the left vertical axis) and the latency of the estimate of speed (plotted against the right vertical axis).

Figure 15

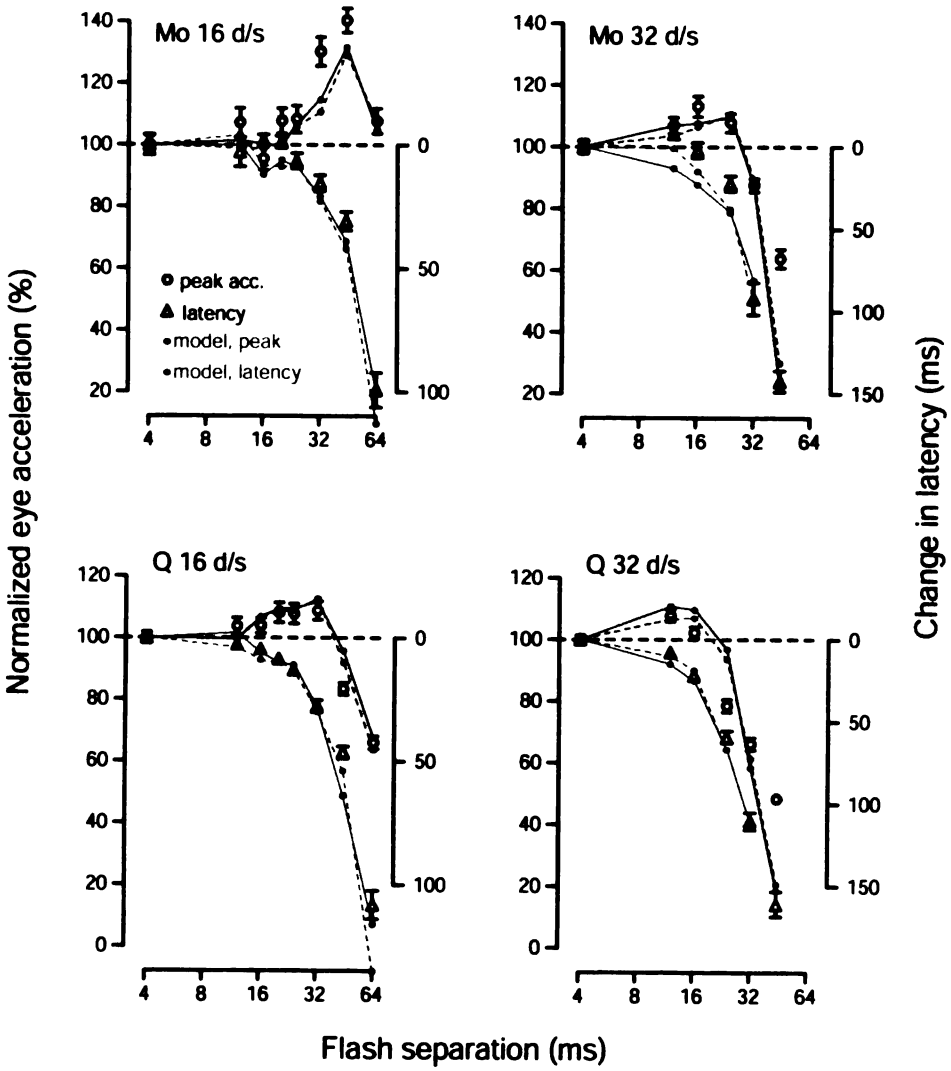
Mo 16 d/s
Mo 32 d/s
Q 16 d/s
Q 32 d/s
peak acc.
latency
model, peak
model, latency
Normalized eye acceleration (%)
Change in latency (ms)
Flash separation (ms)
140
120
100
80
60
40
20
0
50
150
4
8
16
32
64

Figure 16. Cartoon illustration of three hypothetical MT population responses. Neural response is plotted as a function of preferred speed, with rightward preferences on the right and leftward preferences on the left. The blue trace shows a response with a large directional component and a small non-directional component. The red trace shows a response with large directional and non-directional components. The green trace shows a response with a small directional component and a large non-directional component.

Figure 16

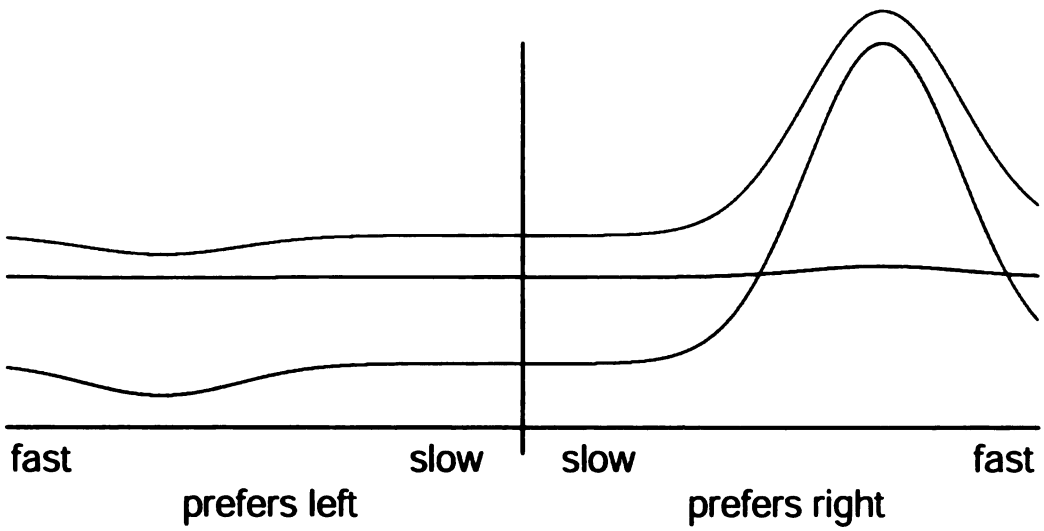

Future directions

The research in this thesis fails to address a number of important questions regarding how image speed is extracted from the firing of motion sensitive neurons. We have shown that an 'opponent vector-average' successfully accounts for the transformation from neural responses to behavior, and that alternative vector-average methods fail to do so. However, we did not explore some other potential methods, such as winner take-all. A pure winner take all computation, in which the most active neuron dominates the estimate, is unrealistic. Nonetheless it is reasonable to ask how large a contribution is made by neurons with responses much smaller than the peak. The vector-average method assumes that all neurons contribute to the estimate in proportion to their firing, but it is possible that the nervous system selectively singles out the most active neurons. One could distinguish between these possibilities by taking a strong motion component and adding a second weaker component at a different speed, or in the opposite direction. For example, the opponent vector-average predicts that a weak motion component in the opposite direction at a slow speed should, against most expectations, increase the estimate of speed. This effect is different from that created by motion contrast and is expected to reverse if the secondary component is faster than the primary component. A winner take all computation would be unaffected by the secondary component. The difficulty in employing this strategy is that the two motion components must be presented in such a way that they are both integrated into the same estimate of speed. If two directions of motion are seen, the strategy has failed. We are currently exploring methods for achieving this goal.

The technical hurdle described above highlights another gap in our knowledge. We do not know how (or even to what degree) the nervous system segregates the motion signals related to different objects, so that an accurate estimate can be made for the object of interest. This problem is simplest when objects are spatially separated, so that spatially separate populations of MT neurons are activated by each object. The problem becomes more difficult when objects are nearby or overlapping, and the nervous system must have some method for deciding which signals belong to which object (the so called 'binding problem'). Our work suggests a tool for addressing this issue. Apparent motion allows the strength of different motion signals to be varied by the experimenter, which could aid an exploration of how such signals are segregated or combined. Apparent motion is a more predictable method for achieving changes in neural response than changing the contrast or size of the object. For the same reason, apparent motion could be a useful tool for investigating how the many motion signals associated with an object are combined to create a single estimate of velocity.

This thesis also does not address how well the vector-average reconstruction of speed approximates the ideal. The vector-average shows biases and errors resulting from the non-uniform sampling of preferred speeds, and from the asymmetry of some neurons' tuning. Given our sample of neurons, how much better could one do? To what degree are the same issues faced by the nervous system? Our neural data could potentially be used as a starting point in answering such questions. The accuracy of the reconstruction of speed also depends upon the variability of the neural responses. Our data cannot address this issue because a) different random dot patterns were used for each trial, and b) only one neuron was recorded from at a time, so that the degree of shared noise is not

known. As mentioned in Chapter 1, we also do not know how (or to what degree) the nervous system accounts for the spatial-frequency dependence of speed tuning.

Lastly, this thesis does not address why MT neurons react the way they do to apparent motion. The basis of directionality in MT is only incompletely understood. Mikami et al. (1986) used apparent motion as a tool to study the basis of directionality, and our results largely replicate theirs and support their conclusions. However, there is some divergance between our findings and theirs, likely due to stimulus differences. Some of these points of divergence, such as the largest limiting Δx, may be informative. Additionally, apparent motion may provide a useful method for testing the utility of the conception of MT neurons as motion energy filters (e.g. Adelsen and Bergen 1985). In this conception, MT neurons are described as responding to particular combinations of temporal and spatial frequency. In the frequency domain, apparent motion produces 'aliases', combinations of temporal and spatial frequency that are not present in the corresponding smooth motion. Thus, apparent motion is distinguished from real motion by the *presence* of something new (the aliases). This seems very different from the space-time conception of apparent motion, in which it is distinguished from smooth motion by what is *missing* (the presence of the stimulus between flashes). The finding that large flash separations can uncover responses in the null direction seems to support the idea that MT neurons act as motion energy filters. We believe that new stimuli, combining apparent motion with smooth motion, will resolve the issue of whether MT neurons fail to respond directionally to apparent motion because they stop receiving sufficient directional drive, or because they start receiving inhibition or non-directional

excitation. Thus, it is likely that stimuli employing apparent motion can continue to play a role in elucidating the basis of directional responses.

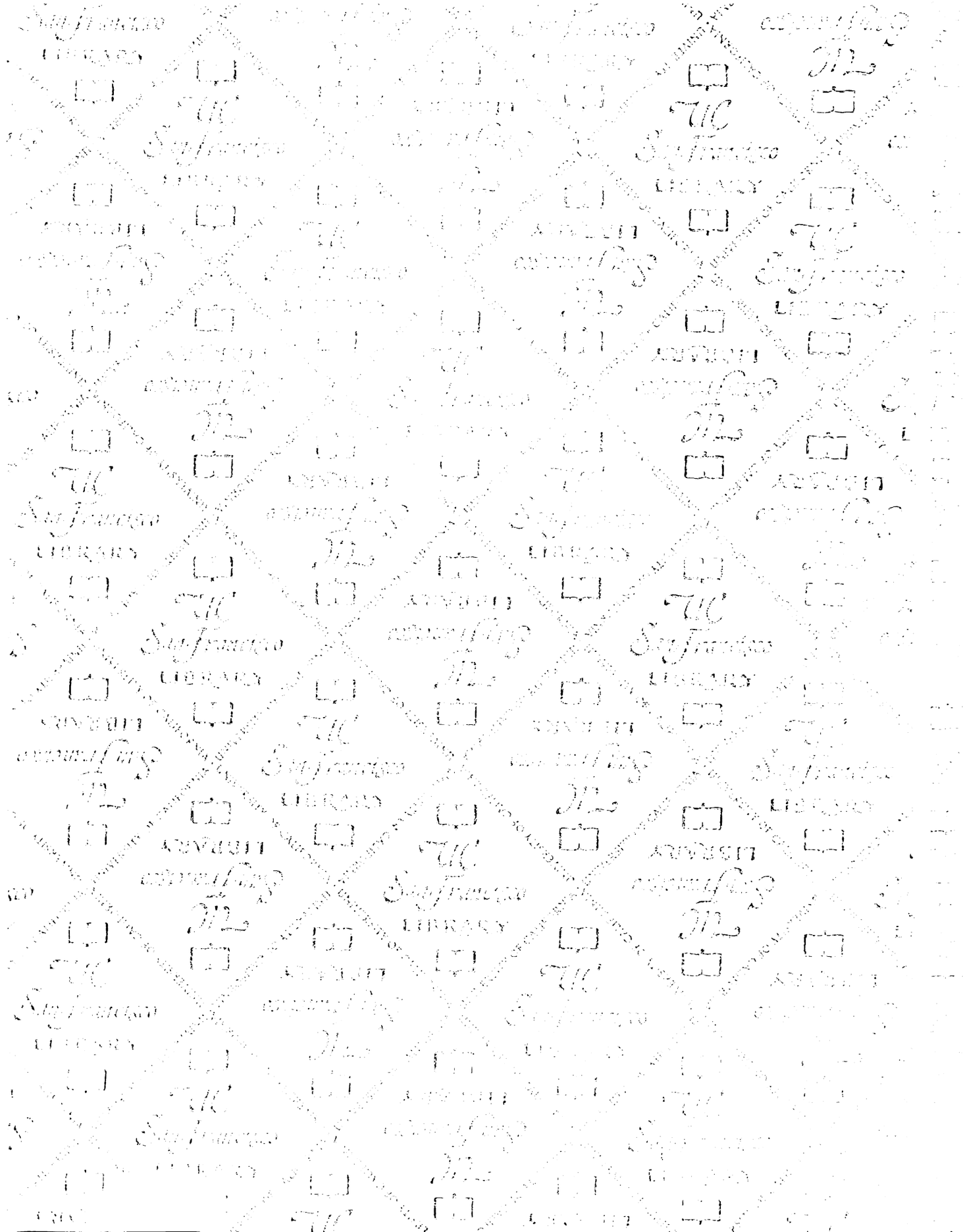
San Francisco
PUBLIC
LIBRARY